RFP-3678
UC-60

ANALYSIS OF WIND TURBINES IN YAW

Robert E. Wilson
Somsak Chaiyapinunt

September 1983

Prepared by

Department of Mechanical Engineering
Oregon State University
Corvallis, Oregon 97331

For

Rockwell International Corporation
Energy Systems Group
Rocky Flats Plant
Wind Energy Research Center
Golden, Colorado 80402-0464

Subcontract No. ASC 51298PB

As a part of the

UNITED STATES DEPARTMENT OF ENERGY
WIND ENERGY TECHNOLOGY DIVISION
FEDERAL WIND ENERGY PROGRAM

Contract No. DE-AC04-76DP03533

Rocky Flats
Wind Energy Research Center

DISCLAIMER

Printed in the United States of America

Available from

National Technical Information Service
U.S. Department of Commerce
5285 Port Royal Road
Springfield, VA 22161

Printed Copy A08 Microfiche A01

DISCLAIMER

RFP--3678

DE84 013620

ANALYSIS OF WIND TURBINES IN YAW

Robert E. Wilson
Somsak Chaiyapinunt

September 1983

Prepared by

Department of Mechanical Engineering
Oregon State University
Corvallis, Oregon 97331

For

Rockwell International Corporation
Energy Systems Group
Rocky Flats Plant
Wind Energy Research Center
Golden, Colorado 80402-0464

Subcontract No. ASC 51298PB

As part of the

U.S. DEPARTMENT OF ENERGY
WIND ENERGY TECHNOLOGY DIVISION
FEDERAL WIND ENERGY PROGRAM

Contract No. DE-AC04-76DP03533

PREFACE

One of the major tasks facing wind systems designers is the prediction of yaw behavior--especially its impact on systems loads and fatigue life--on downwind, horizontal-axis, free yaw machines. Comprising a large portion of the operating units in this country, these types of wind systems are popular within the industry for their simplicity of design. However, these turbines also possess the inherent disadvantage of potential yaw instabilities or excessive yaw tracking error problems.

This report describes an investigation of this problem which was performed by Oregon State University (OSU) under contract to Rockwell International Corporation. What evolved from the work at OSU was a procedure for identifying the relative impact various machine and operating parameters have on yaw behavior. This was accomplished by examining coefficients of the equations of motion rather than solving them explicitly, thus simplifying the analysis. Results from a case study are encouraging and demonstrate the applicability of this approach to the understanding of yaw behavior.

Future work on yaw behavior at Rocky Flats will build upon the approach used by OSU, resulting ultimately in a yaw behavior model. Research will also be conducted to verify these analytical tools by way of controlled velocity experiments and field testing of a horizontal-axis testbed.

The work described herein resulted from Contract No. ASC51298PB and was monitored by M. P. Schroeder of the Rocky Flats Wind Energy Research Center. Other Rocky Flats employees contributing to the completion of this project were: T. E. Hausfeld, J. L. Tangler, P. K. C. Tu, and A. D. Wright.

ABSTRACT

The yaw problems of a three-bladed, downwind, horizontal axis wind turbine are examined in this report. A four-degree-of-freedom system was chosen to model the turbine. Linearized equations of rotor and nacelle motion were developed using the energy method and Lagrange's equations. Quasi-steady blade element and momentum theories were used in developing the axial induction factor and aerodynamic loads. A computer code was developed to obtain the numerical values of coefficients of the equations of motion, thus allowing the cause of yaw instability to be studied. The study indicated that yaw tracking error is primarily caused by tower shadow. However, the wind turbine studied--besides being unstable in yaw under normal operating conditions--has an additional problem in that the nacelle shape contributes to additional instability. Blade coning, in the present design, is inadequate to overcome this instability. The sensitivity of the system stiffness coefficients to the selected input parameters was studied, and results indicate that the system stiffness coefficient is highly sensitive to the coning angle. Increasing the coning angle would significantly increase the stiffness coefficient and lead to improvement of system stability.

TABLE OF CONTENTS

LIST OF TABLES

LIST OF FIGURES

NOMENCLATURE

a	axial induction factor
A	area
B	number of blades
c	blade chord
C_D	drag coefficient
C_L	lift coefficient
C_{F_n}	force coefficient in the direction normal to the rotor
C_{F_t}	force coefficient in the direction tangential to the rotor
C_n	normal force coefficient
C_P	power coefficient
C_Q	torque coefficient
C_t	tangential force coefficient
C_T	thrust coefficient
D	drag force
e	distance from mass center to shear center of the blade cross section
e_1	distance from 1/4 blade chord to shear center of the blade cross section
e_2	distance from 3/4 blade chord to shear center of the blade cross section
e_3	distance from mid-blade chord to shear center of the blade cross section
E	modulus of elasticity

f_1	mode shape of the blade twisting
f_2	mode shape of the blade deflection
f_3	mode shape of the lead-lag deflection
f_4	mode shape of the yaw displacement
F	tip loss factor
F_1	linearized aerodynamic force term
F_2	linearized aerodynamic force term
F_3	linearized aerodynamic force term
F_4	linearized aerodynamic force term
g	gravitational force
G	shear modulus of rigidity
G_1	linearized aerodynamic force term
G_2	linearized aerodynamic force term
G_3	linearized aerodynamic force term
G_4	linearized aerodynamic force term
h	a function defined in gravitational force
I	moment of inertia
I_1	mass moment of inertia in n_1 direction
I_2	mass moment of inertia in n_2 direction
I_3	mass moment of inertia in n_3 direction
j_η	Glauert coefficient
J	polar moment of inertia
J_1	moment of inertia in n_1 direction
J_2	moment of inertia in n_2 direction
J_3	moment of inertia in n_3 direction
k_η	Glauert coefficient
$k_{\eta\eta}$	stiffness coefficient of the system

ℓ	distance from nacelle yaw axis to rotor center
L	lift force
$m_{\eta\eta}$	mass coefficient of the system
M	moment
n_η	unit vector
N_η	linearized normal force
P	power
q_∞	dynamic pressure $\frac{1}{2}\rho_\infty V_\infty^2$
q_1	generalized coordinate of pitch angle
q_2	generalized coordinate of flap deflection
q_3	generalized coordinate of the variation of azimuth angle
q_4	generalized coordinate of yaw angle
q_s	static tip deflection
r	local blade radius
r_N	local blade radius in the rotor plane
r_S	distance of the local blade radius to blade root
R	blade radius
R_H	hub radius
R_S	distance from blade tip to blade root
S	cross-sectional area of nacelle
t	time
H_η	linearized tangential force
u	axial velocity at the rotor
u_η	radial displacement
U	strain energy
v_η	normal displacement

V_∞	wind velocity
V_R	wind velocity at reference point
w	flap deflection
W	relative velocity
W_e	relative velocity excluding the pitching velocity at 3/4 blade chord
W_n	normal relative velocity
W_t	tangential relative velocity
x	local tip speed ratio
X	tip speed ratio
x_1, x_2, x_3	coordinate system on the blade cross section after blade pitching
$x_\theta, y_\theta, z_\theta$	coordinate system on the blade cross section after blade flapping
$x_\beta, y_\beta, z_\beta$	coordinate system on the blade cross section after accounting for the pretwist angle
x_ρ, y_ρ, z_ρ	coordinate system at rotor center accounting for the coning angle
$\underline{x}, \underline{y}, \underline{z}$	coordinate system fixed to the blade at azimuth angle ψ
$\hat{x}, \hat{y}, \hat{z}$	coordinate system with its origin is at the rotor center and the system is fixed to the nacelle
x,y,z	coordinate system fixed to the nacelle and its origin located at nacelle yaw axis
X,Y,Z	coordinate system located on top of the tower

Greek Symbols

θ	pitch angle
χ	variation of azimuth angle
ψ	azimuth angle ($\Omega t + \chi$)
γ	yaw angle
ρ	coning angle
ρ_∞	density
η	dummy variable
Ω	rotor angular velocity
β	pretwist angle
ω_1	blade angular velocity in x_1 direction
ω_2	blade angular velocity in x_2 direction
ω_3	blade angular velocity in x_3 direction
α	angle of attack
α_E	angle of attack plus the effect of pitching velocity
Π_i	integral term for the variation of axial induction factor

1. INTRODUCTION

Wind powered machines can be classified into two types according to the orientation of the axis of rotation: horizontal axis wind turbines and vertical axis wind turbines. For a horizontal axis wind turbine, the system can be further distinguished as either a downwind rotor or an upwind rotor system. When the rotor is upwind of the tower, the system usually has a yaw controller to control the wind turbine to track the wind mechanically. There is generally no need for the yaw controller in the downwind rotor case. When the rotor is downwind of the tower, the wind turbine will usually track the wind. Most of the downwind turbines are free yaw systems.

Unfortunately, a free yaw system quite often suffers from a yaw problem: instead of tracking with the wind the turbine yaws away from the wind.

One of the effects of yaw angle on turbine performance is that it decreases the power output of the rotor.

Little work has been done on the wind turbine in yaw. Most of the previous work is on the dynamics, structure, and control of wind turbine systems. The cause of the yaw problem is still not fully understood.

The technology and methodology used to develop present day wind turbines are adopted from the fixed and rotating wing aircraft technology. Ribner [1] has done the analysis on propellers in yaw. He has developed the analysis to express variation of induction velocity and side force in terms of the shape of the blade when the propeller is yawing. For wind turbines, Miller [2] looked into the static stability characteristics of horizontal axis wind turbines with a free yawed

system. Hirschbaum [6] analyzed the dynamics and control of large horizontal axis axisymmetric wind turbines in his Ph.D. thesis. He modeled the blade motion by considering the blades to be composed of an inboard series of massless, rigid links restrained by linear springs and dampers with a much larger, massive blade attached to the outermost link.

In this analysis, yaw of wind turbines will be studied by using a four-degree-of-freedom system to represent the wind turbine system. The study will be concentrated on the effect of the other variables on the yaw angle, and the cause of yaw tracking errors. This will be done by developing the equations of motion of the system, then studying the coefficients of the equations.

This analysis is developed for a three-bladed, downwind, horizontal axis turbine but it can also be applied to an upwind horizontal axis wind turbine system. With the coefficients of the equations of motion, the dynamic behavior and the stability of the system can be studied further.

2. ANALYSIS

Development of the Equations of Motion

The objective of this study is the aerodynamic and dynamic analyses of horizontal axis wind turbines in yaw. A four-degree-of-freedom system is chosen to model the turbine system. The degrees of freedom are blade pitch deflection, blade flap, nacelle yaw, and rotor speed. Blade pitch is defined as the rotation of the blade cross section around the control axis. Blade flap is defined as the deflection of the blade in the direction perpendicular to the blade chord. Rotor speed variation is defined as the variation of the rotor speed from the nominal value. Nacelle yaw angle is defined as the angle of the nacelle around the yaw axis with respect to the wind.

The equations of motion are developed using the Lagrange method. Since each of the variables is a function of time and distance, the partial derivatives of these variables will be encountered during the development of the equations of motion.

To avoid dealing with partial differential equations, the assumed modes method [4] is used in this study. The purpose of this method is to eliminate the spatial dependence from the dependent variable by discretizing the spatial variable. So each of the system's degrees of freedom is expressed as the product of the displacement function (assumed mode shape), which is the function of the spatial coordinate, and the time-dependent generalized coordinate. By this method, the equations of motion of the system will be developed in ordinary rather than partial differential forms.

In order to attack the problem, the kinematics of the rotor are first developed. Then, the kinetic energy is obtained from the expression of the kinematics. The potential energy expression is developed from the strain energy of the rotor system. With quasi-steady blade element theory, the aerodynamic forces and moments are developed. Then, the nonconservative forces in Lagrange's equation are derived from the virtual work of the aeroforces and moments. Finally, with the Lagrangian functions and nonconservative forces substituted back into Lagrange's equation, we obtain a set of nonlinear equations of motion of the rotor system.

For the wind turbine system, the rotor will extract the energy from the wind converting it into mechanical energy. Since the energy is extracted from the airstream, the velocity of the wake will be decreased. To represent the reduction of the wind velocity at the rotor and in the wake, the axial induction factor 'a' [9,10] is introduced. In this study the nonrotating wake model is used. We can calculate the local value of the axial induction factor by equating the windwise force developed by using the momentum theory, and the same force developed by using the blade element theory. The Glauert empirical relationship [14] is used instead of the momentum theory when the axial induction factor is greater than 0.38. The tip loss model is used to account for the flow at the tip of the turbine blade. The development of the axial induction factor and the tip loss model is presented in Appendix II.

The above steps lead to a set of nonlinear equations. If we restrict the ranges of values of the dependent variables, the system may be well approximated as linear. In this study we will analyze the system in the linear range.

In the process of equation linearization, we will deal with the variation of the axial induction factor with yaw, pitch, flap, and rotational speed. The linear functions of aeroforces and moments are developed.

Let us define the variation of the induction factor with the dependent variables as the summation of two terms: 1) the product of a coefficient and the distance along the yaw axis of the rotor, and 2) the product of a coefficient and the distance along the rotor pitch axis

$$\frac{\partial a}{\partial \eta} = j_\eta \frac{r}{R} \cos\psi + k_\eta \frac{r}{R} \sin\psi$$

Here ψ is the blade azimuth angle.
The value of these two coefficients can be calculated by equating the derivative of yaw or pitch moment developed by the momentum theorem to the derivative of yaw or pitch moment developed by the blade element theory.

With the known values of the coefficients, j_η and k_η, we can determine the variation of the axial induction factor. The result shows that the variation of the axial induction factor exists only for the yaw and yaw rate variables in the uniform flow case.

The linearization of the aerodynamic forces and the variation of the axial induction factor are presented in Appendix II.

The linearized rotor equations of motion are expressed in matrix form

$$[M]\{\ddot{q}_i\} + [C]\{\dot{q}_i\} + [K]\{q_i\} = \{G\}$$

where $\{q_i\}$ is a four-dimensional generalized coordinate column vector representing the system's degrees of freedom; $\{G\}$ is a four-dimensional forcing function column vector; [M], [C], and [K] are the four-dimensional square mass, damping, and stiffness coefficient matrices, respectively.

For a large wind turbine system, the gravity effect is very important in the dynamic and structural analyses. To make the analytical model for the turbine system applicable regardless of the size of the system, the gravity effect is included in this study. The gravitational force is added to the system by means of a potential function.

For a downwind system, the rotor is located behind the nacelle and tower. The effect of the nacelle and tower shadow on the system will be studied.

The nacelle is considered as a slender body. The shape of the nacelle is assumed to be a cylinder with hemispheres on both ends. The equation of motion of the nacelle will be developed by using the Lagrange method. We will consider the nacelle as a rigid body rotating around its yaw axis when we calculate the kinetic and potential energy. The nonconservative force on the nacelle is derived from the virtual work of the nacelle. The forces on the nacelle are calculated by using the slender body theory with forces generated only from the forebody part of the nacelle.

The tower shadow is modeled as the velocity deficit from the rotor axial velocity value over a selected region of the rotor disk. The system's equations of motion are developed with the tower shadow.

Throughout this analysis the wind turbine is modeled with a three-bladed rotor. The turbine blades are elastic. The hub, nacelle and

tower are rigid. The nacelle is allowed to yaw freely. The center of mass of the nacelle and rotor is located over the central axis of the tower. We refer to this axis as the nacelle yaw axis.

The absolute motion of the turbine blade is determined by the motion of blade deflection relative to the hub, the motion due to rotor rotation, and the motion of the nacelle and tower. Since in this analysis no movement of the tower is allowed, we consider the tower as the inertial reference frame. A series of coordinate systems is used to describe a point on the blade. A series of transformation matrices is used to transform the coordinate systems that describe motion of a point on the blade in its original reference frame into the inertial reference frame.

A computer code has been written to handle the numerical analyses which yield the coefficients for the equations of motion. The inputs of the computer code are the geometric as well as the wind and operating conditions. This computer program will calculate the axial induction factor along the blade at a particular tip speed ratio. At the same time it also calculates the integral terms for variation of the axial induction factor with yaw and yaw rate. Finally, the program will calculate the constant coefficients in the equations of motion (mass, damping, stiffness and forcing functions). Besides the coefficients of the equations of motion, the code also calculates the thrust and power coefficients of the rotor.

The geometry and properties of the turbine system are needed as inputs to the computer code. The Enertech 1500 Wind Turbine is examined. Then, the analytical solutions from the system are verified with the experimental data of the Enertech 1500 obtained from the Rocky Flats Wind Energy Research Center.

3. ENERTECH 1500

The Enertech 1500 is a downwind system with a three-bladed rotor. The geometry and material properties of a blade off an actual Enertech 1500 wind turbine were measured. The blade has linear twist with slight linear taper over the outer 22% of the rotor blade and the blade's thickness is varied from root to tip. For the calculation of the aerodynamic forces and moments, the blade profile section was represented by the NACA 4415 airfoil section. The airfoil lift and drag coefficients are plotted as functions of Reynolds number and angle of attack in Figure 3.1. These data are obtained from Reference 7. This rotor is designed to operate at tip speed of 117 fps (170 rpm). The physical characteristics of the rotor are presented in Table 3.1.

Table 3.1. Rotor physical and operating characteristics.

Rotor Diameter	13.12 ft.
Blade Chord	6.8 in. from root to r/R = 0.6545 linear taper to 6.1 in. at r/R = 1.0
Airfoil Type	NACA 4415*
RPM	170
Tip Speed	117 fps
Number of Blades	3
Root Cut-out	0.84 ft.
Twist	5° from root linear to 1° at blade tip
Precone	0°

*Used as representative airfoil section.

The profile of the blade cross-sections are measured at six stations along the blade. The weight of the blade was measured. By knowing the weight and the profile of each cross section, properties of

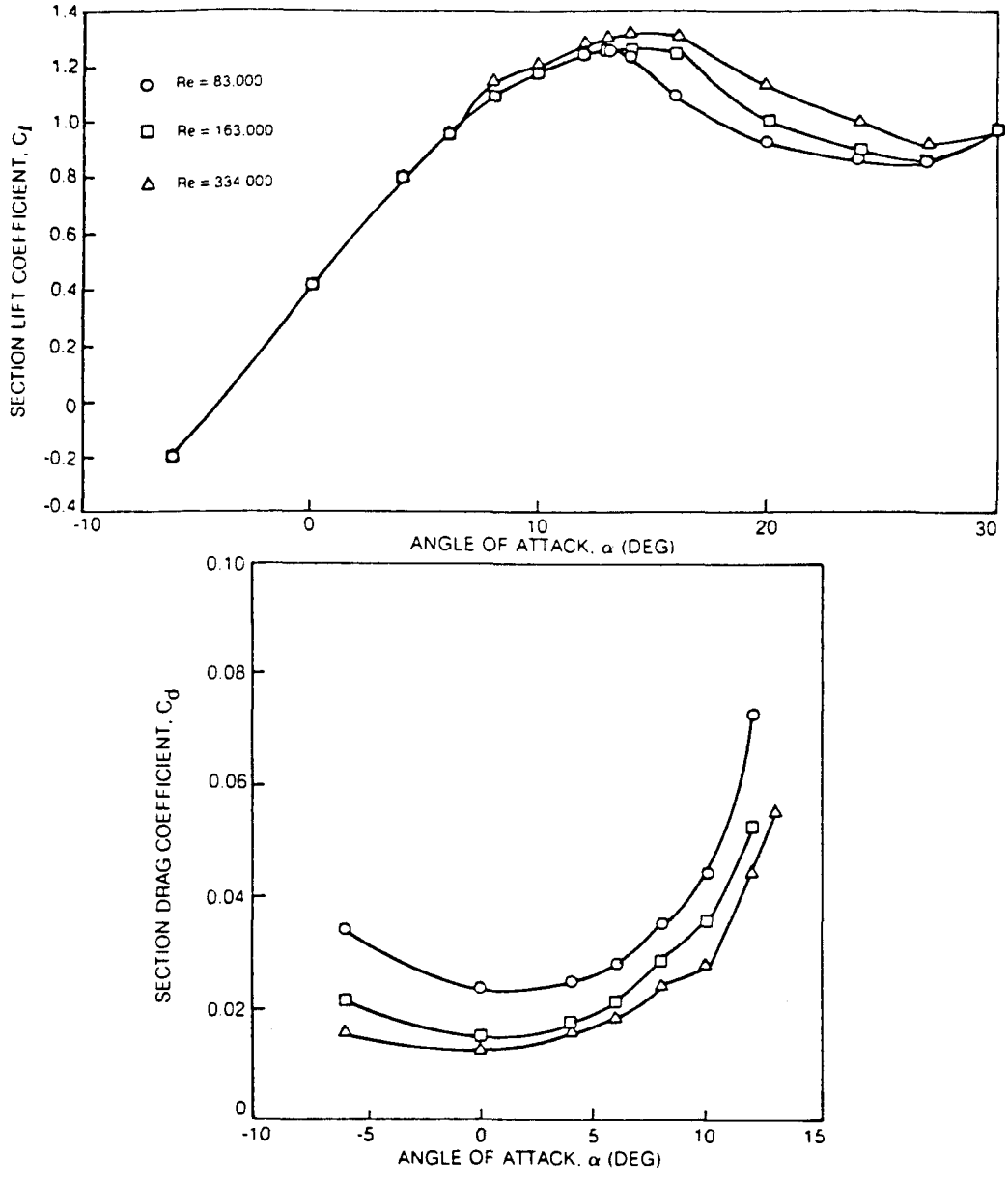

Figure 3.1 Lift and drag coefficient for the NACA 4415 airfoil section (Ref. 7)

the blade were calculated. The expressions for the moment of inertia and mass distribution per unit length of the blade were written as a function of the distance along the blade. These expressions are given in Tables 3.2 and 3.3.

Table 3.2. The moment inertia of the blade cross-section.

r/R	J_2 (in 4)	J_3 (in 4)
1-0.6545	5.673 exp(-3.313 r/R)	67.3636 exp(-2.0236 r/R)
0.6545-0.3648	2.111 exp(-1.802 r/R)	29.44 exp(-0.76 r/R)
0.3648-0.244	2.111 exp(-1.802 r/R)	11.3726 $(r/R)^{-0.6585}$
0.244 -0.1393	4.5679 exp(-4.8604 r/R)	11.3726 $(r/R)^{-0.6585}$
0.1393-0.128	2.3210	41.924

Here J_i's are the moment of inertias of the blade cross section at the mass center in x_i direction and $J_1 = J_2 + J_3$.

Table 3.3. Mass distribution of the blade.

r/R	μ (slug/ft)
1-0.6545	0.090898 exp(-1.3266 r/R)
0.6595-0.3648	0.05847 exp(-0.6447 r/R)
0.3648-0.1393	0.081772 $(r/R)^{-0.3695}$
0.1393-0.128	0.06593

Since the blade is made of wood (orthotropic material), its material properties depend on the orientation of wood grain. It is difficult to find the mechanical properties of a nonuniform orthotropic beam by experiment. Thus it was decided to treat the blade as an isotropic material and use the values given by J.Y. Liu from the U.S.

Forest Products Laboratory on Sitka Spruce with 10 percent moisture content. The values are:

$$E_L = 1.84 \times 10^6 \text{ psi}, \; G_{LR} = 1.089 \times 10^5 \text{ psi}, \; \nu_{LR} = 0.25$$

For simplicity, the elastic axis was assumed to be a straight line which is parallel to the trailing edge of the blade. The location of the elastic axis on the blade cross section was chosen arbitrarily. The location of the axis is then varied to see the effect on the system.

The nacelle of the Enertech 1500 has a cylindrical shape with a hemisphere on each end. The properties and geometry of the nacelle are given in Table 3.4.

Table 3.4. Nacelle properties.

Distance of the nacelle yaw axis to the blade hub	2.46 ft
Length of the nacelle	5.896 ft
The radius of the nacelle cross-section	0.84 ft
The mass moment inertia of the nacelle around the yaw axis	14.41 slug-ft^2

The generator for the Enertech 1500 is a single phase induction motor connected to a gearbox having a measured 11:28 to 1 ratio.

With the lift and drag data obtained from references 7 and 8, the lift and drag curves were modified to use in the computer code.

The lift coefficient curve is approximated and can be described in a simple yet fairly accurate form by six parameters. The curve consists of four straight line segments as follows:

$$C_L = 2\pi m \sin(\alpha+\alpha_{L_o}) \qquad \alpha < \alpha_{C_{L_{max}}}$$

$$C_L = C_{L_{max}} \qquad \alpha_{C_{L_{max}}} < \alpha < \alpha_{BR}$$

$$C_L = C_{L_{flat}} \qquad \alpha_{BR} < \alpha < \alpha_{stall}$$

$$C_L = C_{L_{flat}} \frac{\sin(\frac{\pi}{2} - \alpha)}{\sin(\frac{\pi}{2} - \alpha_{stall})} \qquad \alpha > \alpha_{stall}$$

The six parameters are:

m - lift curve slope divided by 2π

α_{L_o} - zero lift angle of attack

$C_{L_{max}}$ - maximum lift coefficient

α_{BR} - angle at which C_L drops to $C_{L_{flat}}$

$C_{L_{flat}}$ - an approximation to the average C_L on the far side of C_L curve, this can be adjusted up or down depending upon the characteristics of the airfoil

α_{stall} - angle at which C_L begins to decrease

For the Enertech 1500 blade, these six parameters are as follows:

$m = 0.89$

$C_{L_{max}} = 1.35$

$C_{L_{flat}} = 1.0$

$\alpha_{LO} = 4.2°$

$\alpha_{BR} = 15°$

$\alpha_{stall} = 45°$

The drag curve of the Enertech 1500 blade can be approximated in a series of curve fits. These curve fits are shown as follows:

$$C_D = C_{D_o}[1 + 53.81\alpha^2] \qquad \alpha < 12^0$$

$$C_D = 3.36\, C_{D_o} + (\tan\alpha - \tan 12^0) \qquad 12^0 < \alpha < 15^0$$

$$C_D = 2.439\, C_{L_{flat}} (\tan\alpha)^{2.15} \qquad 15^0 < \alpha < \alpha_2$$

$$C_D = C_{L_{flat}} \tan\alpha \qquad \alpha_2 < \alpha < 45^0$$

$$C_D = C_{D_2} \frac{\sin^2\alpha}{1 + \sin\alpha} \qquad \alpha > \frac{\pi}{4}$$

where

$$C_{D_o} = 0.014$$

$$C_{D_2} = 3.4142$$

$$\alpha_2 = \arctan\left[\left(\frac{.41}{C_{L_{flat}}}\right)^{.87}\right]$$

4. RESULTS AND DISCUSSION

The Enertech 1500 was used as a test case. With the numerical values of the characteristics and physical properties of the Enertech 1500 as the inputs to the computer code, the code generates the numerical values of power coefficient, thrust coefficient, and static tip deflection, the coefficients accounting for the variations of the axial induction factor, coefficients in the rotor equations of motion and the forcing function at a particular value of tip speed ratio.

For the aerodynamic part, the code is verified by comparing the predicted power coefficients with the test results. The test results were obtained from the Rocky Flats Wind Energy Research Center. The test procedure is explained in reference 11. The comparision of the predicted values and data is given in Figure 4.1. Agreement is good at high tip speed ratios. At the low tip speed ratios, where the agreement was only fair, the blade angle of attack is large and stalled flow occurs over most of the blade. This introduces two sources of uncertainty. First, there is some doubt as to the accuracy of the aerodynamic input (lift and drag curve) associated with stall since there is little data on the NACA 4415 at any Reynolds number. Secondly, the use of quasi-static analysis may be questioned when the turbine is operated under a large yaw angle.

To find the cause of the yaw problem, the numerical values of coefficients in the equations of motion are studied.

The static pitch angle is examined by first setting the dynamic terms in the linearized equation of motion in pitch equal to zero and then calculating the static pitch angle that deviated from the nominal

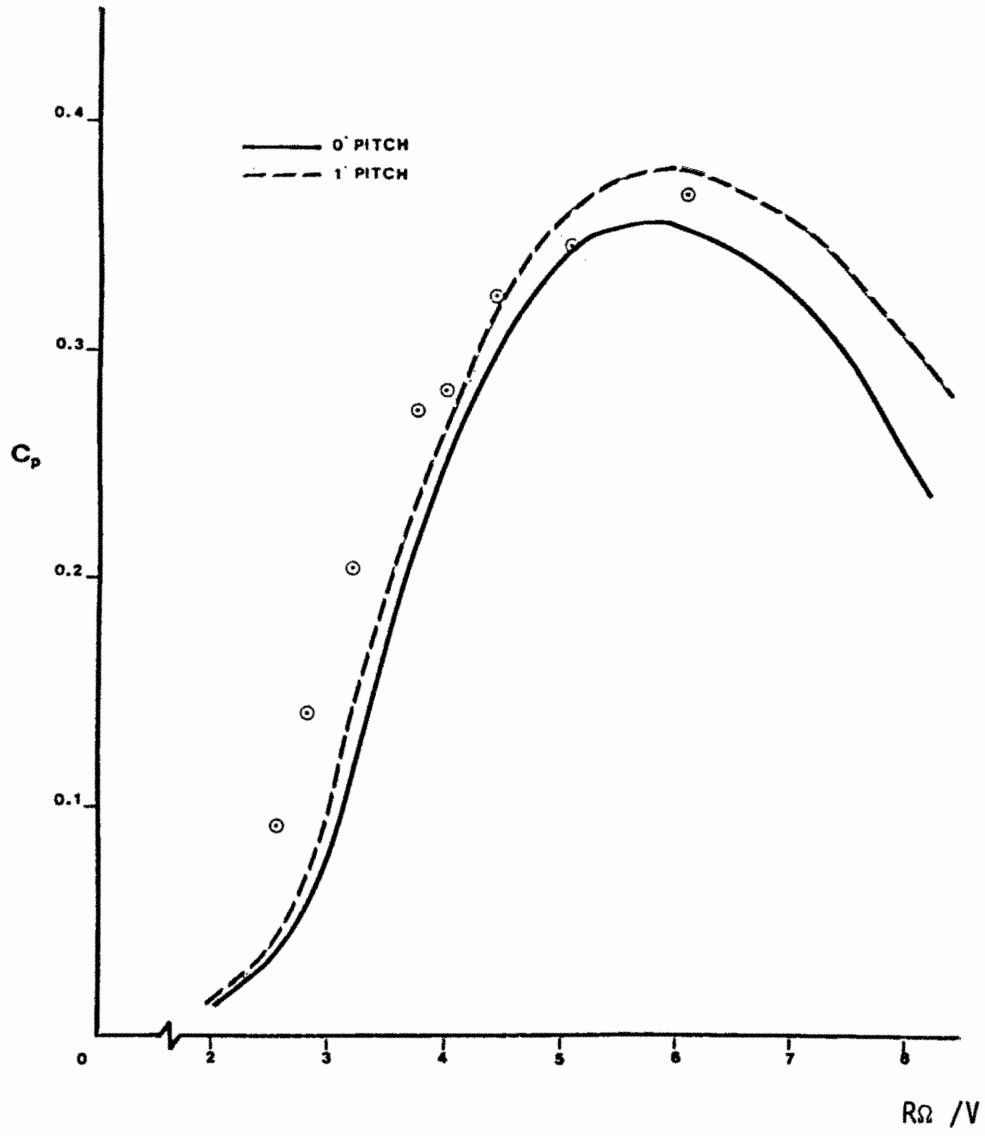

Figure 4.1 Power Coefficient VS. Tip Speed Ratio

value. The static tip pitch angles are given in Table 4.1. These angles are so small that they have negligible effect on the system.

Table 4.1. Static tip pitch angles under nominal operating condition.

x	θ_{st} (degree)
2	0.0430
3	0.0323
4	0.0312
5	0.0305
6	0.0218
7	0.0177
8	0.0147

The static condition of the equation of motion in flap is considered. Because the static flapwise displacement appears implicitly and explicitly in the force and moment expressions, the iteration method is used in order to calculate for a numerical value of static deflection.

The static tip deflection is first calculated by setting the value of the derivative of flapwise deflection, radial displacement, and its derivative, to zero. Then, by using the value obtained as the initial value, the static tip deflection is iterated until the final value is converged within the given criterion.

The results show that the difference between the initial value and final value is negligibly small. So for this study the code will use the first calculation method (without the iteration) to calculate for static tip deflection

The static tip deflections for the nominal operating condition are given in Table 4.2.

Table 4.2. Static tip deflections under nominal operating condition.

x	ds (ft)
2	0.01644
3	0.01279
4	0.01269
5	0.01057
6	0.00839
7	0.00676
8	0.00558

For the uniform flow condition, there is no coupling between the yaw angle and the other three variables explicitly on the equations of motion.

For the nacelle, the equation of motion appears in the form of an undamped second order system in yaw. The stiffness coefficient of the nacelle is not dependent on tip speed ratios.

Because of the linearity of the system, the nacelle equation of motion can be added directly to the rotor equation of motion in yaw. The nacelle is destabilized to the system in yaw. The coefficients in the equation of motion in yaw are shown in Tables 4.3 and 4.4.

Table 4.3. Coefficients of equation of motion in yaw.

x	m_{44R}*	c_{44R}	k_{44R}	m_{44n}*	k_{44n}
2	0.01605	0.01486	-0.00226	0.01315	-0.036477
3	0.03605	0.02666	-0.01716	0.02958	-0.036477
4	0.06409	0.06306	-0.00909	0.05259	-0.036477
5	0.10007	0.11496	0.00803	0.08217	-0.036477
6	0.14398	0.13952	0.01457	0.11833	-0.036477
7	0.19585	0.17117	0.01554	0.16106	-0.036477
8	0.25569	0.20538	0.01592	0.21036	-0.036477

*R subscript for rotor
n subscript for nacelle

Table 4.4. Coefficients of equation of motion of the system in yaw (nacelle and rotor).

x	m_{44}	c_{44}	k_{44}
2	0.02920	0.01486	-0.03874
3	0.06563	0.02666	-0.05364
4	0.11668	0.06306	-0.04557
5	0.18224	0.11496	-0.02845
6	0.26231	0.13952	-0.02191
7	0.35691	0.17117	-0.02094
8	0.46605	0.20538	-0.02056

The equation of motion in yaw is studied to find the cause of the yaw problem. The gravity effect on the system is also considered when the equations of motion are developed. The gravitational force is added to the system by means of a potential function. The analysis shows that the gravitational force appears in the harmonic terms (terms associated with sine and cosine of the azimuth angle). The gravitational force terms are dropped out of the system when we add the effect that accounts for the three-bladed rotor.

The effect of the blade cyclic force on the cyclic pitch angle is also examined by considering the gravitational force on a single blade. With the equation of motion of a rotor blade in pitch, the harmonic terms appear in the stiffness coefficient and forcing function as the component of gravitational force. These harmonic terms are given in the following forms:

$$(C_g\cos\psi + D_g\sin\psi)q_1 = (E_g\cos\psi + F_g\sin\psi)$$

The coefficients C_g, D_g, E_g and F_g are given in Table 4.5. The stiffness coefficient and forcing function are also given in Table 4.5.

Table 4.5. Coefficients of harmonic terms (C_g, D_g, E_g, F_g), stiffness coefficient and forcing function of a single blade equation of motion in pitch.

x	k_{11}	G_{01}	$C_g x10^5$	$D_g x10^4$	$E_g x10^5$	$F_g x10^4$
2	13.845	0.0101	-.1380	1.0649	-.2140	-.1423
3	31.152	0.0167	-.3105	2.3961	-.3745	-.3201
4	55.383	0.0289	-.5520	4.2598	-.6605	-.5692
5	86.367	0.0392	-.8626	6.6559	-.8604	-.8894
6	124.607	0.0457	-1.2806	9.5845	-.9829	-1.2421
7	169.602	0.0506	-1.6907	13.0456	-1.0786	-1.7431
8	221.043	0.0541	-2.2082	17.0392	-1.1629	-2.2767

For the static condition, the cyclic tip pitch angle is given in the following form

$$q_{1s} = \frac{G_{01}/3 + (E_g\cos\psi + F_g\sin\psi)}{k_{11}/3 + (C_g\cos\psi + D_g\sin\psi)}$$

We can see that the blade cyclic force has negligible effect on the static pitch angle by comparing the magnitude of the coefficients given in Table 4.5.

With no forcing function on the system's (rotor + nacelle) equation of motion in yaw, the turbine will always stay at zero yaw angle for the static case at any tip speed ratio.

But according to the data obtained from Rocky Flats, the system was operating with the static yaw angle. The yaw tracking error is shown in Figure 4.2. The discrepancy between the analysis results and data in yaw angle indicates that our model fails to include the effect causing the static yaw angle.

The tower shadow effect is then added to the system. The tower shadow is modeled as a velocity deficit from the axial velocity value over a selected region of the rotor disk, centered about the tower center line. The development of the rotor equation of motion with tower shadow is given in Appendix III.

Because of the different values of the axial velocity on the rotor between the inside and outside of the tower shadow region (i.e., when the blade is in the 6 o'clock position and 12 o'clock position), there will be different values of relative velocity that lead to the difference in aerodynamic force values inside the shadow. And the difference of tangential force in the shadow produces the net yaw moment around the yaw axis creating the static yaw angle. This yaw moment turns out to be the forcing function we needed in the yaw equation.

Since our analysis used the linear approximation method, our results are valid only in a small region around the zero yaw angle. The data in Figure 4.2 shows a linear part and a sign change in yaw angle

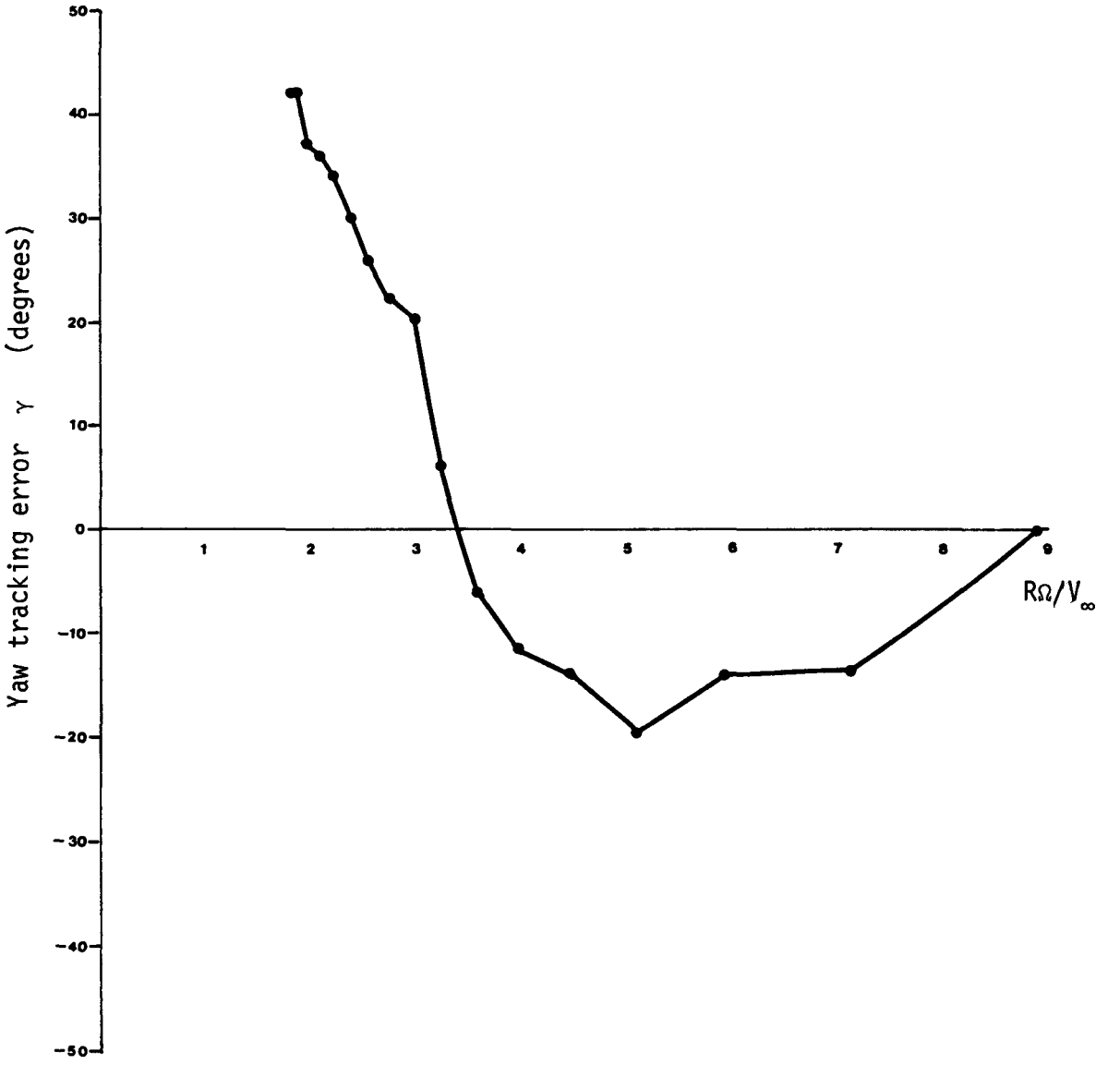

Figure 4.2 Yaw tracking error vs. tip speed ratio

occurred between tip speed ratios 3 and 4. Our linearized model would represent the system operating in the region of this linear part and a sign change of static yaw angle in the analytical results would verify the analysis.

The explanation for a sign change in static yaw angle from the analysis can be obtained by studying the relationship between the tangential forces and velocity ratios. The curves of the tangential forces versus tip speed ratios and velocity ratios are shown in Figures 4.3 and 4.4. From Figure 4.4, with a given value of wind velocity and velocity deficit inside the shadow, we can find the values of the average tangential force on the shadow region and the other region on the rotor. These values will change with the velocity ratios (wind velocity for constant rotor speed). The difference of the tangential forces between the one inside the shadow and the one outside the shadow will change sign at a particular value of velocity ratio. Since the static yaw angle is dependent on the difference of tangential forces on the rotor, the angle will also change sign when the forces do.

To illustrate this idea, the numerical values of the width and velocity deficit of tower shadow are chosen. Then, the coefficients of the equations of motion in yaw with the tower shadow are calculated.

The coupling between the yaw variable and the other variables appears in the equation due to the tower shadow effect. These coupling terms and the forcing function are dependent on the values of the width and velocity deficit of tower shadow. The developing of the coefficient and forcing function terms due to tower shadow is given in Appendix III.

Now considering the static condition and neglecting the coupling terms, we can calculate for the static yaw angle. The static terms on

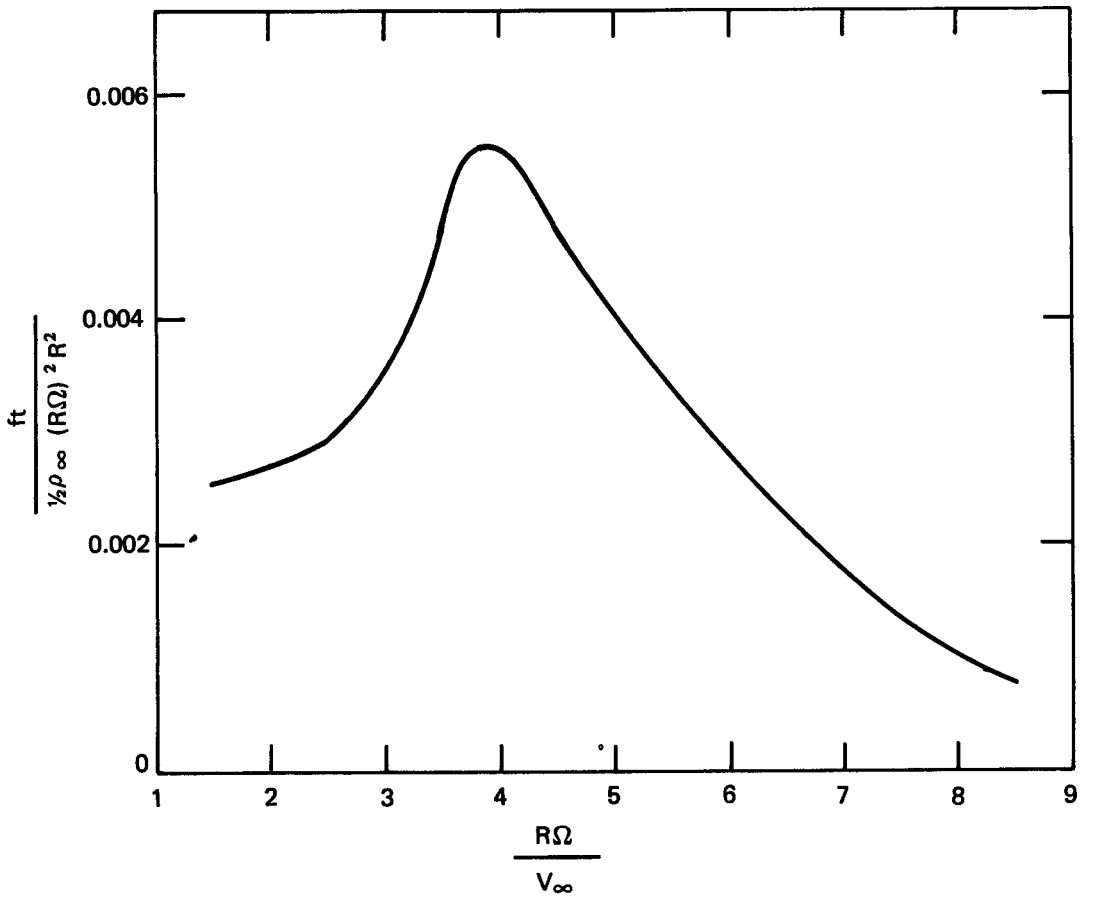

Figure 4.3 Tangential Force on the Rotor VS. Tip Speed Ratio

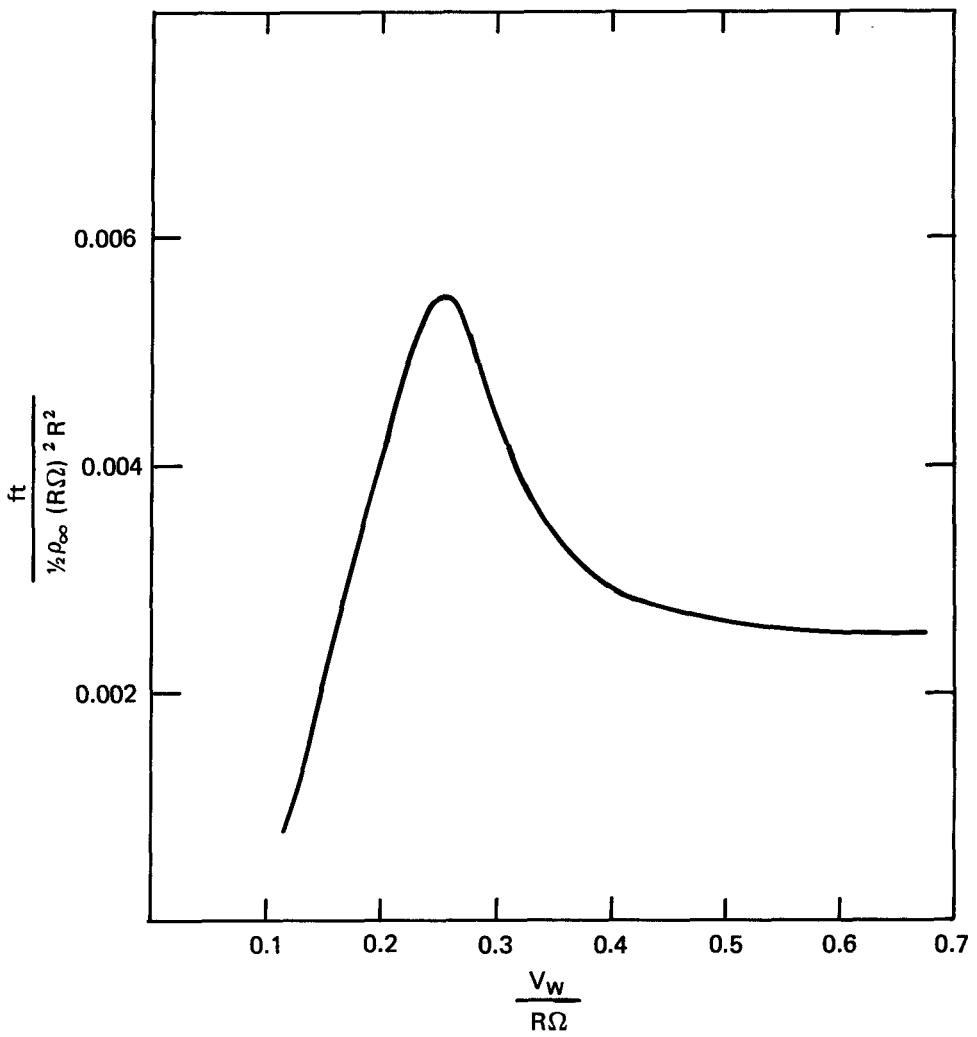

Figure 4.4 Tangential Force on the Rotor VS. Velocity Ratio

the system's equation of motion in yaw for a 20° segment of shadow width and 50% velocity deficit are given in Table 4.6.

Table 4.6. Stiffness coefficient and forcing function in yaw equation with 20° shadow width and velocity deficit = 50%.

x	k_{44_T}	G_{o_4}
2	-0.03874	0.00106
3	-0.05364	0.00025
4	-0.04557	-0.00330
5	-0.02845	-0.00455
6	-0.02191	-0.00449
7	-0.02094	-0.00391
8	-0.02056	-0.00321

For a stable system, if a sign change occurs in the yaw forcing function, the same sign change also occurs in the static yaw angle. Unfortunately, according to the linear analysis, the Enertech 1500 has very poor stability (negative stiffness coefficient). Instead of calculating the static yaw angle from the system, we consider a sign change in the yaw forcing function (a change in direction of yaw moment) as the verification of the analysis. From Table 4.6, there is a sign change in the yaw forcing function occurring between tip speed ratios 2 and 3. This result confirms that the static yaw moment created by tower shadow is the one that causes the machine to yaw in one direction at low wind speeds and to yaw in the opposite direction at high wind speeds.

The effect of the tower shadow model on the static yaw moment (yaw forcing function) is also considered. The yaw forcing function for velocity deficit values of 33.3%, 50% and 66.7% is shown in Figure

4.5. The yaw forcing function with 10°, 20°, 30°, 45°, 60°, and 90° shadow width is shown in Figure 4.6.

The effects of the magnitude of the velocity deficit on the yaw forcing function are the value of the zero forcing function cross-over point and its slope. The magnitude of the velocity deficit is varied reversely to the value of the tip speed ratio that the sign change takes place at. For the tower shadow width effect, we can see that increasing shadow width also increases the slope of the yaw forcing function. The cross-over point is not affected by shadow width.

Sensitivity Study

The stability of the system in yaw is investigated. For the nominal operating condition, the system is unstable because of the negative stiffness coefficient. This negative value is dominated by the nacelle. The sensitivity study of the parameters on the system's equation in yaw indicates that the mass and damping coefficient always have positive values. So the indication of the stability of the system in yaw is the sign on the system (rotor + nacelle) stiffness coefficient.

Usually when we do the stability analysis (i.e., root locus) we will deal with the terms of stiffness and damping coefficients divided by mass coefficient rather than the stiffness and damping coefficients themselves. But in our study, we primarily emphasize the positive stiffness coefficient to insure the system stability. So the sensitivity of the system stiffness coefficient in yaw to the selected input parameters will be studied.

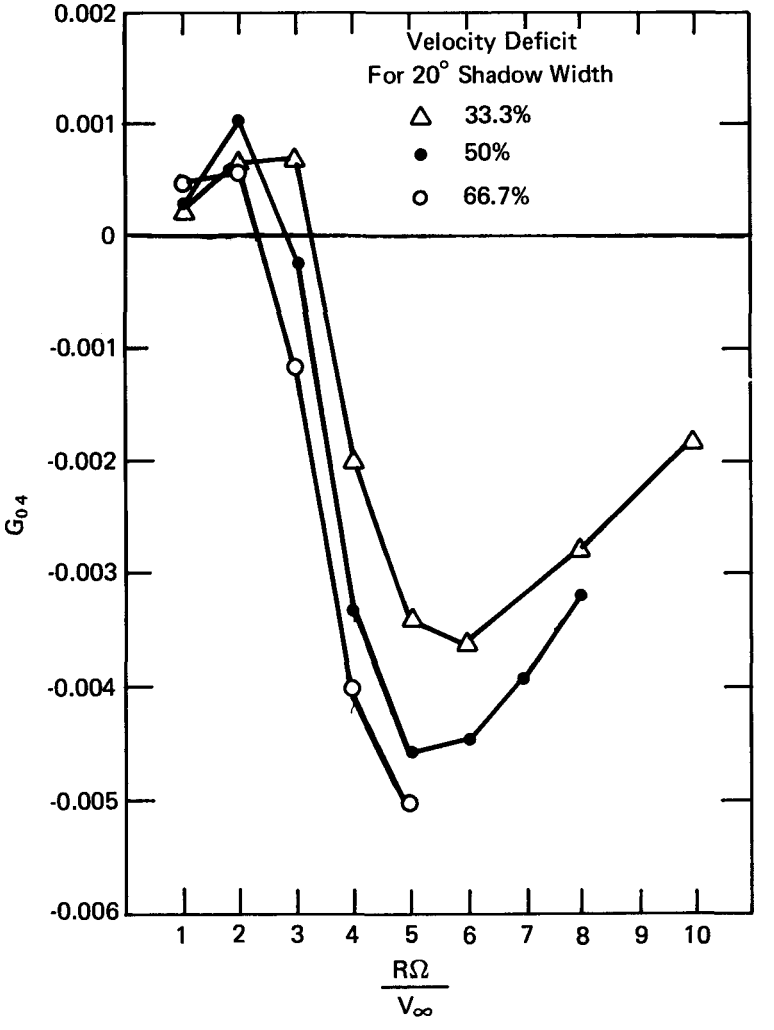

Figure 4.5 Effects of Velocity Deficit on Yaw Forcing Function

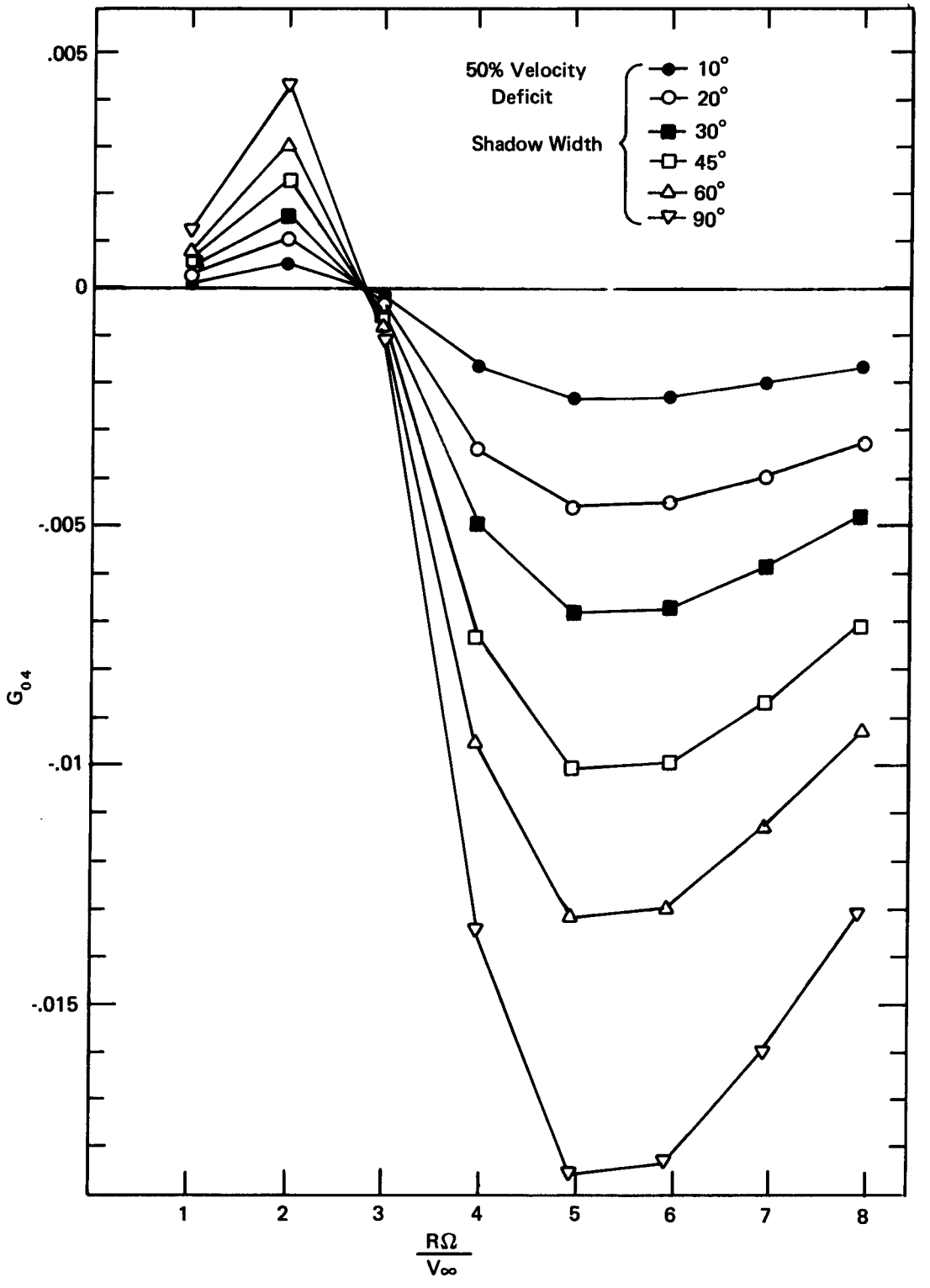

Figure 4.6 Effects of Shadow Width on Yaw Forcing Function

Torsional Stiffness and Pitch Angle

The effect of torsional stiffness is considered by changing the values of the shear modulus G. The result shows that its only effect is on the pitch equation. Unless the static pitch angle is significantly differed from the zero value, there will not be any effect on the yaw equation.

The influence of the pitch angle on the rotor stiffness coefficients is shown in Figure 4.7. Increasing the pitch angle will shift the curve to the left side of the zero pitch angle curve. Decreasing the pitch angle will shift the curve to the right side of the zero pitch angle curve and also increase the stiffness coefficients values. But when the nacelle effect is added, the system is still unstable. This is shown in Figure 4.8.

Modulus of Elasticity and Flapwise Deflection

The static flapwise deflection is defined as the product of the static tip deflection and its mode shape. The static flapwise deflection is dependent on the blade stiffness and the aerodynamic load. The effect of the blade stiffness on the static tip deflection is shown in Figure 4.9 for the values of modulus of elasticity of 1.0×10^5, 1.84×10^6, and 2.3×10^6 psi. Figure 4.9 shows that the stiffer blade will experience smaller deflection. The flat part of the curves between the tip speed ratios 3 and 4 is due to the transition of the flat part and the maximum lift value on the modeled lift curve. In other words, the flat part is caused by the use of a simple model curve to represent the stall part of the real lift curve.

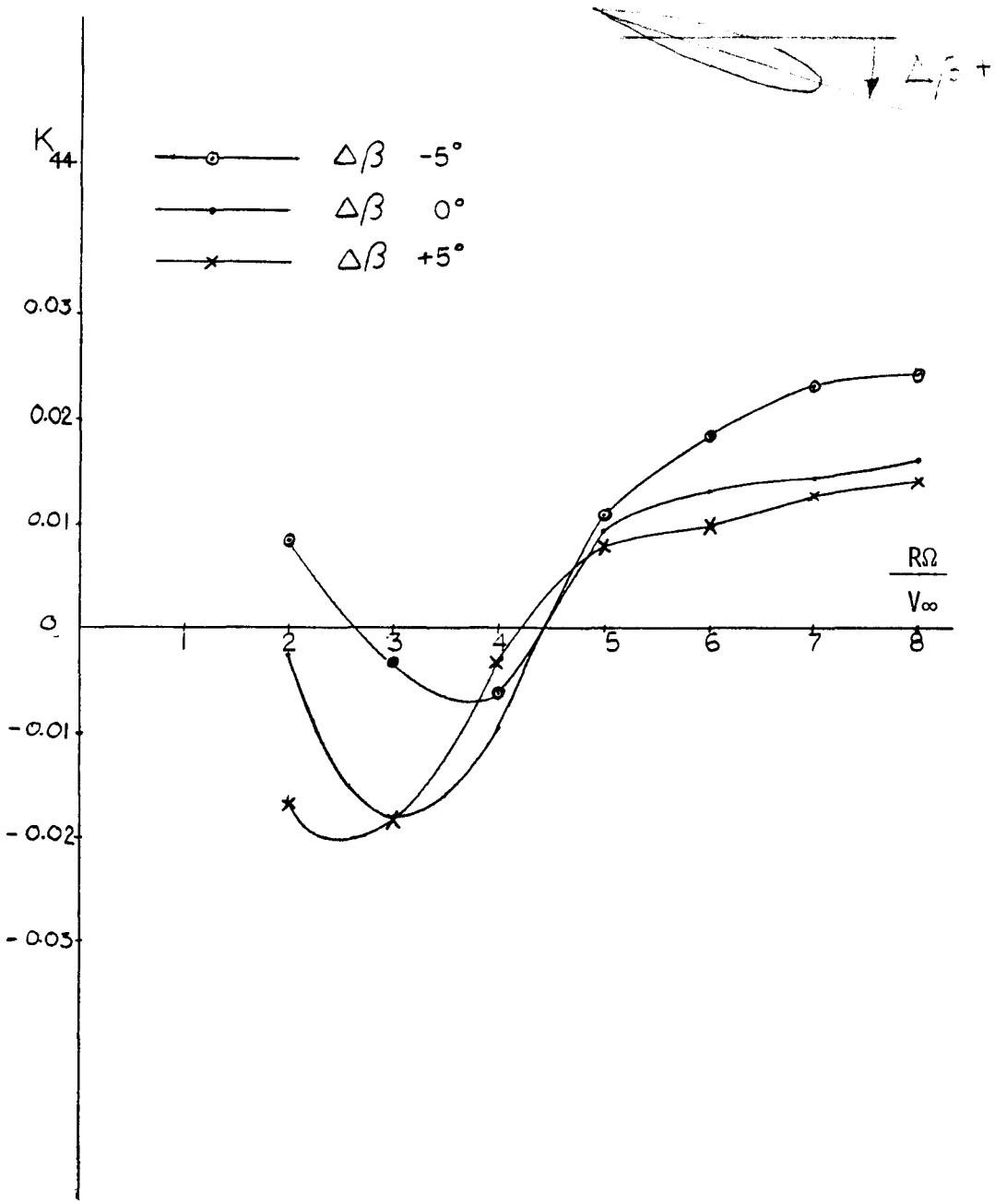

Figure 4.7 Effect of pitch angle on the rotor yaw stiffness coefficient

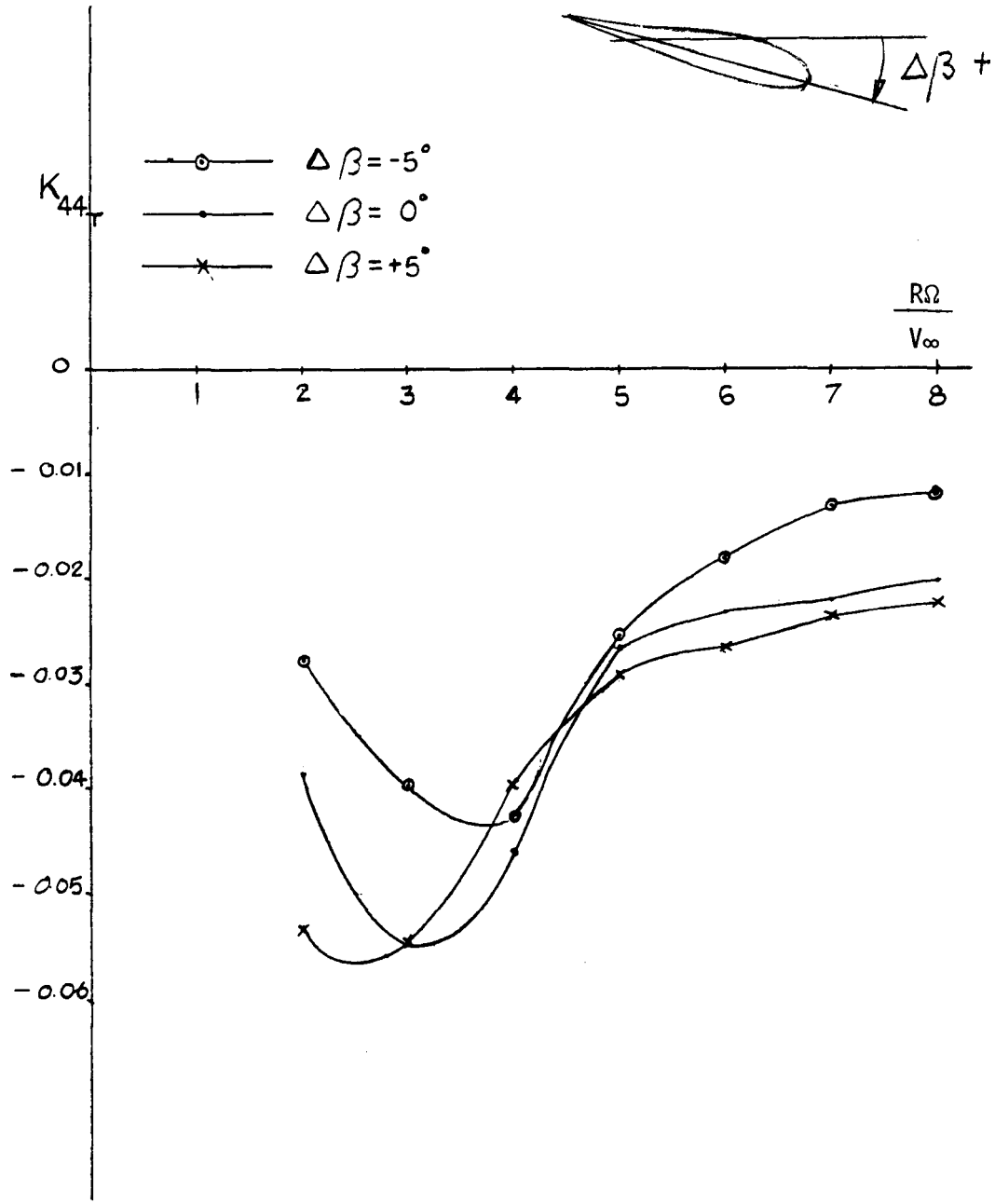

Figure 4.8 Effect of pitch angle on the system stiffness coefficient in yaw

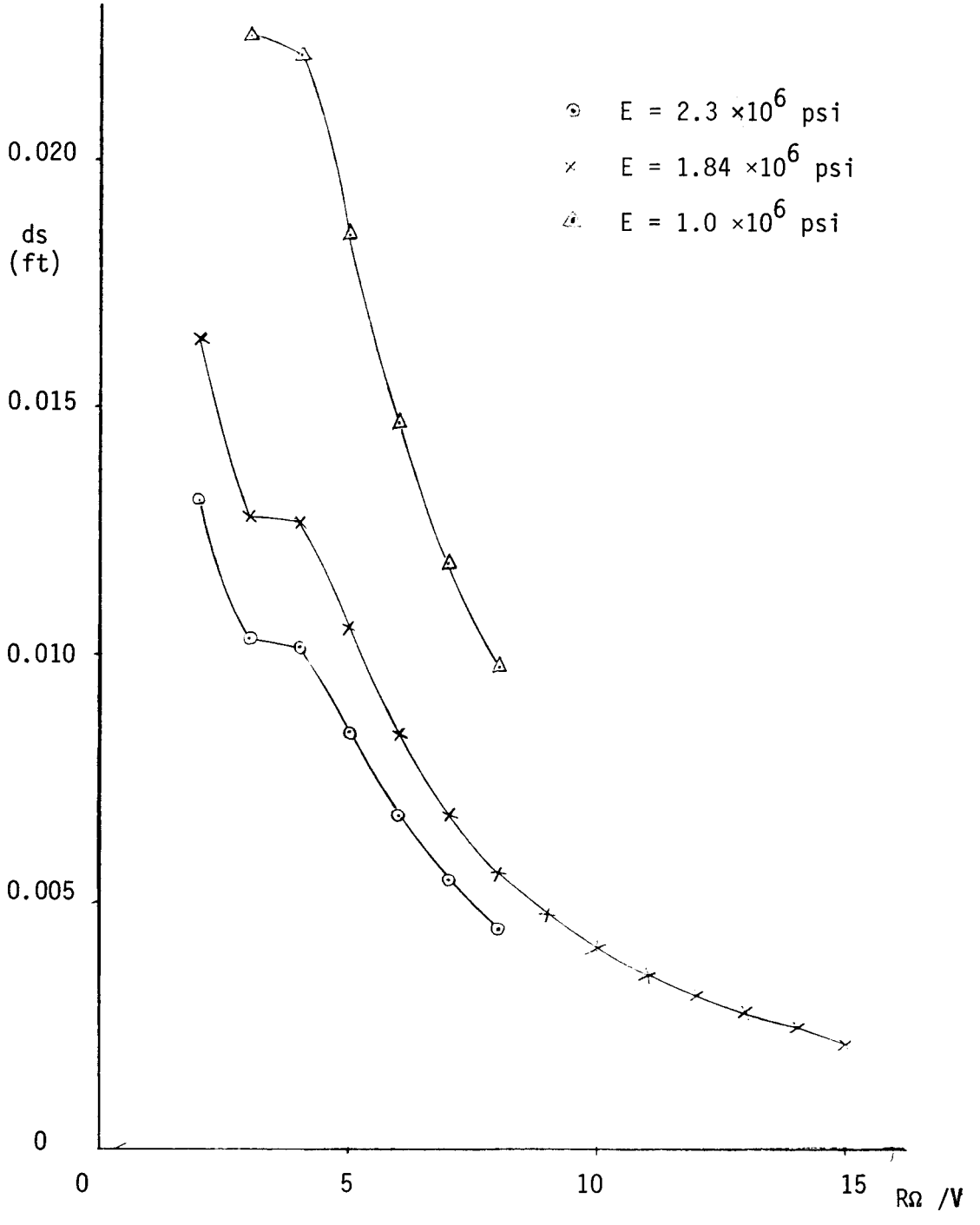

Figure 4.9 Effect of blade stiffness on the static tip deflection

Under the values of blade stiffness considered, the magnitudes of the static tip deflections are very small (in order of 0.1-1.0 % of the blade length). The effect of the flapwise deflection on the system in yaw is negligible. The rotor stiffness coefficients with different values of blade stiffness (flapwise deflection) are shown in Figure 4.10. The rotor stiffness coefficient is increased when we decrease the blade stiffness but the relative magnitude is very small.

Speed

The effect of a change in rotor speed on the stiffness coefficient is studied. The expressions of nondimensionalized rotor mass, damping coefficient, and nacelle mass coefficient are dependent on the dynamic pressure head. By changing the rotor speed, these coefficients change quite dramatically due to the change in dynamic pressure head for the same value of tip speed ratio. The rotor stiffness coefficient is the least sensitive term to the change in the rotor speed. The curves for the rotor stiffness coefficients for the rotor speed of 120, 170, and 220 rpm are shown in Figure 4.11. The effects of the speed change on the rotor stiffness coefficient is small. Increasing the rotor speed also increases the rotor stiffness coefficient. Figure 4.12 shows the system stiffness coefficient for varying rotor speed values. Since the total mass coefficient value changes dramatically with the rotor speed, the value of the system stiffness coefficient divided by the total mass coefficient is considered. These values are plotted against the tip speed ratios in Figure 4.13. From Figures 4.12 and 4.13, we can conclude that within the rotor speed considered the system is still unstable and increasing the rotor speed increases the stiffness

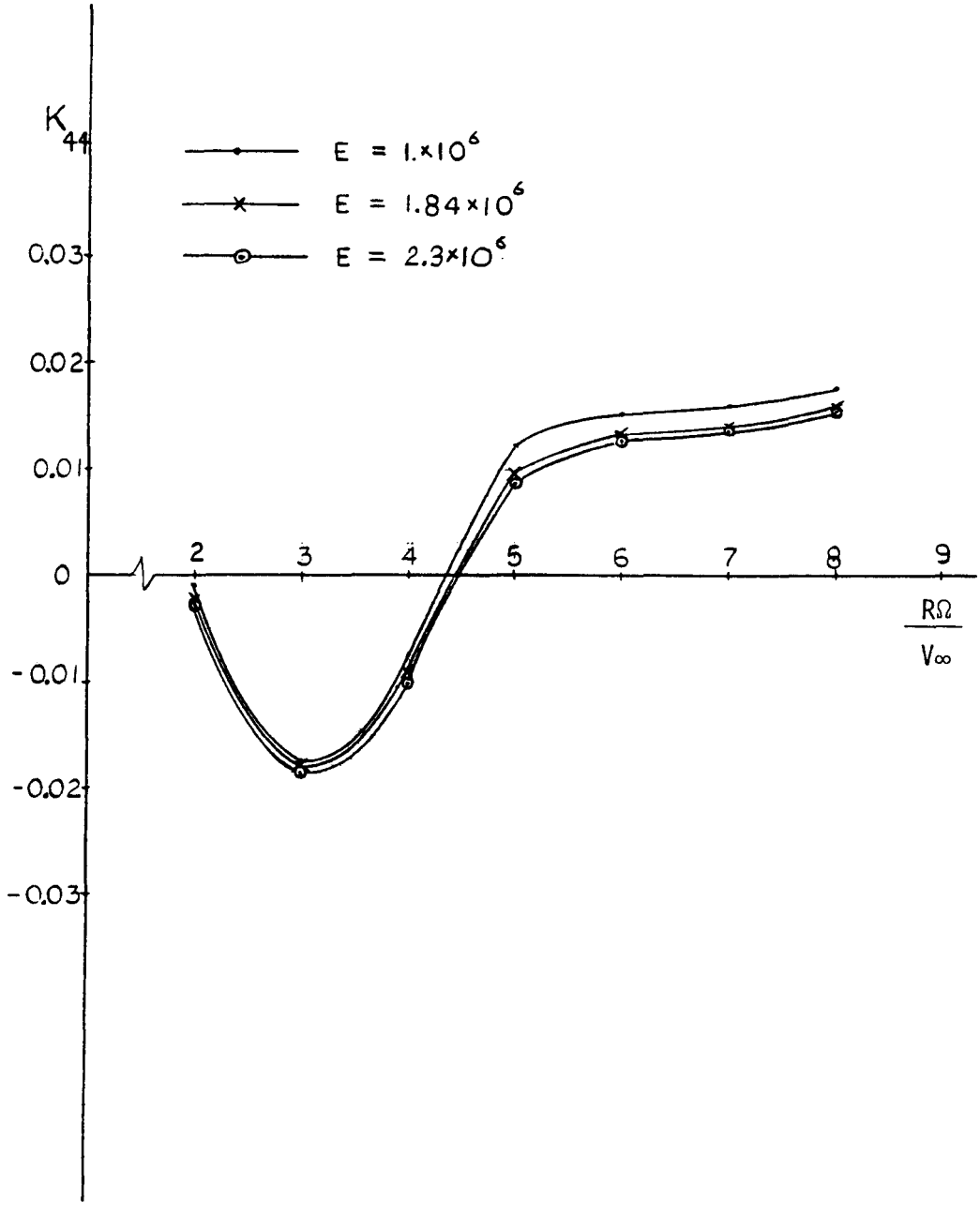

Figure 4.10 Effect of blade stiffness on rotor yaw stiffness coefficient

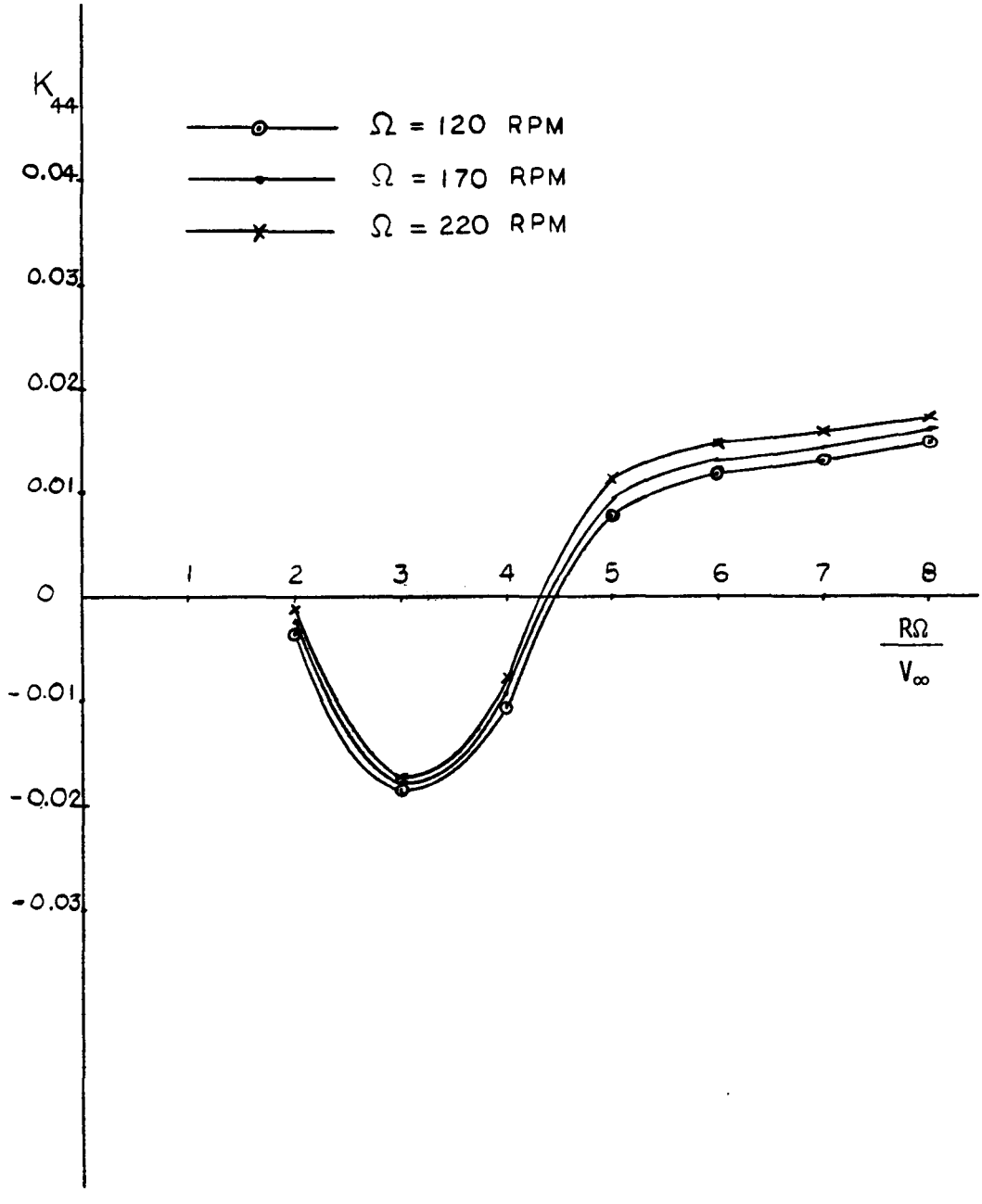

Figure 4.11 Effect of rotor speed on the rotor yaw stiffness coefficient

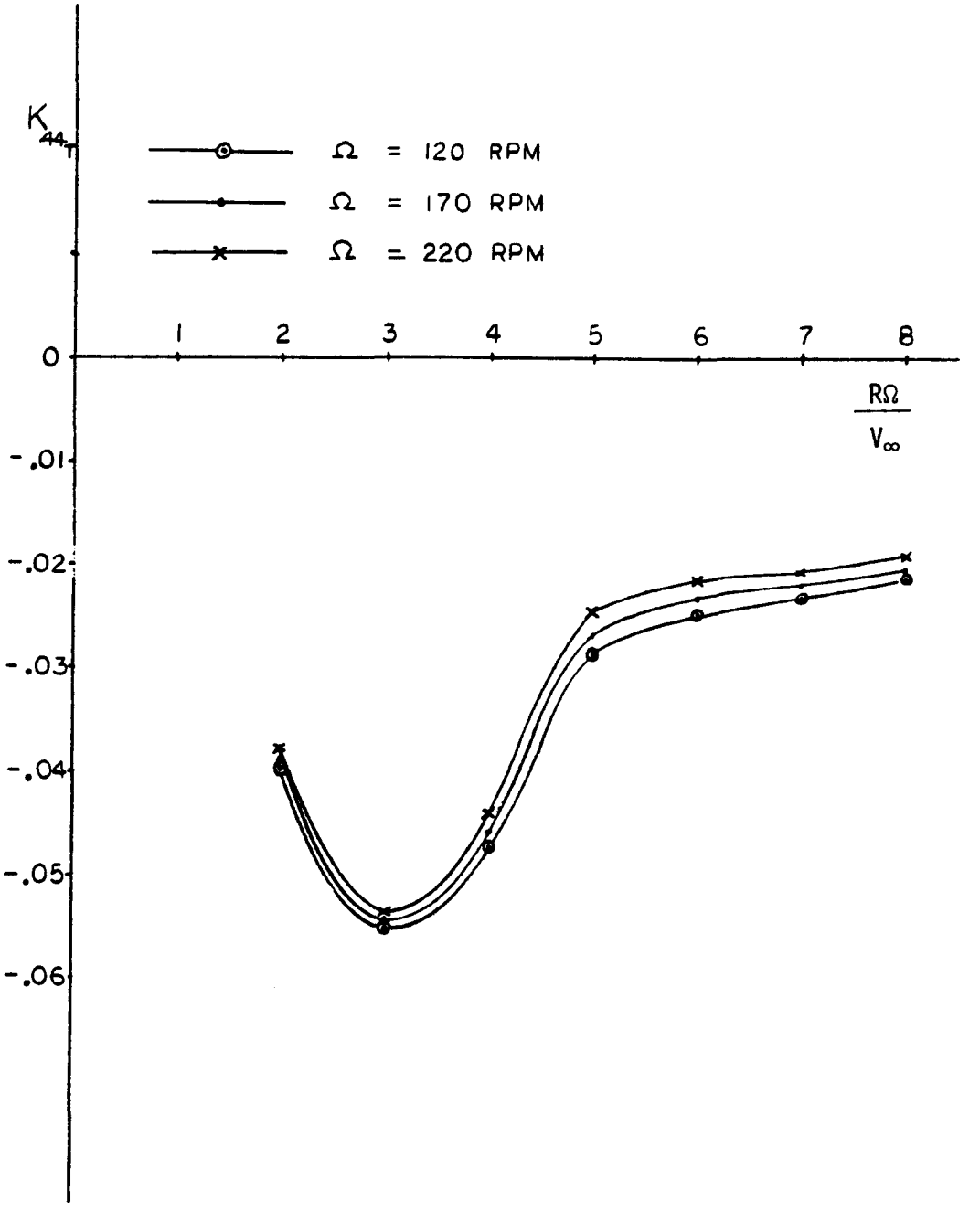

Figure 4.12 Effect of rotor speed on the system yaw stiffness coefficient

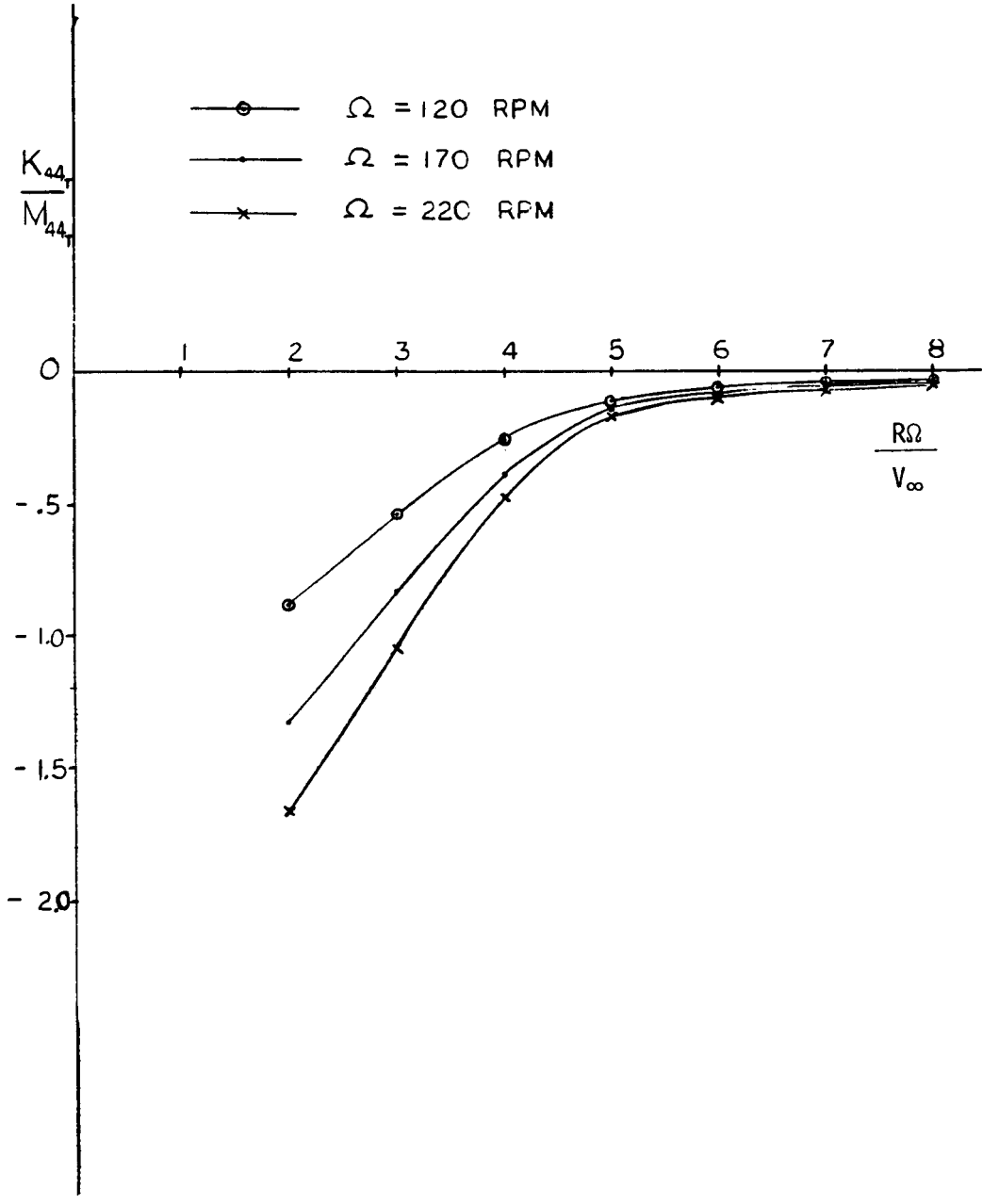

Figure 4.13 Effect of rotor speed on $k_{44T}/\ m_{44T}$

coefficient. It does not necessarily mean, however, that the smaller value of the stiffness coefficient leads to improved stability, especially when the mass coefficient is changed significantly with the speed.

Shear Center Position

The shear center position of the blade cross-section is assumed to be a constant value of the blade chord. The elastic axis will be a straight line parallel to the trailing edge of the turbine blade. The shear center position is varied to see the effect on the stiffness coefficient in yaw. The rotor stiffness coefficients in yaw with shear center positions at 10%, 25%, 50%, and 75% of the blade chord, measured from the leading edge of the turbine blade, are shown in Figure 4.14. The rotor stiffness coefficients are increased by moving the shear center closer to the trailing edge. But when we add the nacelle effect, the system is still unstable. This is shown in Figure 4.15.

The Distance From the Rotor to the Nacelle Yaw Axis

Figure 4.16 shows the rotor stiffness coefficient in the yaw equation for different values of ℓ: the distance from the rotor to the nacelle yaw axis. For $\ell/R = 0.1$, the stiffness coefficient values are positive for all of the tip speed ratios considered. Unfortunately, the nacelle stiffness coefficient is also changed by the change of ℓ. The curves of the total system (nacelle + rotor) stiffness coefficient are shown in Figure 4.17. For $\ell/R = 0.1$ we yield the lowest values in the system stiffness coefficients. Increasing the value of ℓ/R also

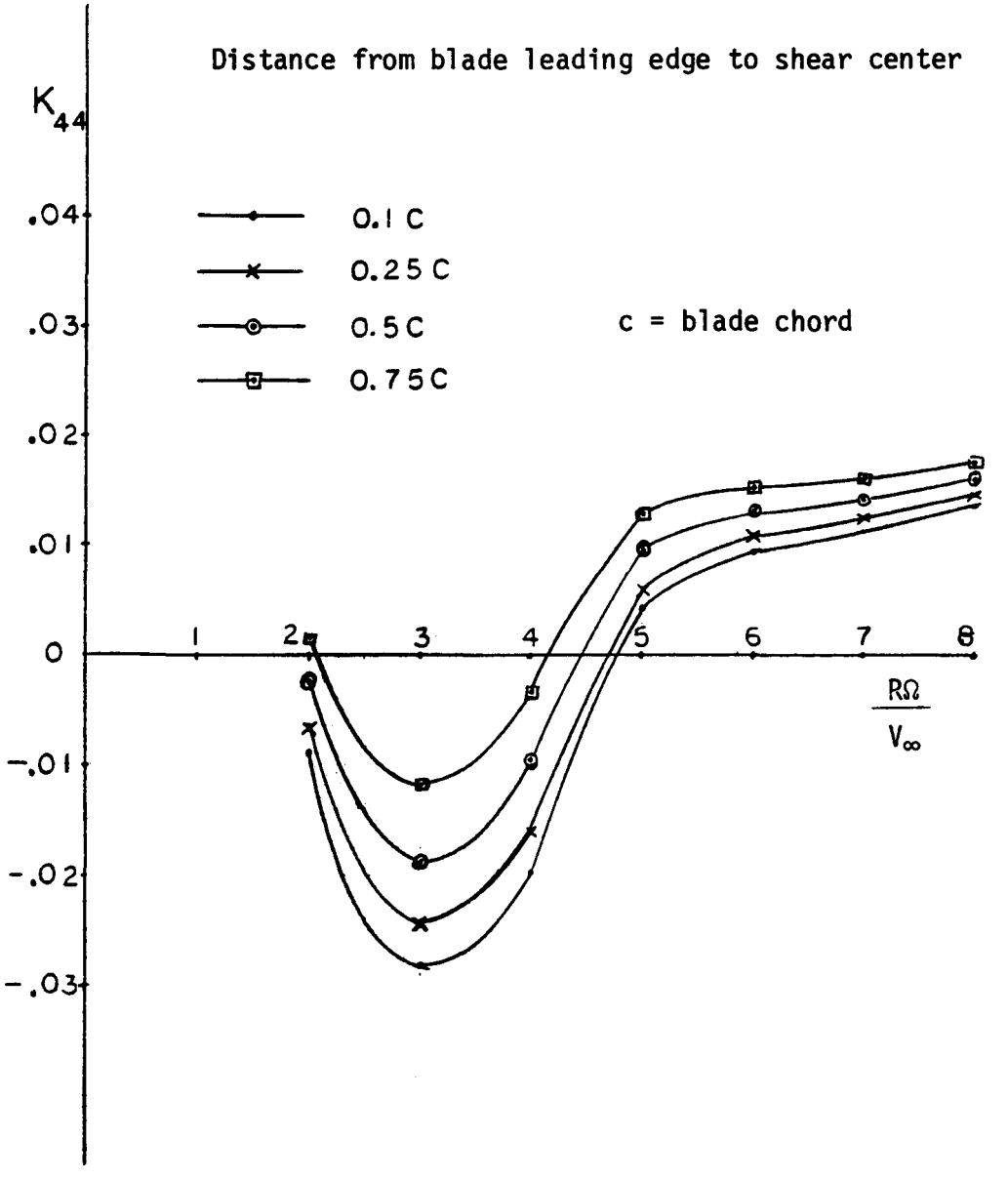

Figure 4.14 Effect of blade cross section's shear center position on rotor stiffness coefficient in yaw.

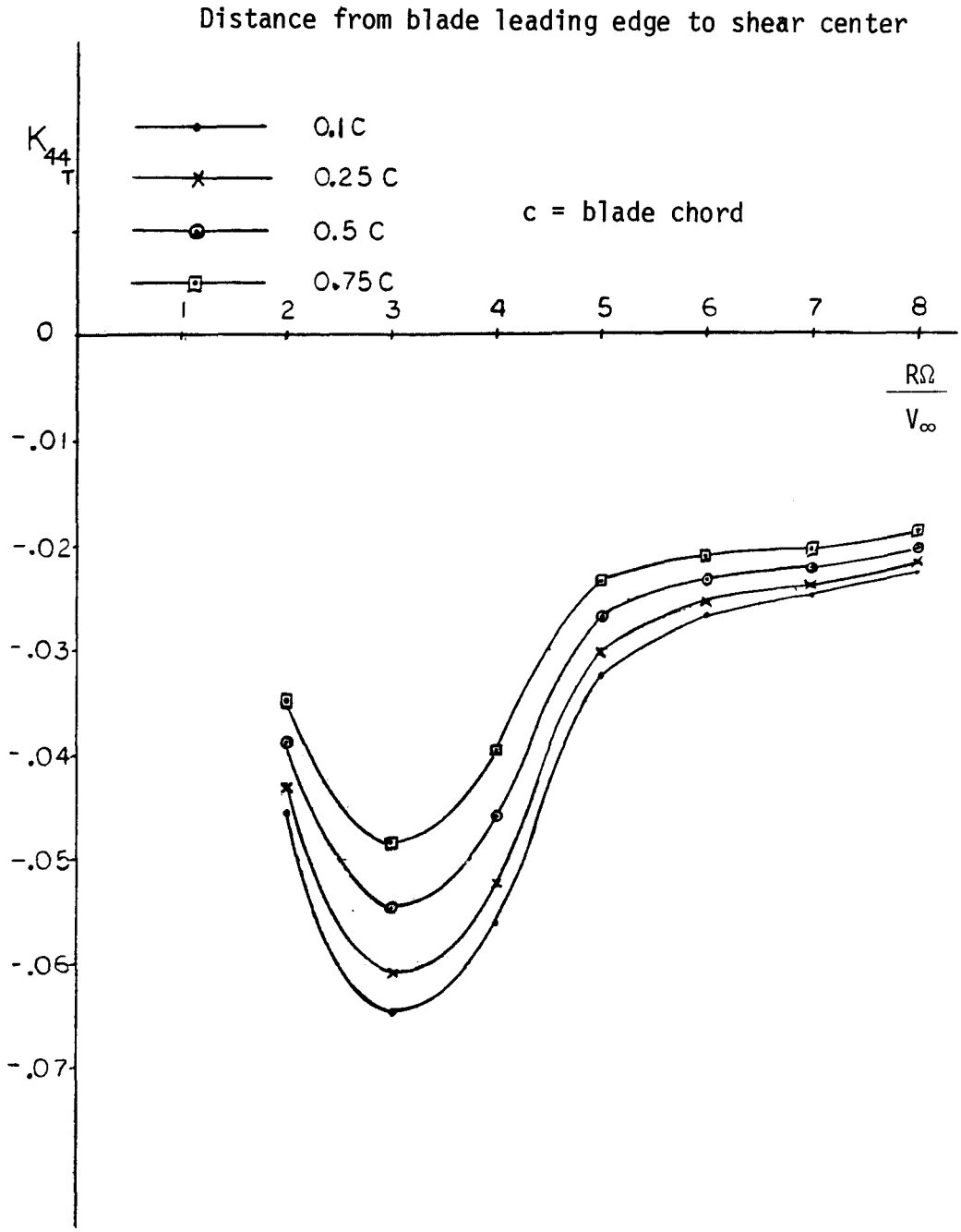

Figure 4.15 Effect of blade cross section's shear center position on the system yaw stiffness coefficient

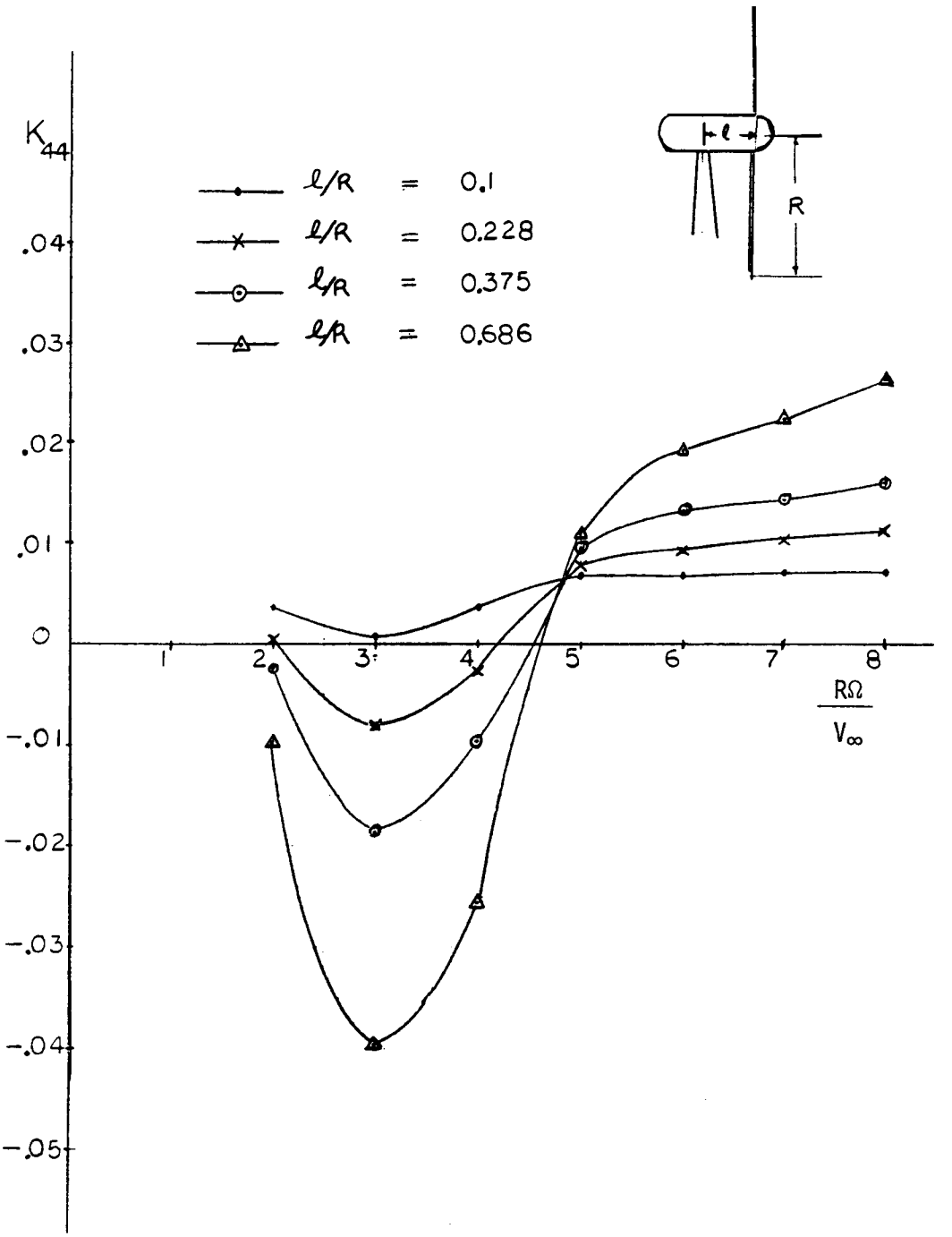

Figure 4.16 Effect of the distance from the nacelle yaw axis to rotor plane on rotor yaw stiffness coefficient

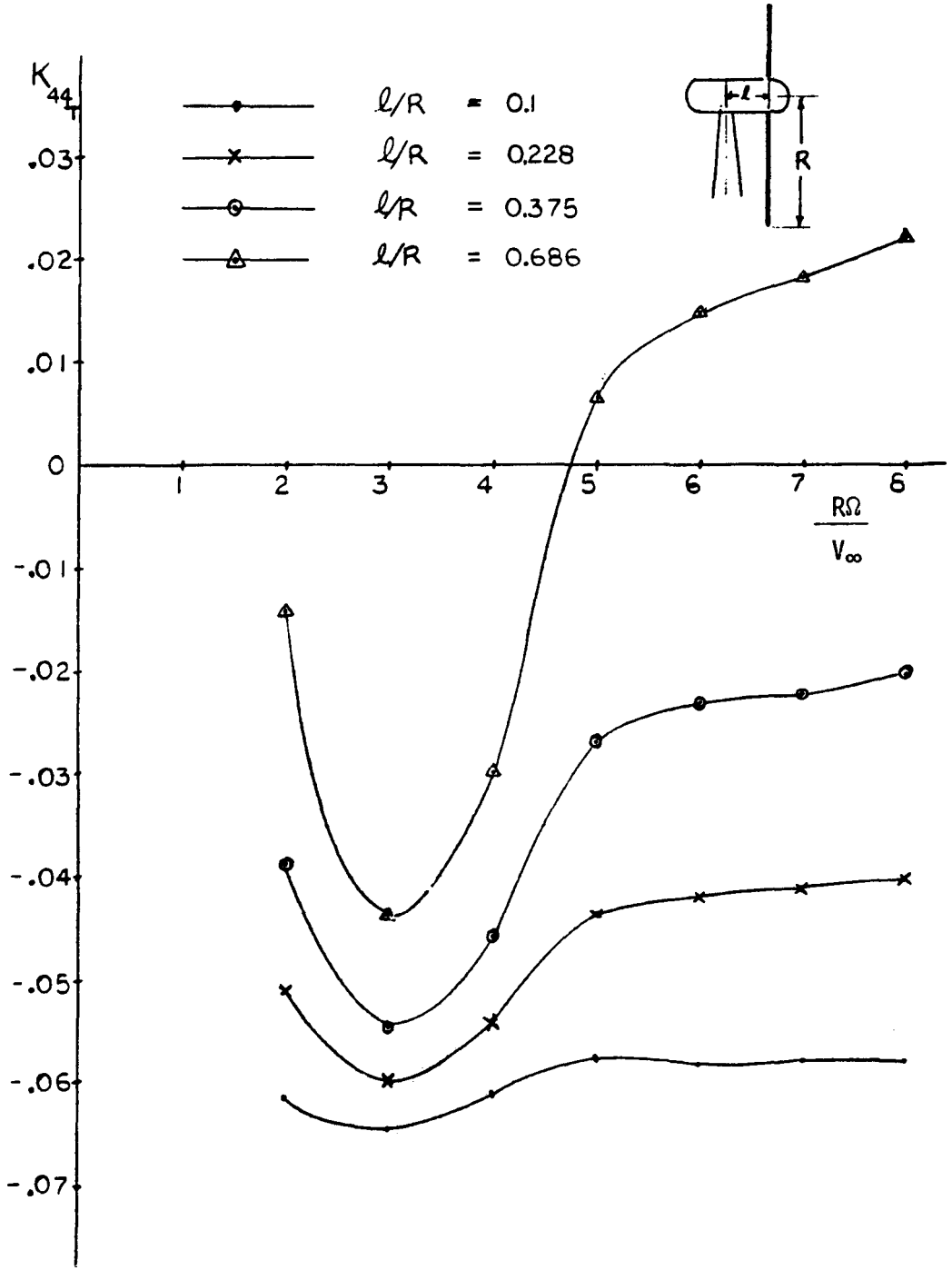

Figure 4.17 Effect of the distance from the nacelle yaw axis to rotor plane on the system yaw stiffness coefficient

increases the system stiffness coefficient. For ℓ/R = 0.686 (ℓ = 4.5 ft) the system is stable at tip speed ratio from 4.5 up. Increasing the distance from the rotor to the nacelle yaw axis improves the system stability, but the value of ℓ is limited by the nacelle geometry. The limitation of the value of ℓ will be discussed in the following section.

Nacelle

The nacelle plays an important role in the system stability because the largest negative value in the system stiffness coefficient comes from the nacelle. So reducing the negative value of the nacelle stiffness coefficient would mean improving the system stability.

Two parameters that affect the nacelle stiffness coefficient are distance from rotor to yaw axis and the configuration of the nacelle forebody part (radius of the forebody part).

By considering the expression of the nacelle stiffness coefficient (shown in Appendix III), we can calculate for the critical value of nacelle parameters.

The criteria of stability (positive value of nacelle stiffness coefficient) for this specific nacelle is obtained from the expression of stiffness coefficient by varying one parameter at a time. These values are given in Table 4.7. To insure the stability of the nacelle system, either parameter has to be greater than its critical value.

Table 4.7. The critical nacelle parameters for the Enertech 1500

$\ell_{critical}$	4.774 ft
$R_{n\ critical}$	7.788 ft

We can see that neither of these two parameters can be greater than its critical value because of the configuration of the nacelle. For the radius of forebody part, the critical value of this radius is greater than the radius of the rotor itself. It is impractical and inefficient to have a large nacelle. As ℓ approaches $\ell_{critical}$, the distance from the yaw axis to the rotor is limited by the space necessary to install the generator unit. Thus these two parameters can be varied only slightly to improve the stability.

Coning Angle

The Enertech 1500 has no built-in coning angle to relieve the blade root bending moment. However, the flexible wood blade will cone to an angle that puts the bending moment along the blade, due to the centrifugal force, in equilibrium with the moment created by aerodynamic forces. The effect of coning on the yaw system is investigated. Figure 4.18 shows the curves for the rotor stiffness coefficient for 10°, 0°, and -10° of the coning angle versus tip speed ratios. For the positive coning angle, the stiffness coefficient has positive values for all of the tip speed ratios considered. The negative coning angle makes the stiffness coefficient decrease. Figure 4.19 shows the system stiffness coefficient in yaw obtained by adding the nacelle effect to the rotor system. We can see that for a positive coning angle, the system stability is improved significantly. The negative coning angle effect on the system is to destabilize the system.

So in conclusion, the parameter that the system stiffness coefficient is most sensitive to is the coning angle. Increasing positive coning angle improves the system stability.

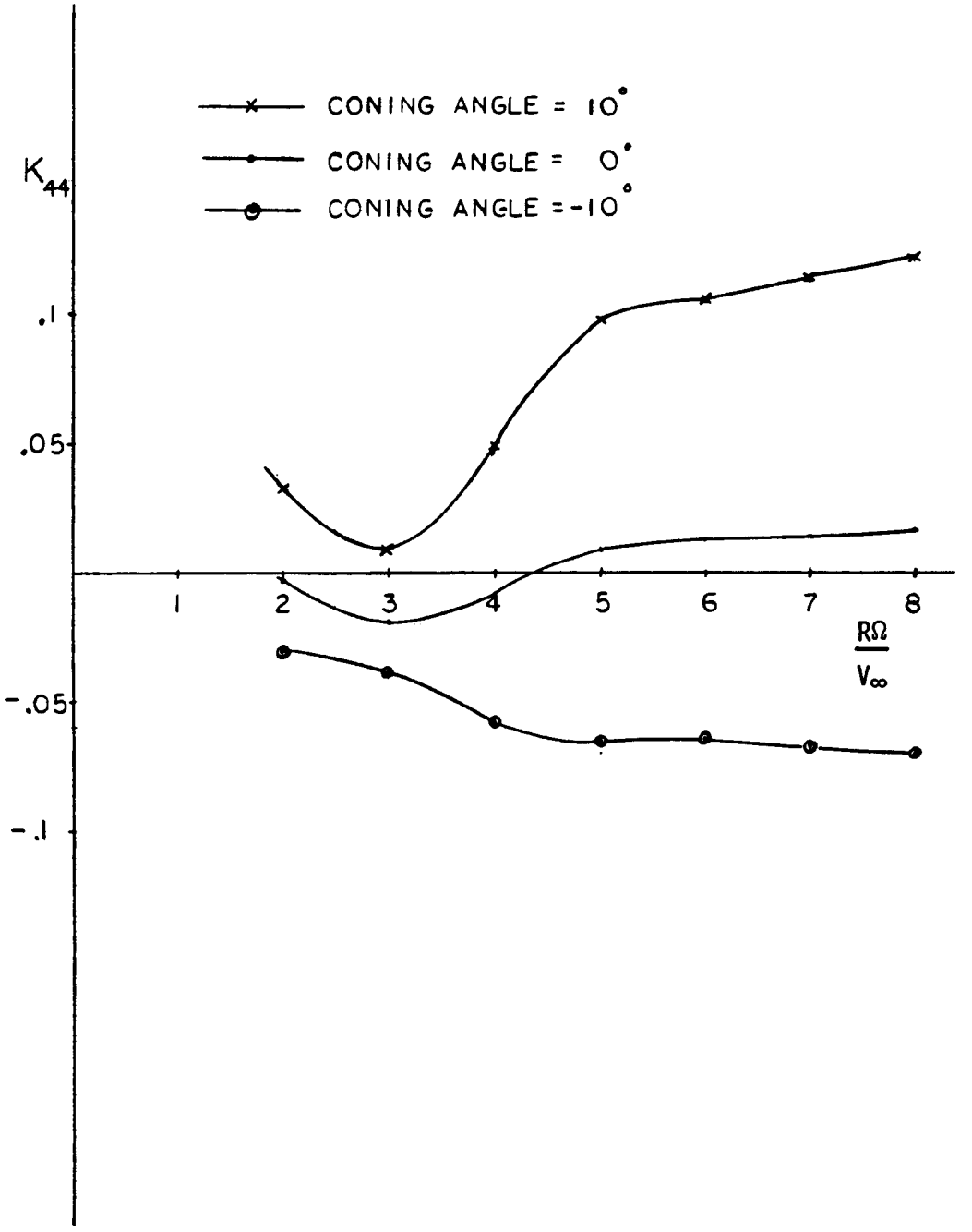

Figure 4.18 Effect of coning angle on rotor yaw stiffness coefficient

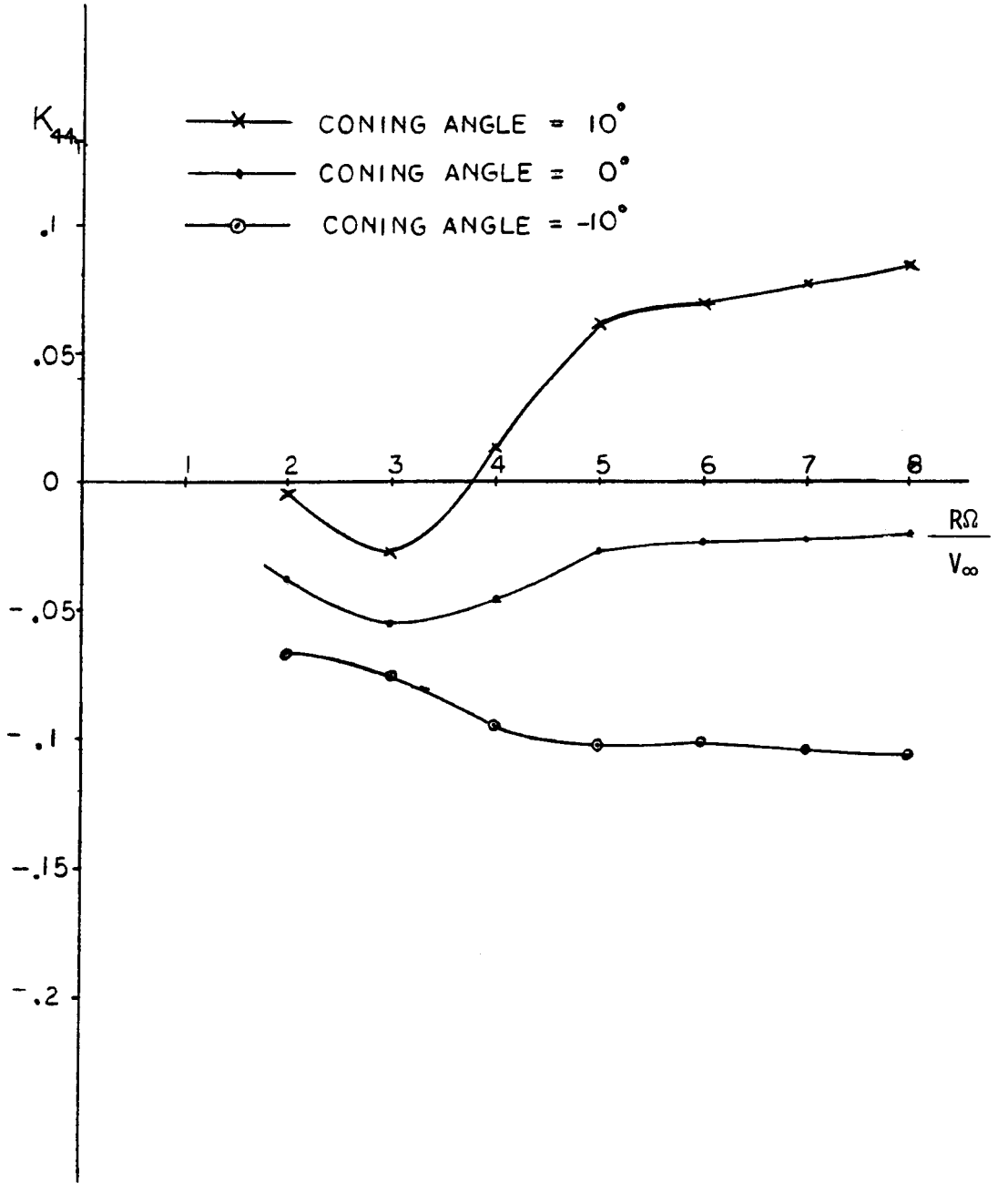

Figure 4.19 Effect of coning angle on system yaw stiffness coefficient.

5. CONCLUSIONS

Two areas of wind turbine research are studied in this report: cause of poor yaw tracking and system stability in yaw. The results are obtained for the Enertech 1500: a three-bladed horizontal axis wind turbine with free yaw.

The cause of the yaw problem is analyzed by studying the linearized equations of motion around the zero yaw angle. The study of the equation of motion in yaw shows that the yaw tracking error is primarily caused by tower shadow. Tower shadow is crudely modeled as a velocity deficit from the axial velocity value over a selected region of the rotor disk. The values of the width and velocity deficit of the tower shadow are arbitrarily chosen. Because of the poor yaw stability of the system (negative stiffness coefficient), due largely to the nacelle, the focus of the problem turns to the yaw forcing function. With the given values of velocity deficit and shadow width, the static yaw moment (yaw forcing function) is calculated and its sign change verifies the analysis.

The effect of the tower shadow model on the yaw forcing function is also studied. The results show that the tower shadow model with smaller value of velocity deficit yields the larger tip speed ratio that the forcing function's sign change takes place at. There is no effect on the cross-over point of the zero yaw forcing function due to the different values of shadow width.

In this study, the system is unstable in yaw due to the negative value of the stiffness coefficient. The nacelle is the primary cause of the system instability because of the magnitude of its negative value of

stiffness coefficient. So this study emphasizes the sign change in the system stiffness coefficient (yield positive value) as an indication of a stable system.

The sensitivity of the system stiffness coefficient to the selected input parameters is studied.

The stiffness coefficient is most sensitive to the coning angle parameter. Increasing the coning angle increases the rotor stiffness coefficient. Decreasing the coning angle (negative coning angle) decreases the rotor stiffness coefficient. With an appropriate coning angle value, the system is stable for a whole range of tip speed ratios.

The next parameter that the stiffness coefficient is sensitive to is the distance from the rotor to the yaw axis. Increasing the value of this distance will increase the value of the system stiffness coefficient. However, the value of this distance is limited by the nacelle configuration.

The system stiffness coefficient is not so sensitive to the following parameters: torsional stiffness, pitch angle, blade stiffness (modulus of elasticity), flapwise deflection, speed, and shear center position.

The stiffness coefficient is slightly increased by decreasing the pitch angle, decreasing the blade stiffness (increasing the flapwise deflection), increasing the speed, and moving the shear center position closer to the blade trailing edge. Because the changes in stiffness coefficient values due to these parameters are so small, they cannot stabilize the system in the presence of the nacelle.

Because of the linearized model, our results (for the Enertech 1500) will be valid for only a small region around the zero yaw angle

(tip speed ratios 2 to 5). The uncertainties introduced from the lack of aerodynamic input (lift and drag curves) associated with stall should be accounted for when the comparison between the data and analysis is made.

The characterization of wind turbine rotors with variable thickness blades by use of single section data (NACA 4415) will cause errors in predicted yaw behavior as well as predicted power output.

In order to obtain more accurate predictions of yaw behavior, accurate power models must be constructed.

In conclusion, the analysis gives the results accurate within the degree of uncertainty given.

REFERENCES

1. Ribner, H.S., "Propellers in Yaw," NACA Technical Report No. 820.
2. Miller, R.H., "On the Weathervaning of Wind Turbines," AIAA Journal of Energy, Vol. 3, No. 5, September-October 1979.
3. Fung, Y.C., An Introduction to the Theory of Aeroelasticity, John Wiley, 1955.
4. Meirovitch, L., Analytical Methods in Vibrations, MacMillan and Co., 1967.
5. Kane, Thomas R., Dynamics, Stanford University, 3rd Edition, 1978.
6. Hirschbein, M.S., "Dynamics and Control of Large Horizontal-Axis Axisymmetric Wind Turbines," Ph.D. Thesis, University of Delaware, 1979.
7. Jacobs, E.N., and A. Sherman, "Airfoil Section Characteristics as Affected by Variations of Reynolds Number," NACA TR 586, 1936.
8. Satrou, D. and M.H. Snyder, "Two-Dimensional Test of GA(w)-1 and GA(w)-2 Airfoils at Angles-of-Attack from 0 to 360 Degrees," WER-1, Wind Energy Laboratory, Wichita State University, Wichita, KS, 1977.
9. Wilson, R.E. and P.B.S. Lissaman, Applied Aerodynamics of Wind Power Machines, Oregon State University, May 1974.
10. Wilson, R.E., P.B.S. Lissaman and S.N. Walker, Aerodynamic Performance of Wind Turbines, Oregon State University, June 1976.
11. Wilson, R.E. and E.M. Patton, "Performance Prediction and Comparison with Test Results for Horizontal Axis Wind Turbines," Report under Subcontract No. PFN-13318W, prepared for Rockwell International Corporation, February 1982.

12. Prandtl, L., Gottinger Nachr., p. 193 Appendix, 1919.

13. Goldstein, S., "On the Vortex Theory of Screw Propellers," Proc. Royal Soc., A123, 440, 1929.

14. Glauert, H., "The Analysis of Experimental Results in the Windmill Brake and Vortex Ring States of an Airscrew," Reports and Memoranda, No. 1026 AE. 222, February 1926.

15. Wilson, R.E. and S.N. Walker, "A Fortran Program for the Determination of Performance, Loads, and Stability Derivatives of Wind Turbines," Oregon State University, 25 October 1974.

APPENDIX I

KINEMATICS

A four-degree-of-freedom wind turbine system is illustrated in Figure I.1. The degrees of freedom of the system are blade pitch deflection, blade flap, speed variation, and yaw angle.

In developing the mathematical model for the turbine system, we use assumed mode shapes and generalized coordinates to represent the dependent variables. By this method we can derive the governing equations in ordinary differential form rather than partial differential form. Each degree of freedom is expressed as the product of the displacement function (assumed mode shape) and the generalized coordinate.

These relations are given as:

$$\theta(r,t) = f_1(\frac{r}{R})q_1(t) \qquad \text{(blade pitch)} \qquad (1)$$

$$w(r,t) = R_S f_2(\frac{r}{R})(q_2(t) + q_s) \qquad \text{(blade flap)} \qquad (2)$$

$$\dot{x}(r,t) = f_3(\frac{r}{R})\dot{q}_3(t) \qquad \text{(speed variation)} \qquad (3)$$

$$\gamma(r,t) = f_4(\frac{r}{R})q_4(t) \qquad \text{(yaw angle)} \qquad (4)$$

where R_S is the distance from the tip of the blade to the hub of the rotor. The $q_i(t)$ terms are the generalized coordinates of the rotor system and the $f_i(\frac{r}{R})$ terms are the assumed mode shapes. The mode shapes are expressed as:

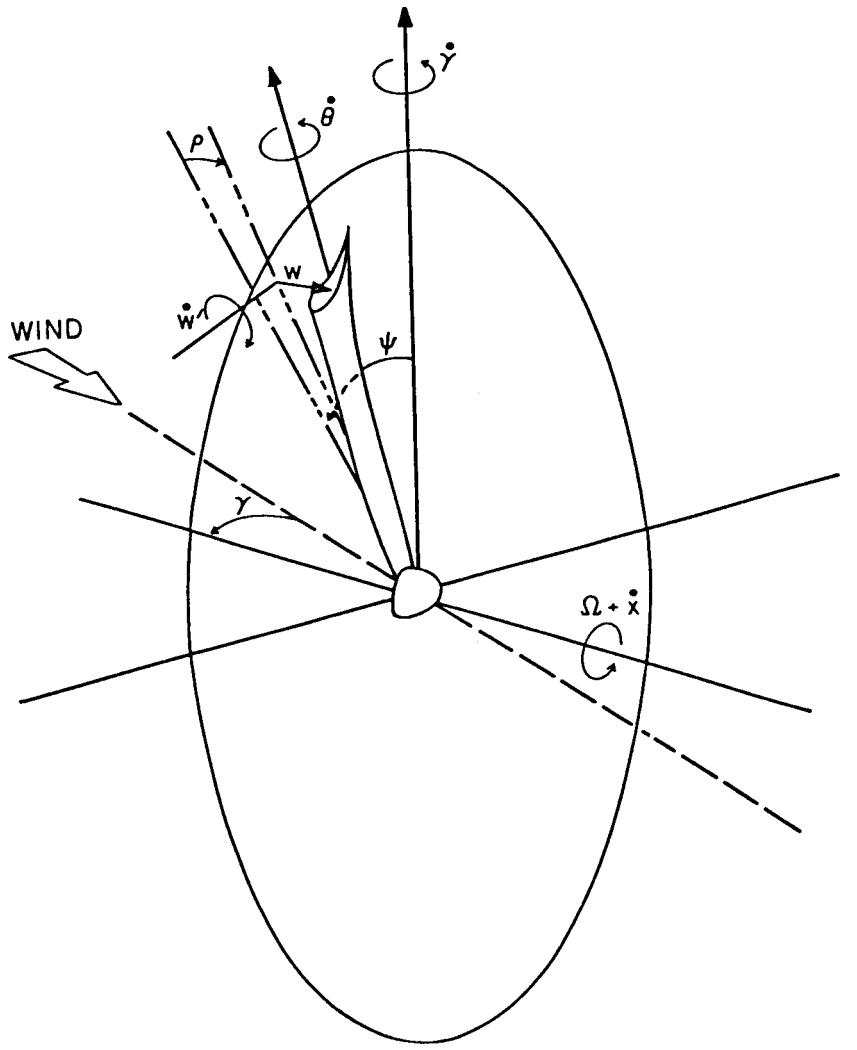

Figure I.1 Rotor system

$$f_1(\frac{r}{R}) = \frac{2r_S}{R_S} - (\frac{r_S}{R_S})^2 \tag{5}$$

$$f_2(\frac{r}{R}) = 6(\frac{r_S}{R_S})^2 - 4(\frac{r_S}{R_S})^3 + (\frac{r_S}{R_S})^4 \tag{6}$$

$$f_3(\frac{r}{R}) = 1 \tag{7}$$

$$f_4(\frac{r}{R}) = 1 \tag{8}$$

Here r_S is the radial distance from the local point on the blade to the blade root.

The mode shape in Eq. (5) is for a uniform cantilever beam in static equilibrium with applied torque at the open end. The mode shape in Eq. (6) is for a uniform cantilever beam in static equilibrium with uniform forces applied on the beam. The mode shapes in Eqs. (7) and (8) are those of a rigid body.

Having defined the degrees of freedom in terms of generalized coordinates, we are now ready to develop the kinematics of the rotor system.

The absolute motion of the turbine blade is determined by the motion of blade deflection relative to the hub, the motion due to rotor rotation, plus the motion of the nacelle and tower. Since in this analysis no movement of the tower is allowed, we consider the reference frame fixed to the tower as the inertial reference frame. Consider the motion of a point on the blade whose absolute position is represented by a series of relative position vectors. A series of coordinate systems is used to describe these vectors. Let the coordinate system X,Y,Z be located on the top of the tower. The coordinate system x,y,z is fixed

on the nacelle and its origin is at the same point as the coordinate system X,Y,Z. The coordinate system $\hat{x},\hat{y},\hat{z}$ is the same as the coordinate system x,y,z except its origin is moved to the center of the rotor. The coordinate system $\underline{x},\underline{y},\underline{z}$ is obtained by rotating the coordinate system $\hat{x},\hat{y},\hat{z}$ by the magnitude of angle ψ (where $\psi = \Omega t + \chi$). The coordinate system x_ρ, y_ρ, z_ρ is obtained by rotating the coordinate system $\underline{x},\underline{y},\underline{z}$ around the $\underline{y}$ axis by the angle ρ. Then, at position r on the blade, the coordinate system $x_\beta, y_\beta, z_\beta$ represents the effect of the pretwist angle, β. The coordinate system $x_\theta, y_\theta, z_\theta$ is obtained by moving the origin of the coordinate system $x_\beta, y_\beta, z_\beta$ in the z_β direction over the distance "w" and rotating it around the y_β axis by the angle w' $(\partial w/\partial r)$. Finally, the coordinate system x_1, x_2, x_3 is located on the shear center of the blade cross section and differs from the coordinates $x_\theta, y_\theta, z_\theta$ by the amount of the pitch angle θ.

These coordinate systems are shown in order from the inertial reference frame to the final reference frame that is fixed on a point on the blade in Figures I.2, I.3, and I.4.

A series of transformation matrices is used to transform from one coordinate system to the others. These transformation matrices are shown in Figure I.5.

Another variable that we will deal with is the radial displacement of the blade. This displacement occurs during the blade deflection when the assumption of an inextensible blade is made. This radial displacement is defined as

$$u_c(r) = -\frac{1}{2}\int_{R_H}^{R} \left(\frac{dv_c}{dr}\right)^2 dr \qquad (9)$$

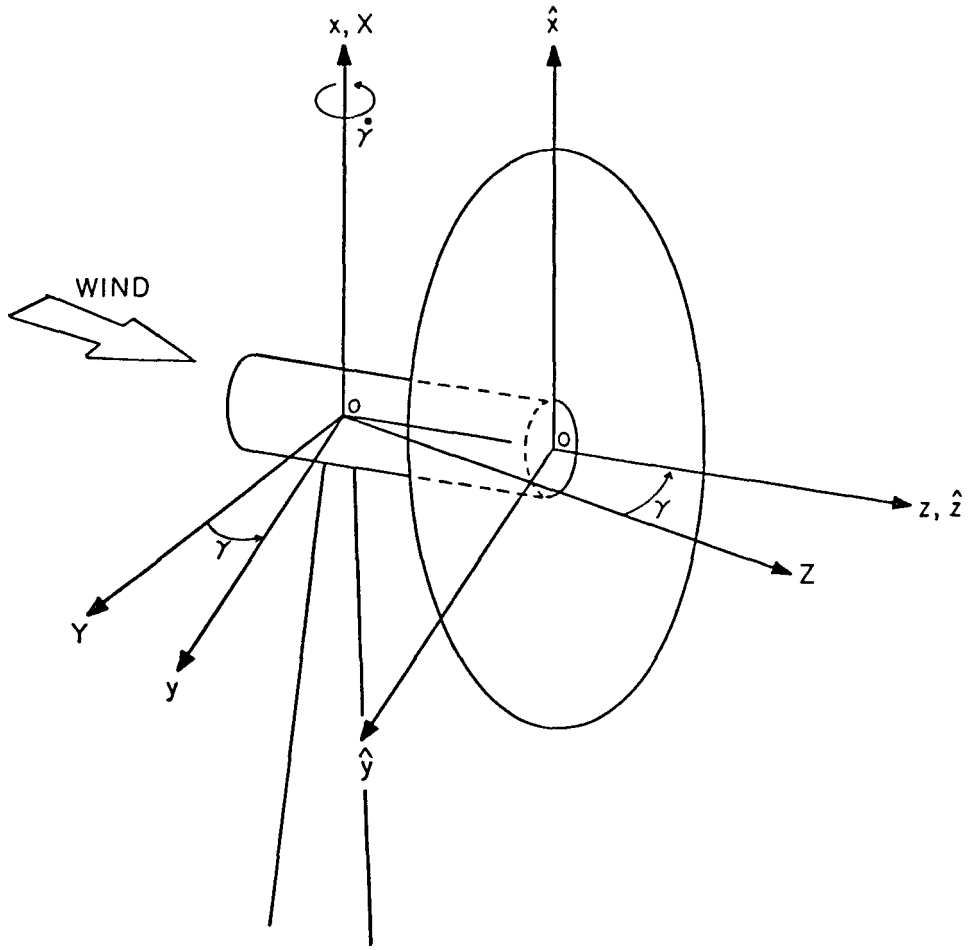

Figure I.2 The coordinate system XYZ, xyz, and $\hat{x}\hat{y}\hat{z}$

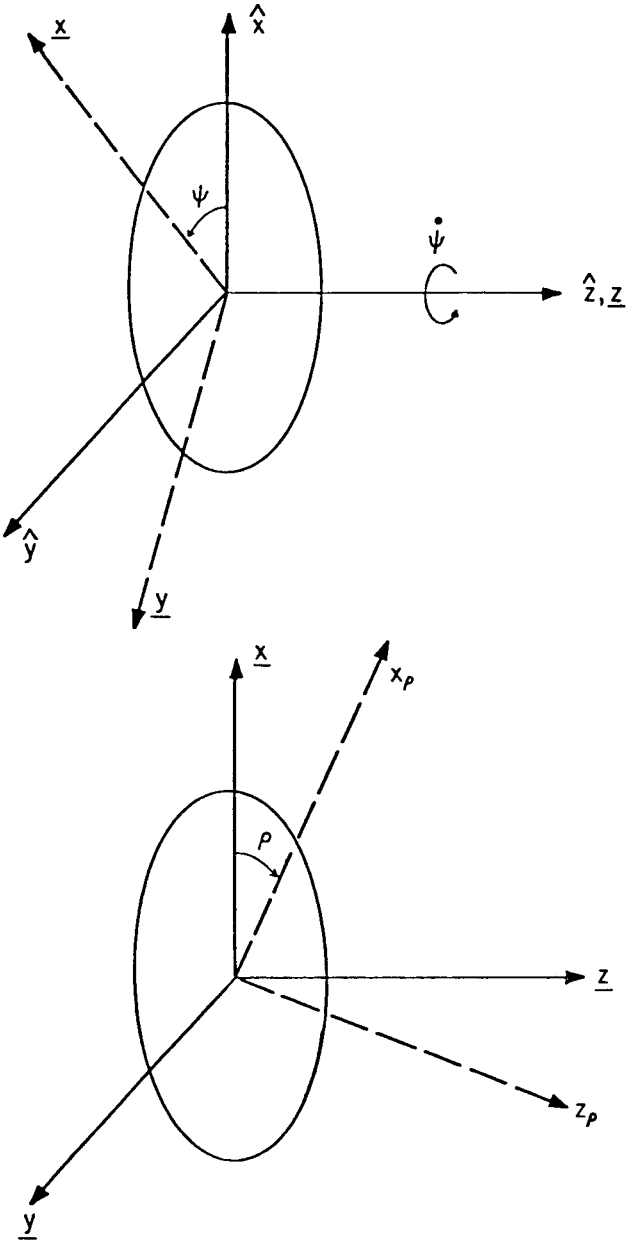

Figure I.3 The coordinate systems xyz, xyz, and $x_\rho y_\rho z_\rho$

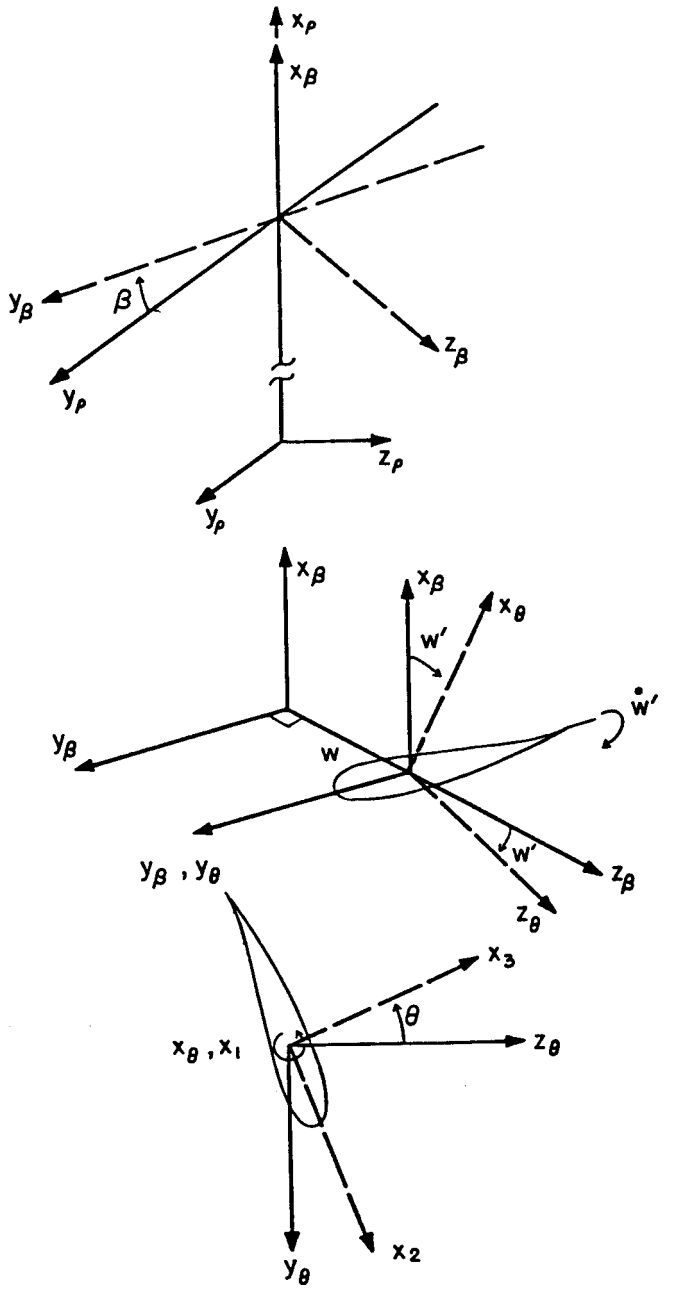

Figure I.4 The coordinate systems $x_\beta y_\beta z_\beta$, $x_\theta y_\theta z_\theta$, and $x_1 y_1 z_1$

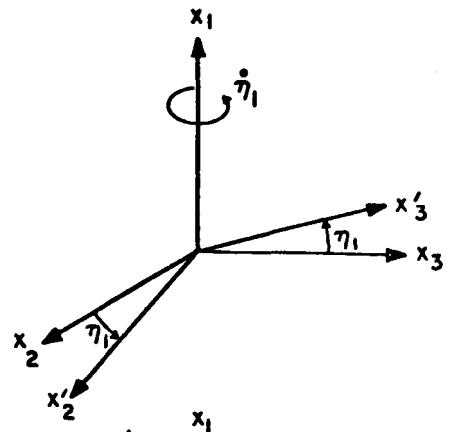

$$(x) = [T]\,(x')$$

$$[T] = \begin{pmatrix} 1 & 0 & 0 \\ 0 & \cos\eta_1 & -\sin\eta_1 \\ 0 & \sin\eta_1 & \cos\eta_1 \end{pmatrix}$$

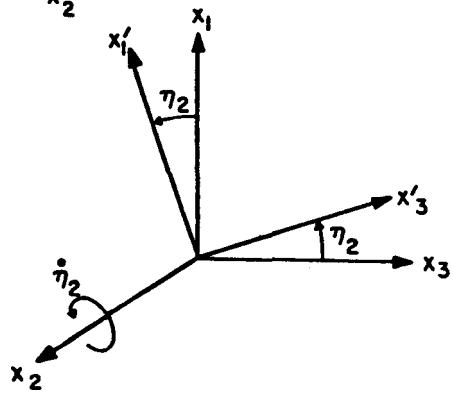

$$(x) = [T]\,(x')$$

$$[T] = \begin{pmatrix} \cos\eta_2 & 0 & \sin\eta_2 \\ 0 & 1 & 0 \\ -\sin\eta_2 & 0 & \cos\eta_2 \end{pmatrix}$$

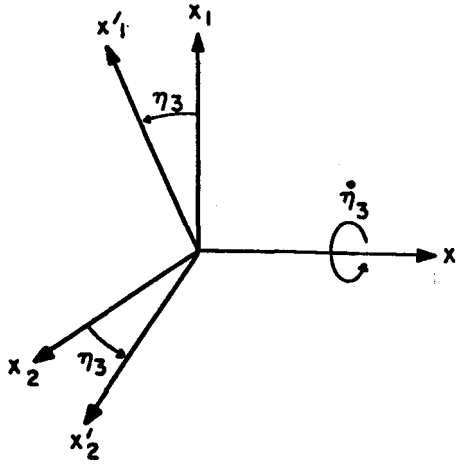

$$(x) = [T]\,(x')$$

$$[T] = \begin{pmatrix} \cos\eta_3 & -\sin\eta_3 & 0 \\ \sin\eta_3 & \cos\eta_3 & 0 \\ 0 & 0 & 1 \end{pmatrix}$$

Figure I.5 Transformation matrices

where v_c is the deflection of the blade in the direction that is perpendicular to the axial line (flapwise direction).

The velocity of a point on the blade is found by using the kinematic relation [5]

$$ {}_R\vec{V}_c = {}_\alpha\vec{V}_c + {}_R\vec{\omega}_\alpha \times \vec{r} \tag{10} $$

where ${}_R\vec{V}_c$ is the velocity of point c in a reference frame R.

${}_\alpha\vec{V}_c$ is the velocity of point c in a reference frame α.

${}_R\vec{\omega}_\alpha$ is the angular velocity of the body that the reference frame α is fixed to, observed from the reference frame R.

$\vec{r}$ is the position vector of point c.

For the angular velocity, we have

$$ {}_R\vec{\omega}_\alpha = {}_R\vec{\omega}_B + {}_B\vec{\omega}_\alpha \tag{11} $$

where ${}_\eta\vec{\omega}_\xi$ is the angular velocity of the body that a reference frame ξ is fixed to, observed from a reference frame η.

The absolute motion of a point on the blade can be found by using the transformation matrices and Eqs. (10) and (11).

The blade velocity and blade angular velocity measured at the center of mass of the blade cross section are:

$$ \vec{V}_c = V_{x\rho}\vec{n}_{x\rho} + V_{y\rho}\vec{n}_{y\rho} + V_{z\rho}\vec{n}_{z\rho} \tag{12} $$

where

$$V_{\eta\rho} = V_{\eta\ell} + V_{\eta r} + V_{\eta w} + V_{\eta e} \qquad \eta = x,y,z$$

and

$$V_{x\ell} = -\ell\dot{\gamma}\cos\rho\sin\psi$$

$$V_{xr} = \dot{u}_c$$

$$V_{xw} = -w\dot{\psi}\sin\beta\cos\rho + w\dot{\gamma}(\sin\rho\sin\beta\cos\psi - \cos\beta\sin\psi)$$

$$V_{xe} = \begin{cases} -e\dot{\theta}\sin w'\cos\theta - e\dot{\psi}\cos\rho(\cos\beta\cos\theta + \cos w'\sin\theta\sin\beta) \\ +e\dot{\gamma}(\sin\beta\cos\theta - \cos\beta\cos w'\sin\theta)\sin\psi \\ +e\dot{\gamma}\sin\rho(\cos\beta\cos\theta + \cos w'\sin\theta\sin\beta)\cos\psi \end{cases}$$

$$V_{y\ell} = -\ell\dot{\gamma}\cos\psi$$

$$V_{yr} = (r + u_c)\dot{\psi}\cos\rho - (r + u_c)\dot{\gamma}\cos\psi\sin\rho$$

$$V_{yw} = \dot{w}\sin\beta - w\dot{\psi}\sin\rho\cos\beta - w\dot{\gamma}\cos\rho\cos\beta\cos\psi$$

$$V_{ye} = \begin{cases} e\dot{\theta}\cos\theta\cos w'\sin\beta - e\dot{w}'\sin\theta\sin w'\sin\beta \\ +e\dot{\psi}[\sin\rho(\sin\beta\cos\theta - \cos\beta\cos w'\sin\theta) - \cos\rho\sin w'\sin\theta] \\ +e\dot{\gamma}\cos\psi[\cos\rho(\sin\beta\cos\theta - \cos\beta\cos w'\sin\theta) + \sin\rho\sin w'\sin\theta] \end{cases}$$

$$V_{z\ell} = \ell\dot{\gamma}\sin\rho\sin\psi$$

$$V_{zr} = (r + u_c)\dot{\gamma}\sin\psi$$

$$V_{zw} = \dot{w}\cos\beta + w\dot{\psi}\sin\beta\sin\rho + w\dot{\gamma}\cos\rho\sin\beta\cos\psi$$

$$V_{ze} = \begin{cases} +e\dot{\theta}\cos\theta\cos w'\sin\beta - e\dot{w}'\sin\theta\sin w'\cos\beta \\ +e\dot{\psi}\sin\rho(\cos\beta\cos\theta + \cos w'\sin\theta\sin\beta) \\ +e\dot{\gamma}\cos\rho(\cos\beta\cos\theta + \cos w'\sin\theta\sin\beta)\cos\psi \\ -e\dot{\gamma}\cos\rho\sin w'\sin\theta\sin\psi \end{cases}$$

where

e = distance from mass center to the shear center of the blade cross section.

ℓ = distance from the rotor plane to the nacelle's yaw axis.

$$w' = \frac{\partial w}{\partial r}$$

$$\dot{w} = \frac{\partial w}{\partial t}$$

$$\dot{w}' = \frac{\partial}{\partial t}\left(\frac{\partial w}{\partial r}\right)$$

$$\dot{\psi} = (\Omega + \dot{\chi})$$

$$\vec{\omega} = \omega_1 \vec{n}_1 + \omega_2 \vec{n}_2 + \omega_3 \vec{n}_3 \qquad (13)$$

where

$$\omega_i = \omega_{\theta i} + \omega_{wi} + \omega_{\psi i} + \omega_{\gamma i} \qquad i = 1,2,3$$

and

$$\omega_{\theta 1} = \dot{\theta}$$

$$\omega_{w1} = 0$$

$$\omega_{\psi 1} = \dot{\psi}(\sin\rho\cos w' + \cos\rho\sin w'\cos\beta)$$

$$\omega_{\gamma 1} = \dot{\gamma}[(\cos\rho\cos w' - \sin\rho\sin w'\cos\beta)\cos\psi - \sin w'\sin\beta\sin\psi]$$

$$\omega_{\theta 2} = 0$$

$$\omega_{w2} = -\dot{w}'\cos\theta$$

$$\omega_{\psi 2} = -\dot{\psi}(\sin\rho\sin w'\sin\theta + \cos\rho\sin\beta\cos\theta - \cos\rho\cos w'\sin\theta\cos\beta)$$

$$\omega_{\gamma 2} = -\dot{\gamma}(\cos\rho\sin w'\sin\theta - \sin\rho\sin\beta\cos\theta + \sin\rho\cos w'\sin\theta\cos\beta)\cos\psi$$
$$- \dot{\gamma}[(\cos\beta\cos\theta + \cos w'\sin\theta\sin\beta)\sin\psi]$$

$$\omega_{\theta 3} = 0$$

$$\omega_{w3} = \dot{w}'\sin\theta$$

$$\omega_{\psi 3} = -\dot{\psi}(\sin\rho\sin w'\cos\theta - \cos\rho\sin\beta\sin\theta - \cos\rho\cos w'\cos\theta\cos\beta)$$

$$\omega_{\dot{\gamma} 3} = -\dot{\gamma}(\cos\rho\sin w'\cos\theta + \sin\rho\sin\beta\sin\theta + \sin\rho\cos w'\cos\theta\cos\beta)\cos\psi$$

$$+ \dot{\gamma}(\cos\beta\sin\theta - \cos w'\cos\theta\sin\beta)\sin\psi$$

APPENDIX II

ROTOR AERODYNAMICS

II.1 Relative Velocity

The relative velocity that the blade element experiences at the rotor is defined as the vector sum of the blade element velocity at mid-chord and the wind velocity at the rotor.

$$\vec{W} = \vec{V}_w - \vec{V}_B \tag{1}$$

Here $\vec{V}_w$ is the wind velocity at the rotor and $\vec{V}_B$ is the blade element velocity at mid-chord, it does not include pitch velocity ($\dot{\theta}$). The wind velocity at the rotor is given by

$$\vec{V}_w = V_w\vec{n}_z - aV_w\vec{n}_z \tag{2}$$

where "a" is the axial induction factor. The development of the axial induction factor will be explained in a later section.

In the strip theory method (2-D assumption), the relative velocity in the spanwise direction does not produce lift force or drag force. The velocity to be considered in evaluation of the aerodynamic forces and moments is the relative velocity in the plane of the blade cross section. Thus the relative velocity is expressed as

$$\vec{W}_e = \{(\vec{V}_w - \vec{V}_B)\cdot\vec{n}_{y\theta}\}\vec{n}_{y\theta} + \{(\vec{V}_w - \vec{V}_B)\cdot\vec{n}_{z\theta}\}\vec{n}_{z\theta} \tag{3}$$

By using the unit vectors $\vec{e}_n$ and $\vec{e}_t$, we obtain

$$\vec{W}_e = W_n\vec{e}_n - W_t\vec{e}_t \tag{4}$$

where

$$W_n = (\vec{V}_w - \vec{V}_B)\cdot\vec{n}_{z\theta} \tag{5}$$

$$W_t = -(\vec{V}_w - \vec{V}_B)\cdot\vec{n}_{y\theta} \tag{6}$$

$$\vec{e}_n = \vec{n}_{z\theta}$$

$$\vec{e}_t = \vec{n}_{y\theta}$$

The expression for $\vec{V}_B$ can be obtained by following the same procedure used in Appendix I.

Substituting the value of $\vec{V}_B$ and $\vec{V}_w$ into Eqs. (5) and (6) we obtain the normal and tangential relative velocities as

$$W_n = V_{wn} + V_{Bn}$$

$$W_t = V_{wt} + V_{Bt}$$

$$V_{wn} = \begin{cases} - V_\infty(\cos\gamma - a)(\sin\rho\sin w' - \cos\rho\cos w'\cos\beta) \\ - V_\infty\sin\gamma[(\cos\rho\sin w' + \sin\rho\cos w'\cos\beta)\sin\psi - \cos w'\sin\beta\cos\psi] \end{cases}$$

$$V_{Bn} = \begin{cases} - \ell\dot{\gamma}[(\sin\rho\cos\beta\cos w' + \sin w'\cos\rho)\sin\psi - \sin\beta\cos w'\cos\psi] \\ + \dot{u}_d\sin w' - (r + u_d)\dot{\psi}\cos w'\cos\rho\sin\beta \\ - (r + u_d)\dot{\gamma}(\cos\beta\cos w'\sin\psi - \sin\rho\sin\beta\cos w'\cos\psi) \\ - \dot{w}\cos w' - w\dot{\psi}\sin w'\cos\rho\sin\beta \\ - w\dot{\gamma}(\sin w'\sin\rho\sin\beta\cos\psi - \sin w'\cos\beta\sin\psi) \\ + e_3\dot{\psi}\cos\theta(\sin\rho\cos w' + \cos\rho\sin w'\cos\beta) \\ + e_3\dot{\gamma}\cos\theta[(\cos\rho\cos w' - \sin\rho\sin w'\cos\beta)\cos\psi - \sin w'\sin\beta\sin\psi] \end{cases}$$

$$V_{wt} = \{- V_\infty(\cos\gamma - a)\cos\rho\sin\beta - V_\infty\sin\gamma(\sin\rho\sin\beta\sin\psi + \cos\beta\cos\psi)\}$$

$$V_{Bt} = \begin{cases} - \ell\dot{\gamma}(\cos\beta\cos\psi + \sin\rho\sin\beta\sin\psi) \\ + (r + u_d)\dot{\psi}\cos\rho\cos\beta - (r + u_d)\dot{\gamma}(\sin\beta\sin\psi + \sin\rho\cos\beta\cos\psi) \\ - w\dot{\psi}\sin\rho - w\dot{\gamma}\cos\rho\cos\psi \\ + e_3\dot{\psi}\sin\theta(\sin\rho\cos w' + \cos\rho\sin w'\cos\beta) \\ + e_3\dot{\gamma}\sin\theta[(\cos\rho\cos w' - \sin\rho\sin w'\cos\beta)\cos\psi - \sin w'\sin\beta\sin\psi] \end{cases}$$

where e_3 is the distance from the mid-chord to the shear center of the blade cross section.

The velocity diagram of the relative velocity at the blade cross section is shown in Figure II.1.1.

II.2 Aerodynamic Forces and Moments

Figure II.1.1 shows a blade profile section at radius r with the relevant velocities and forces. The air flow gives rise to a lift force L and a drag force D whose resultant can be resolved into components of normal force dF_n and tangential force dF_t.

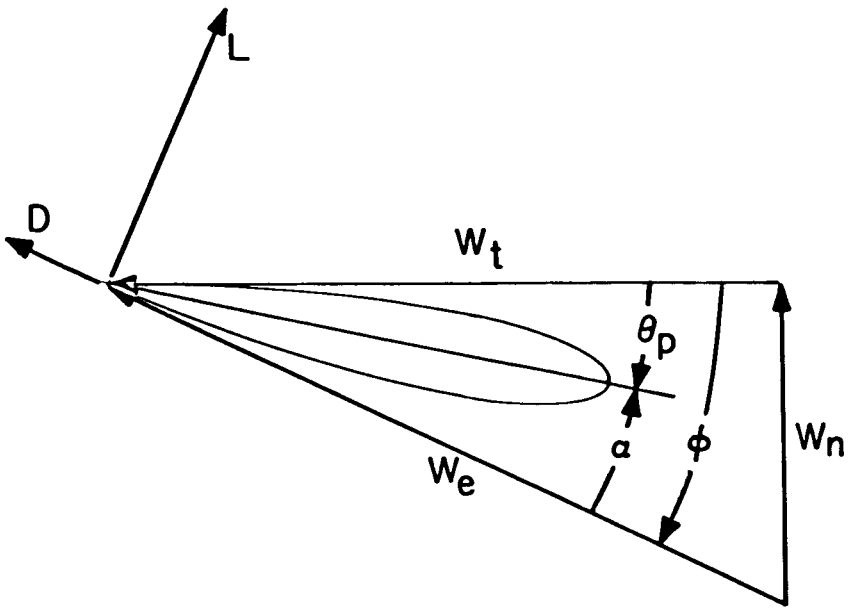

$$\dot{\vec{\theta}}_p = -\dot{\vec{\theta}}$$

Figure II.1.1 Velocity diagram at blade cross section

From the geometry we have

$$dF_n = dL \cos\phi + dD \sin\phi \tag{7}$$

$$dF_t = dL \sin\phi - dD \cos\phi \tag{8}$$

The expression for the normal force and tangential force can also be expressed as

$$dF_n = \frac{1}{2} \rho_\infty w_e^2 c C_n dr \tag{9}$$

$$dF_t = \frac{1}{2} \rho_\infty w_e^2 c C_t dr \tag{10}$$

where

$$C_n = C_L \cos\phi + C_D \sin\phi$$

$$C_t = C_L \sin\phi - C_D \cos\phi$$

The aerodynamic moment at 1/4 chord can be expressed as

$$dM_{c/4}\, \vec{n}_1 = \frac{1}{2} \rho_\infty w_e^2 c^2 C_{M_{c/4}} dr\, \vec{n}_1 \tag{11}$$

and according to Fung [3]

$$C_{M_{c/4}} = -\frac{\pi c}{8} \cos\alpha\, \dot{\theta} \tag{12}$$

Substituting the expression of $C_{M_{c/4}}$ back into Eq. (11), we obtain

$$dM_{c/4} = - \rho_\infty W_e \cos\alpha \frac{\pi c^3}{16} \dot{\theta}\, dr \tag{13}$$

II.3 Linearized Aerodynamic Forces

In this study the linearized aerodynamic forces will be developed. These functions will consist of the nominal terms plus the linear variations of the aerodynamic forces with the dependent variables.

Let us first consider the aerodynamic forces. Figure II.3.1 shows the blade profile section at radius r with the relevant velocities and forces. The components of the aerodynamic forces are expressed as

$$dF_n = \frac{1}{2} \rho_\infty W_e^2 c C_n dr \tag{14}$$

$$dF_t = \frac{1}{2} \rho_\infty W_e^2 c C_t dr \tag{15}$$

where

$$C_n = C_L(\alpha_E)\cos\phi + C_D(\alpha_E)\sin\phi$$

$$C_t = C_L(\alpha_E)\sin\phi - C_D(\alpha_E)\cos\phi$$

$$W_e = W_n + W_t$$

α_E is the effective angle of attack measured at 3/4 chord when including the effect of the pitching velocity at that point.

Normalizing Eqs. (14) and (15) by dividing through with $\frac{1}{2} \rho_\infty V_\infty^2 R^2$ yields

$$C_{F_n} = \left(\frac{W_e}{V_\infty}\right)^2 \frac{c}{R} C_n \frac{dr}{R} \tag{16}$$

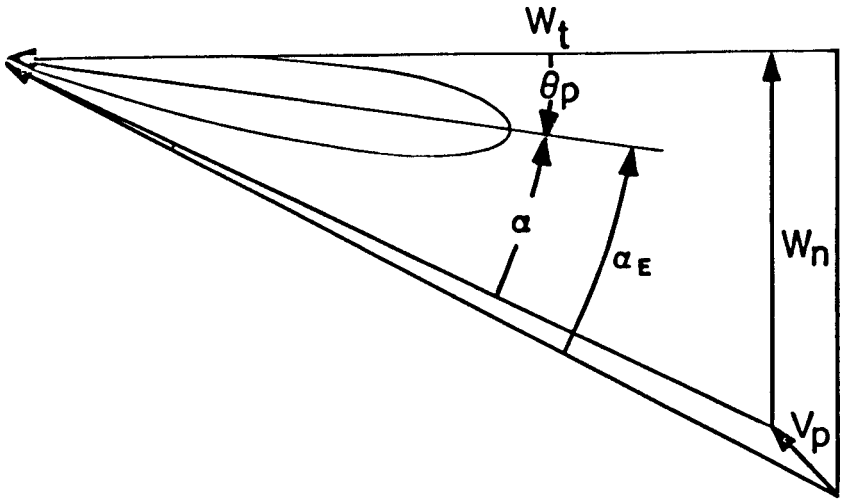

$$\dot{\vec{\theta}}_p = - \dot{\vec{\theta}}$$

Figure II.3.1 Velocity diagram at blade cross section

$$C_{F_t} = \left(\frac{W_e}{V_\infty}\right)^2 \frac{c}{R} C_t \frac{dr}{R} \tag{17}$$

The derivative of the normal force with respect to the dependent variables is defined as

$$N_\eta \frac{dr}{R} = \frac{\partial C_{F_n}}{\partial \eta}$$

$$N_\eta = \frac{c}{R} C_n\left(2 \frac{W_n}{V_\infty} \frac{\partial}{\partial \eta}\left(\frac{W_n}{V_\infty}\right) + \frac{2W_t}{V_\infty} \frac{\partial}{\partial \eta}\left(\frac{W_t}{V_\infty}\right)\right] + \frac{c}{R}\left(\frac{W_e}{V_\infty}\right)^2 \frac{\partial}{\partial \eta} C_n \tag{18}$$

The derivative of C_n with respect to η becomes

$$\frac{\partial C_n}{\partial \eta} = \frac{\partial C_n}{\partial \alpha_E} \frac{\partial \alpha_E}{\partial \eta} + \frac{\partial C_n}{\partial \phi} \frac{\partial \phi}{\partial \eta} \tag{19}$$

The velocity of the fluid that accounts for the pitching velocity at 3/4 chord is expressed as

$$V_p = e_2 \dot{\theta} \cos\theta \vec{e}_n - e_2 \dot{\theta} \sin\theta \vec{e}_t \tag{20}$$

and

$$W^2 = \left(W_n + e_2 \dot{\theta} \cos\theta\right)^2 + \left(W_t + e_2 \dot{\theta} \sin\theta\right)^2$$

From the velocity diagram in Figure II.3.1, the tangent and cosine of the effective angle are expressed as

$$\tan\phi_E = \frac{W_n + e_2 \dot{\theta} \cos\theta}{W_t + e_2 \dot{\theta} \sin\theta} \tag{21}$$

$$\cos\phi_E = \frac{W_t + e_2\dot{\theta}\sin\theta}{W} \tag{22}$$

where

$$\phi_E = \alpha_E - \theta$$

From trigonometric relations we obtain

$$\frac{\partial}{\partial\eta}(\tan\phi_E) = \sec^2\phi_E \frac{\partial\phi_E}{\partial\eta}$$

$$\frac{\partial\alpha_E}{\partial\eta} = \cos^2\phi_E \frac{\partial}{\partial\eta}(\tan\phi_E) + \frac{\partial\theta}{\partial\eta} \tag{23}$$

By substituting Eqs. (21) and (22) into Eq. (23), we obtain the expression of $\frac{\partial\alpha_E}{\partial\eta}$ as

$$\frac{\partial\alpha_E}{\partial\eta} = \frac{1}{W^2}\left[(W_{n_\eta} + e_2\frac{\partial}{\partial\eta}(\dot{\theta}\cos\theta))(W_t + e_2\dot{\theta}\sin\theta)\right.$$

$$\left. - (W_n + e_2\dot{\theta}\cos\theta)(W_{t_\eta} + e_2\frac{\partial}{\partial\eta}(\dot{\theta}\sin\theta))\right] + \frac{\partial\theta}{\partial\eta} \tag{24}$$

where

$$W_{n_\eta} = \frac{\partial W_n}{\partial\eta}$$

$$W_{t_\eta} = \frac{\partial W_t}{\partial\eta}$$

In the same way, the expression of $\frac{\partial\phi}{\partial\eta}$ can be expressed as

$$\frac{\partial \phi}{\partial \eta} = \frac{1}{W_e^2} \left[W_{n\eta} W_t - W_n W_{t\eta} \right] \tag{25}$$

Substituting Eqs. (19), (24), and (25) back into Eq. (18) we then evaluate all the dependent variables at nominal values. The derivative of the normal force can be expressed as

$$\begin{aligned}
N_\eta &= F_1 \frac{W_{n_\eta}}{V_\infty} + F_2 \frac{W_{t_\eta}}{V_\infty} \qquad \text{for } \eta \neq q_1, \dot{q}_1 \\
N_{q_1} &= F_1 \frac{W_{n_{q_1}}}{V_\infty} + F_2 \frac{W_{t_{q_1}}}{V_\infty} + F_4 \\
N_{\dot{q}_1} &= F_1 \frac{W_{n_{\dot{q}_1}}}{V_\infty} + F_2 \frac{W_{t_{\dot{q}_1}}}{V_\infty} + F_3
\end{aligned} \tag{26}$$

where

$$F_1 = \frac{c}{R} \left\{ 2 \frac{W_n}{V_\infty} C_n + C_{n_\nu} \frac{W_t}{V_\infty} \right\}$$

$$F_2 = \frac{c}{R} \left\{ 2 \frac{W_t}{V_\infty} C_n - C_{n_\nu} \frac{W_n}{V_\infty} \right\}$$

$$F_3 = \frac{c}{R} C_{n_\alpha} \frac{e_2}{V_\infty} \frac{W_t}{V_\infty} f_1$$

$$F_4 = \frac{c}{R} \left(\frac{W_e}{V_\infty} \right)^2 C_{n_\alpha} f_1$$

Figure II.3.2 shows the velocity diagram of the blade evaluated at the nominal value. The relation of lift and drag at the nominal value can be expressed as

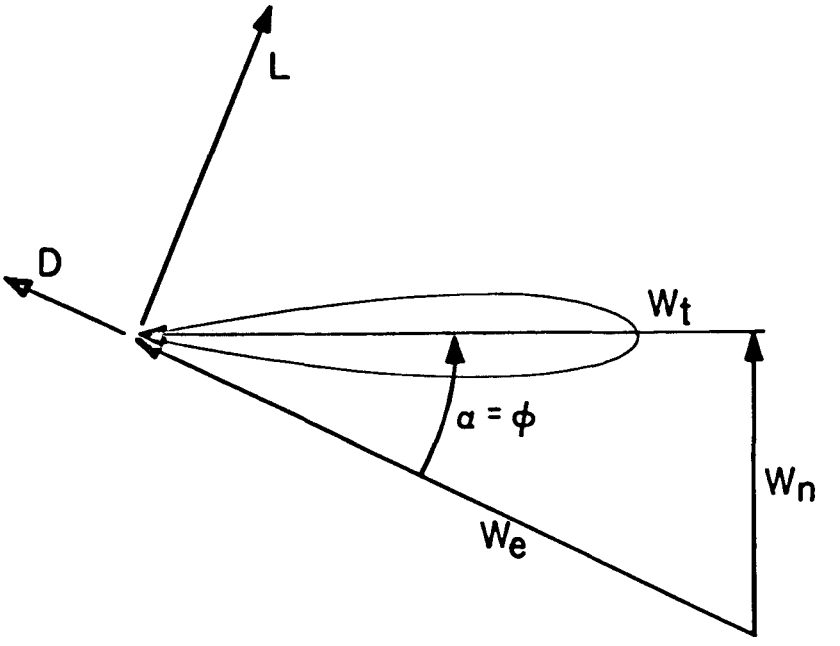

Figure II.3.2 Velocity diagram at blade cross section evaluated at nominal value

$$C_n = C_L \cos\alpha + C_D \sin\alpha$$

$$C_{n_\nu} = C_{L_{\alpha_E}} \cos\alpha + C_{D_{\alpha_E}} \sin\alpha - C_t$$

$$C_t = C_L \sin\alpha - C_D \cos\alpha$$

$$C_{t_\nu} = C_{L_{\alpha_E}} \sin\alpha - C_{D_{\alpha_E}} \cos\alpha + C_n$$

$$C_{n_\alpha} = C_{L_{\alpha_E}} \cos\alpha + C_{D_{\alpha_E}} \sin\alpha$$

$$C_{t_\alpha} + C_{L_{\alpha_E}} \sin\alpha - C_{D_{\alpha_E}} \cos\alpha$$

The variation of the tangential force with the dependent variables can be found in the same way. The derivative of the tangential force is defined as

$$H_\eta \frac{dr}{R} = \frac{\partial C_{F_t}}{\partial \eta}$$

and

$$H_\eta = G_1 \frac{W_{n_\eta}}{V_\infty} + G_2 \frac{W_{t_\eta}}{V_\infty} \qquad \text{for } \eta \neq q_1, \dot{q}_1$$

$$H_{q_1} = G_1 \frac{W_{n_{q_1}}}{V_\infty} + G_2 \frac{W_{t_{q_1}}}{V_\infty} + G_4 \qquad (27)$$

$$H_{\dot{q}_1} = G_1 \frac{W_{n_{\dot{q}_1}}}{V_\infty} + G_2 \frac{W_{t_{\dot{q}_1}}}{V_\infty} + G_3$$

where

$$G_1 = \frac{c}{R}\left\{\frac{2W_n}{V_\infty} C_t + C_{t_\nu} \frac{W_t}{V_\infty}\right\}$$

$$G_2 = \frac{c}{R}\left\{\frac{2W_t}{V_\infty} C_t - C_{t_\nu} \frac{W_n}{V_\infty}\right\}$$

$$G_3 = \frac{c}{R} C_{t_\alpha} \frac{e_2}{V_\infty} \frac{W_t}{V_\infty} f_1$$

$$G_4 = \frac{c}{R} \left(\frac{W_e}{V_\infty}\right)^2 C_{t_\alpha}$$

II.4 Axial Induction Factor "a"

In this analysis, the nonrotating wake model is used. We can calculate the local value of the axial induction factor by equating the windwise force developed on the blade to the momentum flux in an annular ring of radius r.

Applying the momentum theorem to the flow in the annulus "dr" one obtains an expression for the windwise force as

$$dT = \rho_\infty (2\pi r dr) u (V_\infty - V_2)$$

$$= \rho_\infty V_\infty^2 (1 - a) 2a 2\pi r dr \qquad (28)$$

Defining a local thrust coefficient by

$$(C_T)_L = \frac{dT}{\frac{1}{2}\rho_\infty V_\infty^2 dA}$$

Equation (28) becomes

$$(C_T)_L = 4a(1 - a) \qquad (29)$$

The local thrust coefficient based on the blade force in the windwise direction is developed using the blade element theory

$$dT = \frac{1}{2} \rho_\infty W_e^2 Bc \; C_n dr \tag{30}$$

Using the definition of $(C_T)_L$, we obtain

$$(C_T)_L = (\frac{Bc}{r})(\frac{W_e}{V_\infty})^2 \frac{C_n}{2\pi} \tag{31}$$

With a given value of C_L, the local axial induction factor can be found by equating Eqs. (29) and (31).

The simple momentum theory approach leads to the result that the induction factor "a" cannot be greater than 0.5 as this would yield zero downstream velocity. However, increasing thrust coefficient values are obtained for a > 0.5.

When the axial induction factor "a" is greater than $a_{critical}$, the Glauert relationship [14] has been used instead of the simple momentum theorem. The Glauert relationship is shown in Figure II.4.1. This empirical relationship can be approximated by a straight line with good accuracy using wind tunnel test data. The straight line approximation used in this analysis for $a > a_c$ is

$$(C_T)_L = 4a_c(1 - a_c) + 4(1 - 2a)(a - a_c) \tag{32}$$

where $a_c = 0.38$.

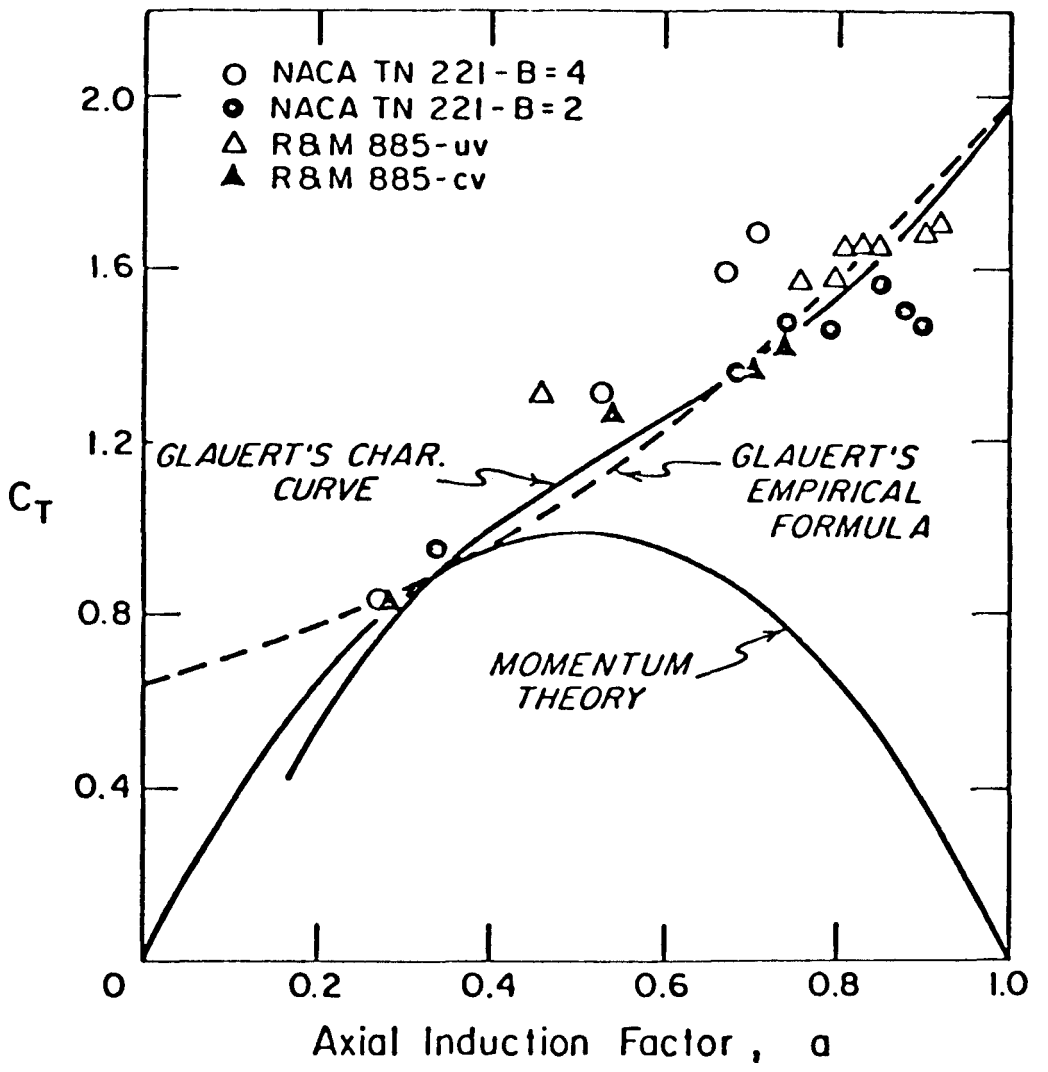

Figure II.4.1 Windmill Brake State Performance

II.5 The Variation of Axial Induction Factor with Generalized Coordinates

In the process of linearizing the aeroforces, the variation of the axial induction factor with the dependent variables is encountered. We can calculate the local variation of the axial induction factor by equating the derivative of the moments developed by the blade force to the derivative of the moments developed by the momentum flux.

Defining the variation of the axial induction factor as

$$\frac{\partial a}{\partial \eta} = k_\eta \frac{r}{R} \sin\psi + j_\eta \frac{r}{R} \cos\psi \tag{33}$$

Substituting the expression for the variation of the axial induction factor back into the linearized aerodynamic forces terms, we now have two new coefficients to solve for, k_η and j_η.

The coefficient k_η can be calculated by equating the derivative of the yaw moment developed by the momentum theorem to the yaw moment derivative developed by the blade element theory. In the same way, the coefficient j_η can be calculated by equating the derivative of the pitching moment developed by the momentum theorem to the pitching moment derivative obtained from the blade element theory.

Considering the segment "$r_N dr_N d\psi$" of the annulus "dr", we obtain the expression of the moment as the cross product of the r_N vector and the windwise force of that segment.

$$d\vec{M} = \vec{r}_N \times d\vec{T} \tag{34}$$

where

$$r_N = (r + u_m)\cos\rho - w\sin\rho \tag{35}$$

$$dT = \rho_\infty V_\infty^2 (\cos\gamma - a)2a\, r_N dr_N d\psi \tag{36}$$

A local moment coefficient is defined as

$$dC_M = \frac{dM}{\frac{1}{2}\rho_\infty V_\infty^2 \pi R^3} \tag{37}$$

Substituting Eqs. (35) and (36) into Eq. (37), we obtain the expression of the yaw moment as the component of the vector "dC_M" in the n_x direction and the pitching moment in the n_y direction.

The expression for the yaw moment is

$$dC_{M_x} = \frac{1}{\pi} 4a(\cos\gamma - a) \frac{r_N^2}{R} \sin\psi \frac{dr_N}{R} d\psi \tag{38}$$

The expression for the pitching moment is

$$dC_{M_y} = \frac{1}{\pi} 4a(\cos\gamma - a) \frac{r_N^2}{R} \cos\psi \frac{dr_N}{R} d\psi \tag{39}$$

By taking the derivative of the yaw moment and the pitching moment with respect to the dependent variables then integrating over the whole rotor, we obtain the expression

$$\frac{\partial C_{M_x}}{\partial \eta} = + \frac{1}{\pi} \int_0^R \int_0^{2\pi} \frac{\partial C_{T_L}}{\partial a} \frac{\partial a}{\partial \eta} \frac{r_N^2}{R^2} \sin\psi d\psi \frac{dr_N}{R} \tag{40}$$

$$\frac{\partial C_{M_y}}{\partial \eta} = - \frac{1}{\pi} \int_0^R \int_0^{2\pi} \frac{\partial C_{T_L}}{\partial a} \frac{\partial a}{\partial \eta} \frac{r_N^2}{R^2} \cos\psi d\psi \frac{dr_N}{R} \tag{41}$$

where

$$C_{T_L} = 4a(1 - a)$$

Substituting the expression of $\frac{\partial a}{\partial \eta}$ from Eq. (33) into Eqs. (40) and (41), we obtain

$$\frac{\partial C_{M_x}}{\partial \eta} = k_\eta \Pi_1 \tag{42}$$

$$\frac{\partial C_{M_y}}{\partial \eta} = - j_\eta \Pi_1 \tag{43}$$

where

$$\Pi_1 = \int_o^R \frac{\partial C_{T_L}}{\partial a} \frac{r_N^3}{R^3} \frac{dr_N}{R} \tag{44}$$

Now we will look into the same yaw moment and the same pitching moment but they will be developed by blade force instead of momentum flux.

Considering the small element of blade "dr", the moment created by the aeroforces and aeromoments are expressed as

$$d\vec{M} = \vec{r}_M \times d\vec{F} + d\vec{M}_{\frac{c}{4}} \tag{45}$$

where

$$\vec{r}_M = (r + u_m)\vec{n}_{x\rho} + w_{z\beta} + e_1\vec{n}_2$$

$$d\vec{F} = dF_n\vec{n}_{z\theta} + dF_t\vec{n}_{y\theta}$$

$$d\vec{M}_{\frac{c}{4}} = dM_{\frac{c}{4}} \vec{n}_1$$

the expression for the yaw moment is obtained from the component of $d\vec{C}_M$ in the n_x direction

$$dC_{M_x} = \frac{N}{\pi} (TL1) \frac{dr}{R} d\psi + \frac{H}{\pi} (TL2) \frac{dr}{R} d\psi \qquad (46)$$

where

$$N = \left(\frac{W_e}{V_\infty}\right)^2 C_n \frac{c}{R}$$

$$H = \left(\frac{W_e}{V_\infty}\right)^2 C_t \frac{c}{R}$$

$$TL1 = \begin{cases} \frac{e_1}{R} \cos\theta[(\cos\rho\cos w' - \sin\rho\sin w'\cos\beta)\cos\psi - \sin w'\sin\beta\sin\psi] \\ -[\frac{(r+u_m)}{R}\cos w' - \frac{w}{R}\sin w'](\sin\rho\sin\beta\cos\psi - \cos\beta\sin\psi) \end{cases}$$

$$TL2 = \begin{cases} -[\frac{(r+u_m)}{R}\sin w' - \frac{w}{R}\cos w' - \frac{e_1}{R}\sin\theta][(\sin w'\sin\beta\sin\psi) \\ \qquad + (\cos\rho\cos w' - \sin\rho\sin w'\cos\beta)\cos\psi] \\ -[\frac{(r+u_m)}{R}\cos w' + \frac{w}{R}\sin w'][(\cos\rho\sin w' + \sin\rho\cos w'\cos\beta)\cos\psi \\ \qquad + \cos w'\sin\beta\sin\psi] \end{cases}$$

Now we take the derivative of this moment with respect to the dependent variables. Then we add the effect which accounts for the "B" turbine

blades in the system. The expression of the average yaw moment derivative is given as

$$\frac{\partial C_{M_x}}{\partial \eta} = \frac{B}{2\pi^2} \int_{R_H}^{R} \int_{o}^{2\pi} N_\eta (TL1) \frac{dr}{R} d\psi + \frac{B}{2\pi^2} \int_{R_H}^{R} \int_{o}^{2\pi} H_\eta (TL2) \frac{dr}{R} d\psi \tag{47}$$

where

$$N_\eta = \frac{\partial N}{\partial \eta}$$

$$H_\eta = \frac{\partial H}{\partial \eta}$$

By substituting the expression of $\frac{\partial a}{\partial \eta}$ from Eq. (33) into N_η and H_η terms, the derivative of the yaw moment is expressed in terms of k_η and j_η.

The expression of the pitching moment developed by the blade force is expressed as the component of $d\vec{C}_M$ in Eq. (45) in the n_y direction. Then the derivative of the pitching moment $\frac{\partial C_{M_y}}{\partial \eta}$ is obtained in the same way as it is done in $\frac{\partial C_{M_x}}{\partial \eta}$.

Now we can equate the derivative of the yaw moment developed by momentum flux to the one developed by blade force and the derivative of pitching moment developed by momentum flux to the one developed by blade force. The analysis results in two equations and two unknowns (k_η and j_η).

The result of this linearized analysis shows that the variation of the axial induction factor exists only for the yaw and yaw rate variables

$$\frac{\partial a}{\partial \eta} = 0 \qquad \eta \neq q_4 \text{ and } \dot{q}_4 \tag{48}$$

The coefficients k_η and j_η for yaw and yaw rate are given by

$$k_{q_4} = \frac{(\Pi_4 + \Pi_5 + \Pi_6 + \Pi_7)(\Pi_1 - \Pi_3) - \Pi_2(\Pi_{12} + \Pi_{13} + \Pi_{14} + \Pi_{15})}{(\Pi_1 - \Pi_3)^2 + \Pi_2^2} \quad (49)$$

$$j_{q_4} = -\frac{\{(\Pi_4 + \Pi_5 + \Pi_6 + \Pi_7)\Pi_2 + (\Pi_1 - \Pi_3)(\Pi_{12} + \Pi_{13} + \Pi_{14} + \Pi_{15})\}}{(\Pi_1 - \Pi_3)^2 + \Pi_2^2} \quad (50)$$

$$k_{\dot{q}_4} = \frac{(\Pi_8 + \Pi_9 + \Pi_{10} + \Pi_{11})(\Pi_1 - \Pi_3) - \Pi_2(\Pi_{16} + \Pi_{17} + \Pi_{18} + \Pi_{19})}{(\Pi_1 - \Pi_3)^2 + \Pi_2^2} \quad (51)$$

$$j_{\dot{q}_4} = \frac{-\{(\Pi_8 + \Pi_9 + \Pi_{10} + \Pi_{11})\Pi_2 + (\Pi_1 - \Pi_3)(\Pi_{16} + \Pi_{17} + \Pi_{18} + \Pi_{19})\}}{(\Pi_1 - \Pi_3)^2 + \Pi_2^2} \quad (52)$$

where Π_i's are the integral terms.

These integral terms are given as follows:

$$\Pi_1 = \int_{R_H}^{R} \frac{\partial C_{T_L}}{\partial a} \left(\frac{r_N}{R}\right)^3 \frac{dr_N}{R}$$

$$\Pi_2 = \begin{cases} \frac{3}{2\pi} \int_{R_H}^{R} (N1)\, \frac{e_1}{R} (\cos\rho\cos w_o' - \sin\rho\sin w_o'\cos\beta)\, \frac{r_N}{R}\frac{dr}{R} \\ -\frac{3}{2\pi} \int_{R_H}^{R} (N1) \left(\frac{(r+u_m)}{R}\cos w_o' + \frac{w_o}{R}\sin w_o'\right)\sin\rho\sin\beta\, \frac{r_N}{R}\frac{dr}{R} \\ +\frac{3}{2\pi} \int_{R_H}^{R} (H1)\left(\frac{(r+u_m)}{R}\sin w_o' - \frac{w_o}{R}\cos w_o'\right)(\cos\rho\cos w_o' \\ \qquad - \sin\rho\sin w_o'\cos\beta)\, \frac{r_N}{R}\frac{dr}{R} \\ -\frac{3}{2\pi} \int_{R_H}^{R} (H1)\left(\frac{(r+u_m)}{R}\cos w_o' + \frac{w_o}{R}\sin w_o'\right)(\cos\rho\sin w_o' \\ \qquad + \sin\rho\cos w_o'\cos\beta)\, \frac{r_N}{R}\frac{dr}{R} \end{cases}$$

$$\Pi_3 = \begin{cases} -\frac{3}{2\pi}\int_{R_H}^{R} (N1)\,\frac{e_1}{R}\,\sin w_o' \sin\beta\,\frac{r_N}{R}\,\frac{dr}{R} \\ \frac{3}{2\pi}\int_{R_H}^{R} (N1)\,\left(\frac{(r+u_m)}{R}\cos w_o' + \frac{w_o}{R}\sin w_o'\right)\cos\beta\,\frac{r_N}{R}\,\frac{dr}{R} \\ -\frac{3}{2\pi}\int_{R_H}^{R} (H1)\left(\frac{(r+u_m)}{R}\sin w_o' - \frac{w_o}{R}\cos w_o'\right)\sin w_o' \sin\beta\,\frac{r_N}{R}\,\frac{dr}{R} \\ -\frac{3}{2\pi}\int_{R_H}^{R} (H1)\left(\frac{(r+u_m)}{R}\cos w_o' + \frac{w_o}{R}\sin w_o'\right)\cos w_o' \sin\beta\,\frac{r_N}{R}\,\frac{dr}{R} \end{cases}$$

$$\Pi_4 = \frac{3}{2\pi}\int_{R_H}^{R} (N2)\left[\frac{e_1}{R}\left(\cos\rho\cos w_o' - \sin\rho\sin w_o'\cos\beta\right) - \left(\frac{(r+u_m)}{R}\cos w_o' + \frac{w_o}{R}\sin w_o'\right)\sin\rho\sin\beta\right] f_4\,\frac{dr}{R}$$

$$\Pi_5 = \frac{3}{2\pi}\int_{R_H}^{R} (N3)\left(\frac{e_1}{R}\sin w_o'\sin\beta - \left(\frac{(r+u_m)}{R}\cos w_o' + \frac{w_o}{R}\sin w_o'\right)\cos\beta\right) f_4\,\frac{dr}{R}$$

$$\Pi_6 = \begin{cases} \frac{3}{2\pi}\int_{R_H}^{R} (H2)\left(\frac{(r+u_m)}{R}\sin w_o' - \frac{w_o}{R}\cos w_o'\right)\left(\cos\rho\cos w_o' - \sin\rho\sin w_o'\cos\beta\right) f_4\,\frac{dr}{R} \\ -\frac{3}{2\pi}\int_{R_H}^{R} (H2)\left(\frac{(r+u_m)}{R}\cos w_o' + \frac{w_o}{R}\sin w_o'\right)\left(\cos\rho\sin w_o' + \sin\rho\cos w_o'\cos\beta\right) f_4\,\frac{dr}{R} \end{cases}$$

$$\Pi_7 = \frac{3}{2\pi}\int_{R_H}^{R}(H3)[(\frac{(r+u_m)}{R}\cos w_o' + \frac{w_o}{R}\sin w_o')\cos w_o'\sin\beta + (\frac{(r+u_m)}{R}\sin w_o' - \frac{w_o}{R}\cos w_o')\sin w_o'\sin\beta]f_4\frac{dr}{R}$$

$$\Pi_8 = \frac{3}{2\pi}\int_{R_H}^{R}(N4)[\frac{e_1}{R}(\cos\rho\cos w_o' - \sin\rho\sin w_o'\cos\beta) - (\frac{(r+u_m)}{R}\cos w_o' + \frac{w_o}{R}\sin w_o')\sin\rho\sin\beta]f_4\frac{dr}{R}$$

$$\Pi_9 = \frac{3}{2\pi}\int_{R_H}^{R}(N5)[\frac{e_1}{R}\sin w_o'\sin\beta - (\frac{(r+u_m)}{R}\cos w_o' + \frac{w_o}{R}\sin w_o')\cos\beta]f_4\frac{dr}{R}$$

$$\Pi_{10} = \begin{cases} \frac{3}{2\pi}\int_{R_H}^{R}(H4)(\frac{(r+u_m)}{R}\sin w_o' - \frac{w_o}{R}\cos w_o')(\cos\rho\cos w_o' - \\ \quad - \sin\rho\sin w_o'\cos\beta)f_4\frac{dr}{R} \\ -\frac{3}{2\pi}\int_{R_H}^{R}(H4)(\frac{(r+u_m)}{R}\cos w_o' + \frac{w_o}{R}\sin w_o')(\cos\rho\sin w_o' \\ \quad + \sin\rho\cos w_o'\cos\beta)f_4\frac{dr}{R} \end{cases}$$

$$\Pi_{11} = \frac{3}{2\pi}\int_{R_H}^{R}(H5)[(\frac{(r+u_m)}{R}\cos w_o' + \frac{w_o}{R}\sin w_o')\cos w_o'\sin\beta + (\frac{(r+u_m)}{R}\sin w_o' - \frac{w_o}{R}\cos w_o')\sin w_o'\sin\beta]f_4\frac{dr}{R}$$

$$\Pi_{12} = \frac{3}{2\pi}\int_{R_H}^{R}(N2)(\frac{e_1}{R}\sin w_o'\sin\beta - (\frac{(r+u_m)}{R}\cos w_o' + \frac{w_o}{R}\sin w_o')\cos\beta)f_4\frac{dr}{R}$$

$$\Pi_{13} = \frac{3}{2\pi}\int_{R_H}^{R}(N3)(\frac{e_1}{R}(\sin\rho\sin w_o'\cos\beta - \cos\rho\cos w_o') + (\frac{(r+u_m)}{R}\cos w_o' + \frac{w_o}{R}\sin w_o')\sin\rho\sin\beta)f_4\frac{dr}{R}$$

$$\Pi_{14} = \frac{3}{2\pi}\int_{R_H}^{R}(H2)\left[\left(\frac{(r+u_m)}{R}\sin w_o' - \frac{w_o}{R}\cos w_o'\right)\sin w_o'\sin\beta\right.$$

$$\left. + \left(\frac{(r+u_m)}{R}\cos w_o' + \frac{w_o}{R}\sin w_o'\right)\cos w_o'\sin\beta\right] f_4\,\frac{dr}{R}$$

$$\Pi_{15} = \begin{cases} -\frac{3}{2\pi}\int_{R_H}^{R}(H3)\left(\frac{(r+u_m)}{R}\sin w_o' - \frac{w_o}{R}\cos w_o'\right)(\cos\rho\cos w_o' \\ \quad - \sin\rho\sin w_o'\cos\beta) f_4\,\frac{dr}{R} \\ +\frac{3}{2\pi}\int_{R_H}^{R}(H3)\left(\frac{(r+u_m)}{R}\cos w_o' + \frac{w_o}{R}\sin w_o'\right)(\cos\rho\sin w_o' \\ \quad + \sin\rho\cos w_o'\cos\beta) f_4\,\frac{dr}{R} \end{cases}$$

$$\Pi_{16} = \frac{3}{2\pi}\int_{R_H}^{R}(N4)\left[\frac{e_1}{R}\sin w_o'\sin\beta - \left(\frac{(r+u_m)}{R}\cos w_o' + \frac{w_o}{R}\sin w_o'\right)\cos\beta\right] f_4\,\frac{dr}{R}$$

$$\Pi_{17} = -\frac{3}{2\pi}\int_{R_H}^{R}(N5)\left[\frac{e_1}{R}\left(\cos\rho\cos w_o' - \sin\rho\sin w_o'\cos\beta\right)\right.$$

$$\left. - \left(\frac{(r+u_m)}{R}\cos w_o' + \frac{w_o}{R}\sin w_o'\right)\sin\rho\sin\beta\right] f_4\,\frac{dr}{R}$$

$$\Pi_{18} = \frac{3}{2\pi}\int_{R_H}^{R}(H4)\left[\left(\frac{(r+u_m)}{R}\sin w_o' - \frac{w_o}{R}\cos w_o'\right)\sin w_o'\sin\beta\right.$$

$$\left. + \left(\frac{(r+u_m)}{R}\cos w_o' + \frac{w_o}{R}\sin w_o'\right)\cos w_o'\sin\beta\right] f_4\,\frac{dr}{R}$$

$$\Pi_{19} = \begin{cases} -\frac{3}{2\pi}\int_{R_H}^{R} (H5)\left(\frac{(r+u_m)}{R}\sin w_o' - \frac{w_o}{R}\cos w_o'\right)(\cos\rho\cos w_o' \\ \qquad - \sin\rho\sin w_o'\cos\beta) f_4 \frac{dr}{R} \\ +\frac{3}{2\pi}\int_{R_H}^{R} (H5)\left(\frac{(r+u_m)}{R}\cos w_o' + \frac{w_o}{R}\sin w_o'\right)(\cos\rho\sin w_o' \\ \qquad + \sin\rho\cos w_o'\cos\beta) f_4 \frac{dr}{R} \end{cases}$$

where

$$N1 = (\sin\rho\sin w_o' - \cos\rho\cos w_o'\cos\beta)F_1 - \cos\rho\sin\beta F_2$$

$$N2 = \cos w_o'\sin\beta F_1 - \cos\beta F_2$$

$$N3 = (\cos\rho\sin w_o' + \sin\rho\cos w_o'\cos\beta)F_1 + \sin\rho\sin\beta F_2$$

$$N4 = \begin{cases} \left(\frac{\ell}{V_\infty}\sin\beta\cos w_o' + \frac{(r+u_d)}{V_\infty}\sin\rho\sin\beta\cos w_o' + \frac{w_o}{V_\infty}\sin w_o'\sin\rho\sin\beta\right)F_1 \\ +\frac{e_3}{V_\infty}(\cos\rho\cos w_o' - \sin\rho\sin w_o'\cos\beta)F_1 \\ -\left(\frac{\ell}{V_\infty}\cos\beta + \frac{(r+u_d)}{V_\infty}\sin\rho\cos\beta + \frac{w_o}{V_\infty}\cos\rho\right)F_2 \end{cases}$$

$$N5 = \begin{cases} \left(\frac{\ell}{V_\infty}(\sin\rho\cos\beta\cos w_o' + \sin w_o'\cos\rho) + \frac{(r+u_d)}{V_\infty}\cos\beta\cos w_o'\right. \\ \qquad \left. + \frac{w_o}{V_\infty}\sin w_o'\cos\beta + \frac{e_3}{V_\infty}\sin w_o'\sin\beta\right)F_1 \\ +\left(\frac{\ell}{V_\infty}\sin\rho\sin\beta + \frac{(r+u_d)}{V_\infty}\sin\beta\right)F_2 \end{cases}$$

The expressions for H1, H2, H3, H4, and H5 are the same as N1, N2, N3, N4, and N5, respectively, except F_1 and F_2 in Ni terms are replaced by G_1 and G_2 in Hi terms.

II.5 Tip Loss Model

In order to account for nonuniform flow in the wake of a wind turbine, flow models have been adapted from the propeller theory. Physically, the tip correction accounts for the fact that the maximum change in axial velocity, $2aV_\infty$, in the wake occurs only at the vortex sheets and the average velocity change in the wake is $2aV_\infty F$, where F is the tip loss factor.

"Tip losses" have been treated in a variety of different manners in the propeller and helicopter industries. The simplest method is to reduce the maximum rotor radius by some fraction of the actual radius, which in helicopter studies is of the order of 0.03R. A more detailed analysis was done by Prandtl [12] as a method for estimation of lightly loaded propeller tip losses. Later Goldstein [13] developed a more rigorous analysis.

For this analysis we will use the combination of the effective radius and Prandtl method for the calculation of tip loss factor.

The effective radius is given by

$$\frac{R_{eff}}{R} = \left[\frac{B^{2/3}x}{B^{2/3}x + 1.32}\right]^{1/2}$$

and

$$\frac{R_{eff}}{R} = \left[\frac{B^{2/3}x}{B^{2/3}x + 0.44}\right]^{1/2} \quad \text{for } x < 3$$

which was obtained from an empirical relation which expresses the maximum power coefficient of wind turbines.

The tip loss factor is expressed as

$$F = \frac{2}{\pi} \arccos(ef)$$

where

$$ef = \left[\cos\left(\frac{0.7\pi}{2}\right)\right]^{(1 - r/R)/(1 - R_{eff}/R)}$$

II.6 Power and Thrust Coefficient

From the blade elementary theory, the windwise force and torque at the nominal value are given as

$$dT = \frac{1}{2} \rho_\infty B W_e^2 c C_N \frac{dr}{R} \tag{53}$$

$$dQ = \frac{1}{2} \rho_\infty B W_e^2 c C_t r \frac{dr}{R} \tag{54}$$

Power is defined as the product of torque and angular speed

$$dP = \Omega dQ \tag{55}$$

Normalizing Eqs. (53) and (55) with $\frac{1}{2} \rho_\infty V_\infty^2 \pi R^2$ and $\frac{1}{2} \rho_\infty V_\infty^3 \pi R^2$, respectively and making use of the relationship of the relative velocities and angles at the blade cross section, one obtains

$$C_P = \frac{\cos^3\rho}{\pi x} \int_{x_{hub}}^{x_{tip}} \frac{Bc}{R} \sqrt{1 + \left(\frac{1-a}{x}\right)^2} \left[(1-a)C_L - xC_D\right]x^2 dx \qquad (56)$$

$$C_T = \frac{\cos^3\rho}{\pi x} \int_{x_{hub}}^{x_{tip}} \frac{Bc}{R} \sqrt{1 + \left(\frac{1-a}{x}\right)^2} \left[xC_L + (1-a)C_D\right]x dx \qquad (57)$$

APPENDIX III

DERIVATION OF GOVERNING EQUATIONS

In order to develop the equations of motion, the Lagrange method is used. The expression of kinetic and potential energy of the system will be developed. Then, by using the virtual work concept an expression for the nonconservative forces can be obtained.

Lagrange's equation is used to develop the equations of motion. The Lagrange equation is given as

$$\frac{d}{dt}\left(\frac{\partial L}{\partial \dot{q}_i}\right) - \frac{\partial L}{\partial q_i} = Q_i$$

where

L = Lagrangian function = KE-PE

Q_i = nonconservative force

q_i = generalized coordinate

With the expression of KE, PE and Q_i substituted back into Lagrange's equations, we obtain the equations of motion.

III.1 Kinetic and Potential Energy

In order to obtain the expression for kinetic energy of the rotor system, the velocity and angular velocity of the blade element are first developed. With known values of mass and mass moment of inertia of the blade element, the kinetic energy is expressed as

$$d(KE) = V_c^2 dm + \omega_1^2 dI_1 + \omega_2^2 dI_2 + \omega_3^2 dI_3 \qquad (1)$$

Here V_c is the velocity of the blade element of length dr, ω_i's are angular velocities of the blade element in the direction normal and tangent to the blade, dm is the mass of the blade element, and dI_i's are the mass moment of inertias of the blade element at mass center in the same direction as the ω_i's.

The total kinetic energy of the blade system is obtained by integrating over the blade length and adding the contributions of each blade

$$KE = \sum_{i=1}^{B} \int_{R_H}^{R} V_c^2 dm + \sum_{i=1}^{B} \int_{R_H}^{R} \omega_1^2 \, dI_1 + \sum_{i=1}^{B} \int_{R_h}^{R} \omega_2^2 dI_2 + \sum_{i=1}^{B} \int_{R_h}^{R} \omega_3^2 dI_3 \tag{2}$$

where B is the number of blades.

The additional kinetic energy due to the hub mass and generator are considered. The additional kinetic energy terms are expressed as

$$KE = \frac{1}{2} I_H \dot{\psi}^2 + \frac{1}{2} I_G (N_G \dot{\psi})^2 \tag{3}$$

Here I_H is the mass moment of inertia of the hub around the rotor shaft, I_G is the mass moment of inertia of generator around the rotor shaft, and N_G is the step-up gearing ratio between the turbine and the generator.

An expression for the potential energy of the rotor system can be derived from the strain energy due to the blade deflection and blade twisting. The expression for the strain energy of an element of a blade is first developed, then integrating along the blade span and adding the contribution of each blade to get the total potential energy. Thus, we obtain

$$U = \sum_{i=1}^{B} \frac{1}{2} \int_{R_H}^{R} EI(r)\left(\frac{\partial^2 W}{\partial r^2}\right)^2 dr + \sum_{i=1}^{B} \frac{1}{2} \int_{R_H}^{R} GJ(r)\left(\frac{\partial \theta}{\partial r}\right)^2 dr \qquad (4)$$

III.2 Virtual Work

The virtual work principle can be stated as, "If a system of forces is in equilibrium, the work done by the externally applied forces through virtual displacements compatible with the constraint of the system is zero," [4].

$$\delta W = \sum_{i=1}^{n} \vec{F}_i \cdot \delta \vec{r}_i = 0$$

where

$\vec{F}_i$ = external force

$\delta \vec{r}_i$ = virtual displacement

Virtual displacement is defined as infinitesimal arbitrary changes in the coordinates of a system. These are small variations from the true position of the system and must be compatible with the constraints of the system.

The total virtual work of the system can be expressed as the summation of the virtual work of conservative forces and the virtual work of nonconservative forces. The conservative forces are the forces that do depend on position and can be derived from a potential function. Conservative forces are the inertia forces, the contact forces, and body forces. The nonconservative forces are energy-dissipating forces, such as friction forces and forces imparting energy to the system, such as external forces. Nonconservative forces are forces that do not depend on position alone and cannot be derived from a potential function.

In this analysis we will consider the virtual work of the nonconservative forces alone. The nonconservative forces in our case are the aerodynamic forces and moments.

III.3 Nonconservative Forces

First, let us redefine the virtual displacement and virtual angular displacement (virtual rotation) of the system. In this analysis, we assume that the aeroforces and moments act at 1/4 chord position of the blade cross section. The virtual displacement and virtual angular displacement are defined as [5]

$$\delta\vec{P} = \frac{\partial\vec{V}_d}{\partial\dot{q}_i}\,\delta q_i \tag{5}$$

$$\delta\vec{\alpha} = \frac{\partial\vec{\omega}}{\partial\dot{q}_i}\,\delta q_i \tag{6}$$

where

$\frac{\partial\vec{V}_d}{\partial\dot{q}_i}$ = the partial rate of change of position with respect to q_i at the 1/4 blade chord in the inertial reference frame.

$\frac{\partial\vec{\omega}}{\partial\dot{q}_i}$ = is the partial rate of change with respect to q_i of orientation of the blade in the inertial reference frame.

The virtual work is defined as the summation of the inner product of the aerodynamic force and the virtual displacement and the inner product of the aerodynamic torque or couple and the virtual angular displacement

$$\delta W = \vec{F} \cdot \delta \vec{P} + \vec{M} \cdot \delta \vec{\alpha} \tag{7}$$

The aerodynamic force and couple at 1/4 chord are defined as

$$\vec{F} = F_n \vec{e}_n + F_t \vec{e}_t \tag{8}$$

$$\vec{M} = M \vec{n}_1$$

Substituting Eqs. (7) and (8) into Eqs. (6) the expression for the virtual work becomes

$$\delta W = Q_1 \delta q_1 + Q_2 \delta q_2 + Q_3 \delta q_3 + Q_4 \delta q_4$$

where Q_i represents the nonconservative force relevant for the right hand side of the Lagrange's equation

$$Q_1 = \vec{F} \cdot \left(\frac{\partial \vec{V}_d}{\partial \dot{q}_1}\right) + \vec{M} \cdot \left(\frac{\partial \vec{\omega}}{\partial \dot{q}_1}\right) \tag{9}$$

$$Q_2 = \vec{F} \cdot \left(\frac{\partial \vec{V}_d}{\partial \dot{q}_2}\right) + \vec{M} \cdot \left(\frac{\partial \vec{\omega}}{\partial \dot{q}_2}\right) \tag{10}$$

$$Q_3 = \vec{F} \cdot \left(\frac{\partial \vec{V}_d}{\partial \dot{q}_3}\right) + \vec{M} \cdot \left(\frac{\partial \vec{\omega}}{\partial \dot{q}_3}\right) \tag{11}$$

$$Q_4 = \vec{F} \cdot \left(\frac{\partial \vec{V}_d}{\partial \dot{q}_4}\right) + \vec{M} \cdot \left(\frac{\partial \vec{\omega}}{\partial \dot{q}_4}\right) \tag{12}$$

Now we have the expression for the Lagrangian function and the non-conservative forces. Substituting these expressions back into Lagrange's equation, we obtain four equations of motion. These equa-

tions can be written in matrix form as

$$[M]\{\ddot{q}_i\} + [C]\{\dot{q}_i\} = \{G(q_1,\ldots q_4,\ \dot{q}_1,\ldots \dot{q}_4,t)\} \tag{13}$$

where

[M] = nonlinear mass coefficient matrix

[C] = nonlinear damping coefficient matrix from $\frac{d}{dt}\left(\frac{\partial L}{\partial \dot{q}_i}\right)$

{G} = a vector consisting of nonlinear terms from $\frac{\partial L}{\partial q_i} + Q_i$

III.4 Nacelle, Gravity

Nacelle

In this analysis we will consider the nacelle as a slender body. The shape of the nacelle is assumed to be a cylinder with a hemisphere on the forebody and afterbody. Figure III.4.1 shows a picture of the nacelle.

Since we assume that the nacelle acts like a rigid body and the only movement it is allowed is rotation around the yaw axis, the kinetic energy and potential energy can be expressed as

$$KE = \frac{1}{2} I_n \dot{\gamma}^2$$

$$PE = 0$$

where I_n is the nacelle's mass moment of inertia around the yaw axis

$$KE = \frac{1}{2} I_n f_4^2 \dot{q}_4^2 \tag{14}$$

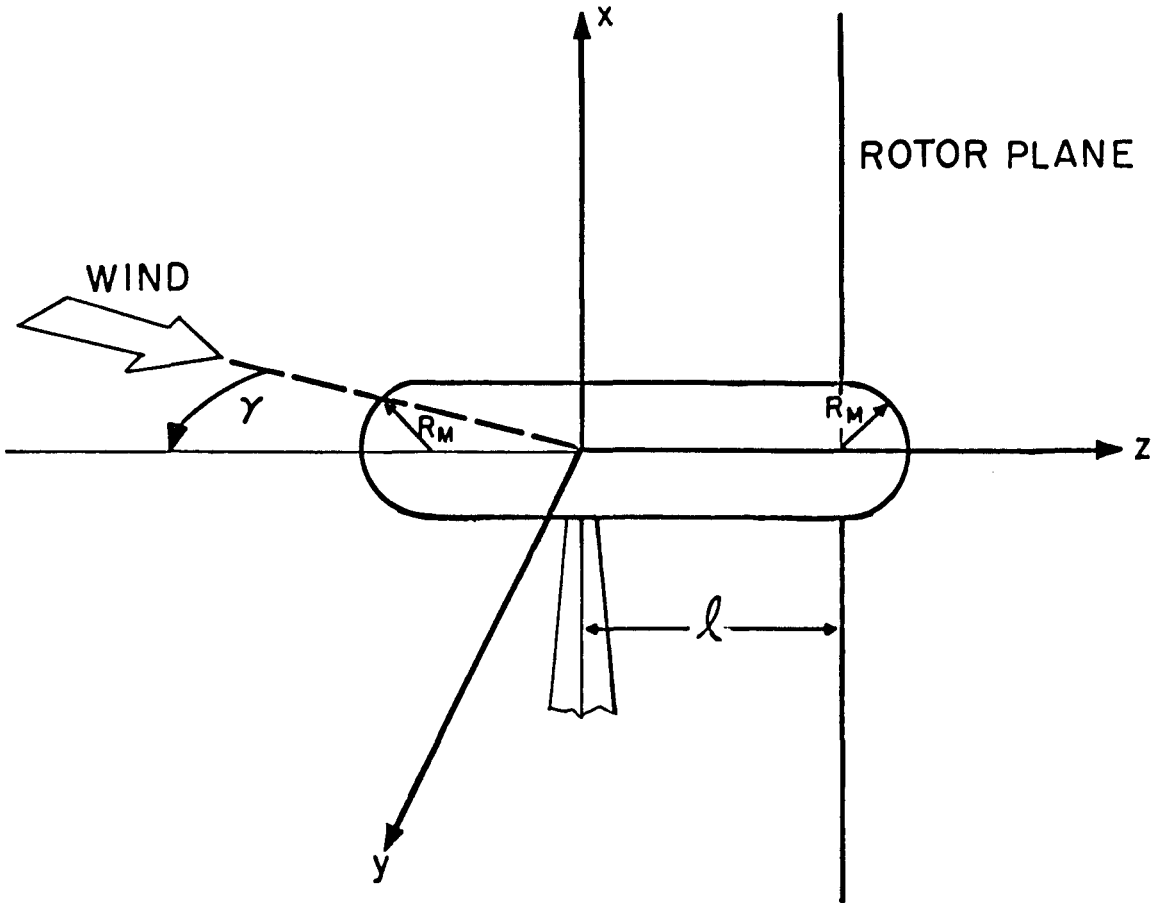

Figure III.4.1 Nacelle geometry

For the nonconservative force, the forces on the nacelle are calculated by using the slender body theorem. The forces on the body can be expressed as

$$dF_y = 2q_\infty \frac{ds}{dz} dz \tag{15}$$

$$dF_z = \{P_\infty - q_\infty(\gamma^2 + \frac{u_{z1}}{V_\infty}(R,z) + (\frac{dR(z)}{dz})^2\} \frac{ds}{dz} dz \tag{16}$$

where

s = the cross section area of the body

R(z) = the radius of the body cross section

The virtual displacement of the nacelle is expressed as

$$\delta\vec{P} = zf_4\delta q_4 \vec{n}_y \tag{17}$$

The virtual work of the nacelle system is given by

$$d(\delta W) = dF_y \delta P$$

$$= (2q_\infty z \frac{ds}{dz} dz f_4^2 q_4)\delta q_4 \tag{18}$$

The nonconservative force for the nacelle is expressed as

$$dQ_N = 2q_\infty z \frac{ds}{dz} dz f_4^2 q_4 \tag{19}$$

The force on the nacelle exists only at the hemispheres at both ends of the nacelle $(\frac{ds}{dz} \neq 0)$.

The afterbody of the nacelle is in the hub area. In real flow, the flow would separate before it reaches the afterbody. Only the forebody part of the nacelle is considered.

The equation of motion of the nacelle is developed by substituting the expression for kinetic energy and the nonconservative force in Lagrange's equation. The nondimensionalized equation of motion is given by

$$m_{44_n} \ddot{q}_4 + k_{44_n} q_4 = 0 \tag{20}$$

where

$$m_{44_n} = \frac{I_n}{q_\infty R^3} f_4^2$$

$$k_{44_n} = -\frac{2}{R^3} \int_{-(\eta - R_M)}^{\eta} z \frac{ds}{dz} f_4^2 \, dz$$

η = distance from the nacelle's yaw axis to the forebody end of the nacelle

R_M = radius of the hemisphere on forebody and afterbody of the nacelle.

Gravity Effect

For a larger wind turbine system, the effect of gravity is very important in dynamic and structural analysis. Although the Enertech

1500 is a small wind turbine system, the gravity effect will be included in the analysis to make the analysis applicable to any size turbine system.

The gravity effect will be added to the system by means of a potential function. The gravitational force of the blade element dr is defined as

$$d\vec{G} = -gdm\ \vec{n}_x \tag{21}$$

The potential function for the gravitational force is given by

$$dP = ghdm \tag{22}$$

where h is a function of q_1, ... q_4, and t, whose absolute value is equal to the distance between the mass center of the blade element cross section and any fixed horizontal plane H.

We are dealing with the expression for the derivative of the potential function $\frac{\partial P}{\partial q_i}$ instead of the potential function itself when we develop the equations of motion by using Lagrange's equation. Therefore we take the derivative of the potential function in Eq. (22) with respect to the generalized coordinate

$$\frac{\partial(dP)}{\partial q_i} = gdm\ \frac{\partial h}{\partial q_i} \tag{23}$$

The velocity of the blade element "dr" measured at the mass center can be expressed as

$$\vec{V}_c = -\frac{dh}{dt}\vec{n}_x + \cdots\cdots\cdots\cdots$$

$$= -\left(\sum_{i=1}^{4}\frac{\partial h}{\partial q_i}\dot{q}_i + \frac{\partial h}{\partial t}\right)\vec{n}_x + \cdots\cdots\cdots \qquad (24)$$

The expression $\frac{\partial h}{\partial q_i}$ be found by dotting Eq. (24) with the unit vector $\vec{n}_x$ and assuming that $\frac{\partial h}{\partial t}$ equals zero.

$$\frac{\partial h}{\partial q_i} = -\frac{\partial \vec{V}_c}{\partial \dot{q}_i}\cdot\vec{n}_x \qquad (25)$$

Substituting the expression $\frac{\partial h}{\partial q_i}$ in Eq. (25) back into Eq. (23), we have the expression $\frac{\partial (dP)}{\partial q_i}$ accounting for the gravity effect to be put into Lagrange's equation

$$\frac{\partial (dP)}{\partial q_i} = gdm\left(-\frac{\partial \vec{V}_c}{\partial \dot{q}_i}\cdot\vec{n}_x\right) \qquad (26)$$

III.5 Tower Shadow

When a rotor is downwind of the tower, the blades pass through the wind shadow cast by the tower. The performance of the wind turbine will be affected by this tower shadow.

In this study, the tower shadow is modeled as the velocity deficit from the rotor axial velocity value over a selected region of the rotor disk, centered about the tower center line. For the simplicity of analysis, the width of the tower shadow is assumed as a segment of the rotor area. The width and the velocity deficit of the tower shadow are dependent on the geometry of the tower. This tower shadow model is shown in Figure III.5.1.

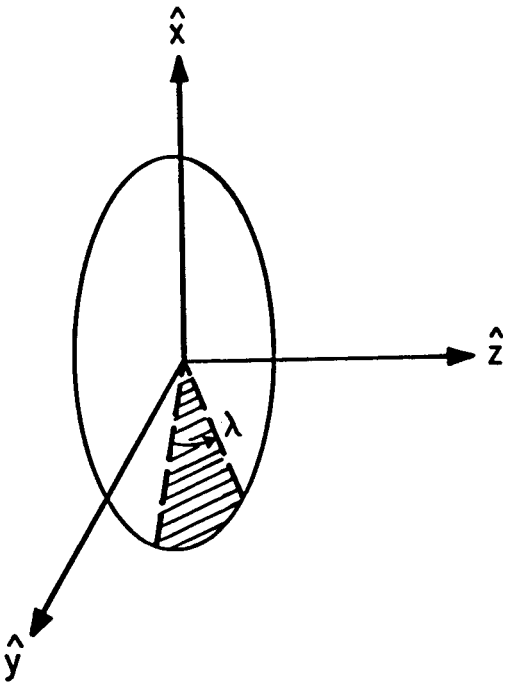

Figure III.5.1 Tower shadow

To account for the tower shadow effect on the equations of motion of the system, the width and the velocity deficit are arbitrarily chosen. Then for this linear system, the superposition method is used. The average forces on the rotor with the tower shadow will be the average forces on the rotor without the tower shadow, plus the difference of average forces in the shadow region between the one with and the one without the velocity deficit due to the tower shadow.

The coefficients of equations of motion will be recalculated for the shadow region. Many terms in the expression for forces and moments that depend on the azimuth angle, which are usually balanced out in the 3-bladed rotor case, will remain in the tower shadow case.

The average forces and moments in the shadow region are given by

$$F_{shadow} = \frac{B}{2\pi} \int_{\pi - \frac{\lambda}{2}}^{\pi + \frac{\lambda}{2}} \int_{R_H}^{R} (dF) d\psi \tag{27}$$

$$\vec{M}_{shadow} = \frac{B}{2\pi} \int_{\pi - \frac{\lambda}{2}}^{\pi + \frac{\lambda}{2}} \int_{R_H}^{R} (\vec{r} \times d\vec{F}) d\psi \tag{28}$$

where

dF = the force on the blade element

λ = the shadow width.

The flow conditions in the tower shadow are developed from a uniform flow model. Thus flow conditions in the tower shadow vary only with velocity deficit and tip speed ratio.

Table III.5.1 gives the values of the integrations from the lower limit of $\pi - \frac{\lambda}{2}$ to $\pi + \frac{\lambda}{2}$.

Table III.5.1. Some Integration Values

$\int_{\pi - \frac{\lambda}{2}}^{\pi + \frac{\lambda}{2}} \sin^2\psi d\psi$	$= \frac{\lambda - \sin\lambda}{2}$
$\int_{\pi - \frac{\lambda}{2}}^{\pi + \frac{\lambda}{2}} \cos^2\psi d\psi$	$= -\frac{(\lambda - \sin\lambda)}{2}$
$\int_{\pi - \frac{\lambda}{2}}^{\pi + \frac{\lambda}{2}} \sin\psi\cos\psi d\psi$	$= 0$
$\int_{\pi - \frac{\lambda}{2}}^{\pi + \frac{\lambda}{2}} \cos\psi d\psi$	$= -2 \sin \frac{\lambda}{2}$
$\int_{\pi - \frac{\lambda}{2}}^{\pi + \frac{\lambda}{2}} \sin\psi d\psi$	$= 0$

APPENDIX IV

LINEARIZED EQUATIONS OF MOTION

IV.1 Linearization

Real systems contain some nonlinearity. If the ranges of values of the dependent variables are sufficiently restricted, the system may be well approximated as linear. In this study we will treat the system in the linear range.

The first thing we need in linearization is the equilibrium value of each dependent variable. Because of the complexity of this rotor system's mathematical model, the equilibrium values have been chosen as

$$\theta_o = 0 \tag{1}$$

$$w_o = R_s f_2(\frac{r}{R}) q_s \tag{2}$$

$$\dot{x}_o = 0 \tag{3}$$

$$\gamma_o = 0 \tag{4}$$

where q_s is the static tip deflection and the subscript 0 indicates that the values are evaluated at nominal values.

We now define the dependent variable as the nominal (equilibrium) term plus a small variation term.

$$q_i(t) = q_{io} + \delta q_i(t) \tag{5}$$

Substituting the value of the generalized coordinate shown in Eq. (5) into the equations of motion and developing a Taylor's Series for the nonlinear function of the generalized coordinates and their derivatives yields the relation given below

$$f(q_i,\dot{q}_i,\ddot{q}_i) = f(q_{i_o},\dot{q}_{i_o},\ddot{q}_{i_o}) + \frac{\partial f(q_{i_o},\dot{q}_{i_o},\ddot{q}_{i_o})}{\partial q_i}\delta q_i + \frac{\partial f(q_{i_o},\dot{q}_{i_o},\ddot{q}_{i_o})}{\partial \dot{q}_i}\delta\dot{q}_i + \frac{\partial f(q_{i_o},\dot{q}_{i_o},\ddot{q}_{i_o})}{\partial \ddot{q}_i}\delta\ddot{q}_i + \cdots\cdots \quad (6)$$

Neglecting higher order terms, we obtain the linearized equation of motion as

$$f(q_i,\dot{q}_i,\ddot{q}_i) = f(q_{i_o},\dot{q}_{i_o},\ddot{q}_{i_o}) + \frac{\partial f(q_{i_o},\dot{q}_{i_o},\ddot{q}_{i_o})}{\partial q_i}\delta q_i + \frac{\partial f(q_{i_o},\dot{q}_{i_o},\ddot{q}_{i_o})}{\partial \dot{q}_i}\delta\dot{q}_i + \frac{\partial f(q_{i_o},\dot{q}_{i_o},\ddot{q}_{i_o})}{\partial \ddot{q}_i}\delta\ddot{q}_i = 0 \quad (7)$$

Linearized Equation of Motion

With the known values of k_η and j_η, the expression for $\frac{\partial a}{\partial \eta}$ in the linearized aeroforce is defined. Then, the linearized equations of motion of the system are expressed in the matrix form as

$$[M^*]\{\delta\ddot{q}_i\} + [C^*]\{\delta\dot{q}_i\} + [K^*]\{\delta q_i\} = \{G\}$$

where

M* = linearized mass coefficient matrix

C* = linearized damping coefficient matrix

K* = linearized stiffness coefficient matrix

G = linearized forcing function vector

The components of the matrices M*, C*, K* and the vector G are:

Mass matrix of the rotor

$$m_{11} = \begin{cases} \frac{3}{q_\infty}\int_{R_H}^{R}\mu\left(\frac{\dot{u}_{c1}}{R}\right)^2\frac{dr}{R} + \frac{3}{q_\infty}\int_{R_H}^{R}\mu\left(\frac{e}{R}\right)^2 f_1^2\frac{dr}{R} - \frac{6}{q_\infty}\int_{R_H}^{R}\mu\frac{\dot{u}_{c1}}{R}\frac{e}{R}\sin w_o f_1\frac{dr}{R} \\ + \frac{3}{q_\infty}\int_{R_H}^{R}\frac{I_1}{R^2}f_1^2\frac{dr}{R} \end{cases}$$

$$m_{12} = m_{21} = \frac{3}{q_\infty}\int_{R_H}^{R}\mu\frac{\dot{u}_{c1}}{R}\frac{\dot{u}_{c2}}{R}\frac{dr}{R} - \frac{3}{q_\infty}\int_{R_H}^{R}\mu\frac{\dot{u}_{c2}}{R}\frac{e}{R}\sin w_o' f_1\frac{dr}{R}$$

$$+ \frac{3}{q_\infty}\int_{R_H}^{R}\mu\frac{e}{R}\frac{R_s}{R}\cos w_o' f_1 f_2\frac{dr}{R}$$

$$m_{13} = m_{31} = \begin{cases} -\frac{3}{q_\infty}\int_{R_H}^{R}\mu\frac{\dot{u}_{c1}}{R}\left(\frac{w_o}{R}\sin\beta\cos\rho + \frac{e}{R}\cos\rho\cos\beta\right)f_3\frac{dr}{R} \\ + \frac{3}{q_\infty}\int_{R_H}^{R}\mu\left(\frac{e}{R}\right)^2\sin w_o'\cos\rho\cos\beta f_1 f_3\frac{dr}{R} \\ + \frac{3}{q_\infty}\int_{R_H}^{R}\mu\left[\frac{e}{R}\frac{(r+u_c)}{R}\cos w_o'\sin\beta\cos\rho + \left(\frac{e}{R}\right)^2\cos w_o'\sin\rho\right]f_1 f_3\frac{dr}{R} \\ + \frac{3}{q_\infty}\int_{R_H}^{R}\mu\frac{e}{R}\frac{w_o}{R}\sin w_o'\sin\beta\cos\rho f_1 f_3\frac{dr}{R} \\ + \frac{3}{q_\infty}\int_{R_H}^{R}\frac{I_1}{R^2}\left(\sin\rho\cos w_o' + \cos\rho\cos\beta\sin w_o'\right)f_1 f_3\frac{dr}{R} \end{cases}$$

$$m_{14} = m_{41} = 0$$

$$m_{22} = \frac{3}{q_\infty}\int_{R_H}^{R}\mu\left(\frac{\dot{u}_{c2}}{R}\right)^2\frac{dr}{R} + \frac{3}{q_\infty}\left(\frac{R_s}{R}\right)^2\int_{R_H}^{R}\mu f_2^2\frac{dr}{R} + \frac{3}{q_\infty}\int_{R_H}^{R}\frac{I_2}{R^2}f_2^2\frac{dr}{R}$$

$$m_{23} = m_{32} = \begin{cases} -\frac{3}{q_\infty}\int_{R_H}^{R} \mu \frac{\dot{u}_{c2}}{R}\left(\frac{w_o}{R}\sin\beta\cos\rho + \frac{e}{R}\cos\rho\cos\beta\right) f_3 \frac{dr}{R} \\ +\frac{3}{q_\infty}\int_{R_H}^{R} \mu\left(\frac{(r+u_c)}{R}\sin\beta\cos\rho + \frac{e}{R}\sin\rho\right)\frac{R_s}{R} f_2 f_3 \frac{dr}{R} \\ +\frac{3}{q_\infty}\int_{R_H}^{R} \frac{I_2}{R^2}\cos\rho\cos\beta f_2' f_3 \frac{dr}{R} \end{cases}$$

$$m_{24} = m_{42} = 0$$

$$m_{33} = \begin{cases} \frac{3}{q_\infty}\int_{R_H}^{R} \mu\left(\frac{w_o^2}{R^2}(\sin^2\beta + \sin^2\rho\cos^2\beta) + \frac{e^2}{R^2}(\cos^2\beta + \sin^2\rho\sin^2\beta)\right. \\ \qquad \left. + \frac{(r+u_c)^2}{R^2}\cos^2\rho\right) f_3^2 \frac{dr}{R} \\ +\frac{6}{q_\infty}\int_{R_H}^{R} \mu\left(\frac{(r+u_c)}{R}\frac{e}{R}\sin\rho\cos\rho\sin\beta - \frac{(r+u_c)}{R}\frac{w_o}{R}\sin\rho\cos\rho\cos\beta\right. \\ \qquad \left. + \frac{w_o}{R}\frac{e}{R}\sin\beta\cos\beta\cos^2\rho\right) f_3^2 \frac{dr}{R} \\ +\frac{3}{q_\infty}\int_{R_H}^{R} \frac{I_1}{R^2}(\sin\rho\cos w_o' + \cos\rho\cos\beta\sin w_o')^2 f_3^2 \frac{dr}{R} \\ \qquad +\frac{3}{q_\infty}\int_{R_H}^{R} \frac{I_2}{R^2}\cos^2\rho\sin^2\beta\, f_3^2 \frac{dr}{R} \\ +\frac{3}{q_\infty}\int_{R_H}^{R} \frac{I_3}{R^2}(\sin\rho\sin w_o' - \cos\rho\cos w_o'\cos\beta)^2 f_3^2 \frac{dr}{R} \\ +\frac{1}{q_\infty R^3}(I_H + n_G^2 I_G) f_3^2 \end{cases}$$

$$m_{34} = m_{43} = 0$$

$$
m_{44} = \left\{
\begin{aligned}
&\frac{3}{2q_\infty}\int_{R_H}^{R} \mu\left[\left(\frac{w_o}{R}\right)^2\left(1+\cos^2\rho\cos^2\beta\right)+\left(\frac{e}{R}\right)^2\left(1+\sin^2\beta\cos^2\rho\right)\right.\\
&\qquad\left.+\frac{(r+u_c)^2}{R^2}\left(1+\sin^2\rho\right)\right] f_4^2\,\frac{dr}{R}\\
&+\frac{3}{q_\infty}\int_{R_H}^{R} \mu\left[\left(\frac{\ell}{R}\right)^2+\frac{2\ell}{R}\frac{w_o}{R}\cos\rho\cos\beta+\frac{2\ell}{R}\frac{(r+u_c)}{R}\sin\rho\right.\\
&\qquad\left.-\frac{2\ell}{R}\frac{e}{R}\cos\rho\sin\beta\right] f_4^2\,\frac{dr}{R}\\
&+\frac{3}{q_\infty}\int_{R_H}^{R} \mu\left(\frac{(r+u_c)}{R}\frac{w_o}{R}\sin\rho\cos\rho\cos\beta-\frac{e}{R}\frac{(r+u_c)}{R}\sin\rho\cos\rho\sin\beta\right.\\
&\qquad\left.-\frac{e}{R}\frac{w_o}{R}\sin\beta\cos\beta\left(1-\sin^2\rho\right)\right] f_4^2\,\frac{dr}{R}\\
&+\frac{3}{2q_\infty}\int_{R_H}^{R} \frac{I_1}{R^2}\left(\cos^2\rho\cos^2 w_o'+\sin^2\rho\sin^2 w_o'\cos^2\beta+\sin^2 w_o'\sin^2\beta\right.\\
&\qquad\left.-2\sin\rho\cos\rho\sin w_o'\cos w_o'\cos\beta\right) f_4^2\,\frac{dr}{R}\\
&+\frac{3}{2q_\infty}\int_{R_H}^{R} \frac{I_2}{R^2}\left(\sin^2\rho\sin^2\beta+\cos^2\beta\right) f_4^2\,\frac{dr}{R}\\
&+\frac{3}{2q_\infty}\int_{R_H}^{R} \frac{I_3}{R^2}\left(\cos^2\rho\sin^2 w_o'+\sin^2\rho\cos^2 w_o'\cos^2\beta+\cos^2 w_o'\sin^2\beta\right.\\
&\qquad\left.+2\sin w_o'\cos w_o'\sin\rho\cos\rho\cos\beta\right) f_4^2\,\frac{dr}{R}
\end{aligned}
\right.
$$

where

μ = blade's mass per unit length

$\dot{u}_{c1} = \dfrac{\partial \dot{u}_c}{\partial \dot{q}_1}$ evaluated at nominal value

$\dot{u}_{c2} = \frac{\partial \dot{u}_c}{\partial \dot{q}_2}$ evaluated at nominal value

I_H = mass moment of inertia of the hub

I_G = mass moment of inertia of the generator unit and gear box

Damping coefficient matrix of the rotor

$$
C_{11} = \left\{
\begin{aligned}
&\frac{3}{q_\infty}\int_{R_H}^{R} \mu\Omega \frac{\partial \dot{u}_{c1}}{R\partial q_1}\left(\frac{w_o}{R}\sin\beta\cos\rho + \frac{e}{R}\cos\rho\cos\beta\right)\frac{dr}{R} \\
&\qquad + \frac{3}{q_\infty}\int_{R_H}^{R} \mu\Omega \frac{\dot{u}_{c1}}{R}\frac{e}{R}\cos\rho\cos w_o'\sin\beta f_1 \frac{dr}{R} \\
&- \frac{3}{q_\infty}\int_{R_H}^{R} \mu\Omega \frac{e}{R}\frac{\partial u_c}{R\partial q_1}\cos w_o'\sin\beta\cos\rho f_1 \frac{dr}{R} - \frac{3}{q_\infty}\int_{R_H}^{R} \mu\Omega \frac{e}{R}\frac{w_o}{R}\sin\rho f_1^2 \frac{dr}{R} \\
&+ \frac{3}{q_\infty}\int_{R_H}^{R} \mu\Omega \frac{e}{R}\frac{(r+u_c)}{R}\cos\beta\cos\rho f_1^2 \frac{dr}{R} + \frac{3\pi}{8}\int_{R_H}^{R} \frac{W_t}{V_\infty}\left(\frac{c}{R}\right)^2 \frac{c}{V_\infty} f_1 \frac{dr}{R} \\
&+ 3\int_{R_H}^{R} \frac{W_t}{V_\infty}\frac{c}{R} C_{n_\alpha} \frac{e_2}{V_\infty}\left(\frac{e_1}{R} f_1 - \frac{\dot{u}_{m1}}{R}\sin w_o'\right) f_1 \frac{dr}{R}
\end{aligned}
\right.
$$

$$
C_{12} = \left\{
\begin{aligned}
&\frac{3}{q_\infty}\int_{R_H}^{R} \mu\Omega \frac{\partial \dot{u}_{c2}}{R\partial q_1}\left(\frac{w_o}{R}\sin\beta\cos\rho + \frac{e}{R}\cos\rho\cos\beta\right)\frac{dr}{R} \\
&\quad + \frac{3}{q_\infty}\int_{R_H}^{R} \mu\Omega \frac{\dot{u}_{c2}}{R}\frac{e}{R}\cos\rho\cos w_o'\sin\beta f_1 \frac{dr}{R} \\
&+ \frac{3}{q_\infty}\int_{R_H}^{R} \mu\Omega \frac{e}{R}\frac{R_s}{R}\sin\beta\sin w_o'\cos\rho f_1 f_2 \frac{dr}{R} \\
&\quad + \frac{3}{q_\infty}\int_{R_H}^{R} \mu\Omega \frac{e}{R}\frac{(r+u_c)}{R}\sin w_o'\sin\beta\cos\rho f_1 f_2' \frac{dr}{R} \\
&+ \frac{3}{q_\infty}\int_{R_H}^{R} \mu\Omega\left(\frac{e}{R}\right)^2\sin\rho\sin w_o' f_1 f_2' \frac{dr}{R} \\
&\quad - \frac{3}{q_\infty}\int_{R_H}^{R} \mu\Omega \frac{e}{R}\cos w_o'\left(\frac{w_o}{R}\sin\beta\cos\rho + \frac{e}{R}\cos\rho\cos\beta\right) f_1 f_2' \frac{dr}{R} \\
&- \frac{3}{q_\infty}\int_{R_H}^{R} \frac{(I_2-I_3)}{R^2}\Omega(\sin\rho\sin w_o' - \cos\rho\cos w_o'\cos\beta) f_1 f_2' \frac{dr}{R} \\
&+ 3\int_{R_H}^{R} \frac{F_1}{V_\infty}\left(R_s\cos w_o' f_2 - R\left(\frac{\dot{u}_{d2}}{R}\right)\sin w_o'\right)\left(\frac{e_1}{R} f_1 - \frac{\dot{u}_{m1}}{R}\sin w_o'\right)\frac{dr}{R}
\end{aligned}
\right.
$$

$$
C_{13} = \left\{
\begin{aligned}
&\frac{6}{q_\infty}\int_{R_H}^{R} \mu\Omega\left(\frac{e}{R}\right)^2(\sin\rho\cos\rho\sin\beta\sin w_o' - \sin\beta\cos\beta\cos w_o'(1-\sin^2\rho))f_1 f_3 \frac{dr}{R} \\
&- \frac{6}{q_\infty}\int_{R_H}^{R} \mu\Omega \frac{e}{R}\frac{w_o}{R}(\cos w_o'(\sin^2\beta+\sin^2\rho\cos^2\beta) \\
&\qquad + \sin\rho\cos\rho\cos\beta\sin w_o')f_1 f_3 \frac{dr}{R} \\
&+ \frac{6}{q_\infty}\int_{R_H}^{R} \mu\Omega \frac{e}{R}\frac{(r+u_c)}{R}(\cos^2\rho\sin w_o' + \sin\rho\cos\beta\cos\rho\cos w_o')f_1 f_3 \frac{dr}{R} \\
&+ \frac{6}{q_\infty}\int_{R_H}^{R} \mu\Omega \frac{\partial u_c}{R\partial q_1}\left(\frac{(r+u_c)}{R}\cos^2\rho\right. \\
&\qquad \left. - \left(\frac{w_o}{R}\cos\beta - \frac{e}{R}\sin\beta\right)\sin\rho\cos\rho\right)f_3 \frac{dr}{R} \\
&- \frac{6}{q_\infty}\int_{R_H}^{R} \frac{(I_2-I_3)}{R^2}\Omega\cos\rho\sin\beta(\sin\rho\sin w_o' - \cos\rho\cos w_o'\cos\beta)f_1 f_3 \frac{dr}{R} \\
&+ 3\int_{R_H}^{R}\left(\left(\frac{(r+u_d)}{V_\infty}\cos w_o' + \frac{w_o}{V_\infty}\sin w_o'\right)\cos\rho\sin\beta\right)F_1\left(\frac{e_1}{R}f_1 - \frac{\dot{u}_{m1}}{R}\sin w_o'\right)f_3 \frac{dr}{R} \\
&-3\int_{R_H}^{R}\frac{e_3}{V_\infty}(\sin\rho\sin w_o' + \cos\rho\sin w_o'\cos\beta)F_1\left(\frac{e_1}{R}f_1 - \frac{\dot{u}_{m1}}{R}\sin w_o'\right)f_3 \frac{dr}{R} \\
&+ 3\int_{R_H}^{R}\left(\frac{w_o}{V_\infty}\sin\rho - \frac{(r+u_d)}{V_\infty}\cos\rho\cos\beta\right)F_2\left(\frac{e_1}{R}f_1 - \frac{\dot{u}_{m1}}{R}\sin w_o'\right)f_3 \frac{dr}{R}
\end{aligned}
\right.
$$

$$C_{14} = 0$$

$$
C_{21} = \left\{
\begin{aligned}
&\frac{3}{q_\infty}\int_{R_H}^{R} \mu\Omega \frac{\partial \dot{u}_{c1}}{R\partial q_2}\left(\frac{w_o}{R}\sin\beta\cos\rho + \frac{e}{R}\cos\rho\cos\beta\right)\frac{dr}{R} \\
&+\frac{3}{q_\infty}\int_{R_H}^{R} \mu\Omega \frac{\dot{u}_{c1}}{R}\frac{R_s}{R}\sin\beta\cos\rho f_2\frac{dr}{R} + \frac{3}{q_\infty}\int_{R_H}^{R}\mu\Omega\left(\frac{e}{R}\right)^2\sin\rho\sin w_o' f_1 f_2'\frac{dr}{R} \\
&+\frac{3}{q_\infty}\int_{R_H}^{R}\mu\Omega\frac{e}{R}\frac{(r+u_c)}{R}\sin\beta\sin w_o' f_1 f_2'\frac{dr}{R} \\
&+\frac{3}{q_\infty}\int_{R_H}^{R}\mu\Omega\frac{e}{R}\frac{R_s}{R}\sin\beta\cos\beta\sin\rho\cos w_o' f_1 f_2\frac{dr}{R} \\
&\quad -\frac{3}{q_\infty}\int_{R_H}^{R}\mu\Omega\frac{\partial u_c}{R\partial q_2}\frac{e}{R}\cos w_o'\sin\beta\cos\rho f_1\frac{dr}{R} \\
&-\frac{3}{q_\infty}\int_{R_H}^{R}\mu\Omega\frac{e}{R}\cos w'\left(\frac{w_o}{R}\sin\beta\cos\rho + \frac{e}{R}\cos\rho\cos\beta\right)f_1 f_2'\frac{dr}{R} \\
&\quad -\frac{3}{q_\infty}\int_{R_H}^{R}\mu\Omega\frac{R_s}{R}\frac{e}{R}\sin w_o'\sin\beta\cos\rho f_1 f_2\frac{dr}{R} \\
&+\frac{3}{q_\infty}\int_{R_H}^{R}\frac{I_1}{R^2}\Omega\left(\sin\rho\sin w_o' - \cos\rho\cos w_o'\cos\beta\right)f_1 f_2'\frac{dr}{R} \\
&+3\int_{R_H}^{R}\frac{W_t}{V_\infty}\frac{e}{R}C_{n_\alpha}\frac{e_2}{V_\infty}\left(\frac{R_s}{R}f_2\cos w_o' - \frac{\dot{u}_{m2}}{R}\sin w_o'\right)f_1\frac{dr}{R}
\end{aligned}
\right.
$$

$$
C_{22} = \left\{
\begin{aligned}
&\frac{3}{q_\infty}\int_{R_H}^{R}\mu\Omega\frac{\partial \dot{u}_{c2}}{R\partial q_2}\left(\frac{w_o}{R}\sin\beta\cos\rho + \frac{e}{R}\cos\rho\cos\beta\right)\frac{dr}{R} \\
&\quad +\frac{3}{q_\infty}\int_{R_H}^{R}\mu\Omega\frac{\dot{u}_{c2}}{R}\frac{R_s}{R}\sin\beta\cos\rho f_2\frac{dr}{R} \\
&+3\int_{R_H}^{R}\frac{F_1}{V_\infty}\left(R_s\cos w_o' f_2 - R\left(\frac{\dot{u}_{d2}}{R}\right)\sin w_o'\right)\left(\frac{R_s}{R}f_2\cos w_o' - \frac{\dot{u}_{m2}}{R}\sin w_o'\right)\frac{dr}{R}
\end{aligned}
\right.
$$

$$
C_{23} = \left\{
\begin{aligned}
&-\frac{6}{q_\infty}\int_{R_H}^{R}\mu\Omega\,\frac{w_o}{R}\,\frac{R_s}{R}\,(\sin^2\beta+\sin^2\rho\cos^2\beta)f_2f_3\,\frac{dr}{R}\\
&\qquad-\frac{6}{q_\infty}\int_{R_H}^{R}\mu\Omega\,\frac{e}{R}\,\frac{R_s}{R}\,\sin\beta\cos\beta(1-\sin^2\rho)f_2f_3\,\frac{dr}{R}\\
&-\frac{6}{q_\infty}\int_{R_H}^{R}\mu\Omega\frac{\partial u_c}{R\partial q_1}\Big(\frac{(r+u_c)}{R}\cos^2\rho-\Big(\frac{w_o}{R}\cos\beta-\frac{e}{R}\sin\beta\Big)\sin\rho\cos\rho\Big)f_3\,\frac{dr}{R}\\
&+\frac{6}{q_\infty}\int_{R_H}^{R}\mu\Omega\,\frac{(r+u_c)}{R}\,\frac{R_s}{R}\,\sin\rho\cos\beta f_2f_3\,\frac{dr}{R}\\
&-\frac{6}{q_\infty}\int_{R_H}^{R}\frac{R(I_2-I_3)}{R^2}\Omega[\sin\rho\cos\rho\cos\beta\cos2w_o'\\
&\qquad+\sin w_o'\cos w_o'(\cos^2\rho\cos^2\beta-\sin^2\rho)]f_2'f_3\,\frac{dr}{R}\\
&+3\int_{R_H}^{R}\Big[\frac{(r+u_d)}{V_\infty}\cos w_o'\cos\rho\sin\beta+\frac{w_o}{V_\infty}\sin w_o'\cos\rho\cos\beta\Big]F_1\Big(\frac{R_s}{R}f_2\cos w_o'\\
&\qquad\qquad-\frac{\dot u_{m2}}{R}\sin w_o'\Big)f_3\,\frac{dr}{R}\\
&-3\int_{R_H}^{R}\Big[\frac{e_3}{V_\infty}(\sin\rho\sin w_o'+\cos\rho\sin w_o'\cos\beta)F_1-\Big(\frac{w_o}{V_\infty}\sin\rho\\
&\qquad-\frac{(r+u_d)}{V_\infty}\cos\rho\cos\beta\Big)F_2\Big]\Big(\frac{R_s}{R}f_2\cos w_o'-\frac{\dot u_{m2}}{R}\sin w_o'\Big)f_3\,\frac{dr}{R}
\end{aligned}
\right.
$$

$$C_{24} = 0$$

$$C_{31} = \begin{cases} 3\int_{R_H}^{R} \frac{W_t}{V_\infty}\frac{c}{R}C_{n_\alpha}\frac{e_2}{V_\infty}\left[\frac{(r+u_m)}{R}\cos w_o'\cos\rho\sin\beta\right. \\ \qquad \left. + \frac{w_o}{R}\sin w_o'\cos\rho\sin\beta\right] f_1 f_3 \frac{dr}{R} \\ 3\int_{R_H}^{R} \frac{W_t}{V_\infty}\frac{c}{R}C_{n_\alpha}\frac{e_2}{V_\infty}\frac{e_1}{R}(\sin\rho\cos w_o'+\cos\rho\sin w_o'\cos\beta) f_1 f_3 \frac{dr}{R} \\ 3\int_{R_H}^{R} \frac{W_t}{V_\infty}\frac{c}{R}C_{t_\alpha}\frac{e_2}{V_\infty}\left(\frac{(r+u_m)}{R}\cos\rho\sin\beta - \frac{w_o}{R}\sin\rho\right) f_1 f_3 \frac{dr}{R} \\ \frac{3\pi}{8}\int_{R_H}^{R} \frac{W_T}{V_\infty}\left(\frac{c}{R}\right)^2\frac{c}{V_\infty}(\sin\rho\cos w_o'+\cos\rho\sin w_o'\cos\beta) f_1 f_3 \frac{dr}{R} \end{cases}$$

$$C_{32} = \begin{cases} 3\int_{R_H}^{R} \frac{F_1}{V_\infty}(K_s\cos w_o' f_2 - \dot{u}_{d2}\sin w_o')\left(\frac{(r+u_m)}{R}\cos w_o'\cos\rho\sin\beta\right. \\ \qquad \left. + \frac{w_o}{R}\sin w_o'\cos\rho\sin\beta\right) f_3 \frac{dr}{R} \\ 3\int_{R_H}^{R} \frac{F_1}{V_\infty}(R_s\cos w_o' f_2 - \dot{u}_{d2}\sin w_o')\frac{e_1}{R}(\sin\rho\cos w_o'+\cos\rho\sin w_o'\cos\beta) f_3 \frac{dr}{R} \\ 3\int_{R_H}^{R} \frac{G_1}{V_\infty}(R_s\cos w_o' f_2 - \dot{u}_{d2}\sin w_o')\left(\frac{(r+u_m)}{R}\cos\rho\sin\beta - \frac{w_o}{R}\sin\rho\right) f_3 \frac{dr}{R} \end{cases}$$

$$C_{33} = \begin{cases} 3\int_{R_H}^{R} N6\left(\frac{(r+u_m)}{R}\cos w_o'\cos\rho\sin\beta + \frac{w_o}{R}\sin w_o'\cos\rho\sin\beta\right. \\ \qquad \left. + \frac{e_1}{R}(\sin\rho\cos w_o'+\cos\rho\sin w_o'\cos\beta)\right) f_3^2 \frac{dr}{R} \\ 3\int_{R_H}^{R} H6\left(\frac{(r+u_m)}{R}\cos\rho\sin\beta - \frac{w_o}{R}\sin\rho\right) f_3^2 \frac{dr}{R} + C_G \end{cases}$$

$$C_{34} = 0$$

$$C_{41} = C_{42} = C_{43} = 0$$

where

$$N6 = \begin{cases} \{\frac{(r+u_d)}{V_\infty} \cos w_o' \cos\rho \sin\beta + \frac{w_o}{V_\infty} \sin w_o' \cos\rho \sin\beta\} F_1 \\ -\frac{e_3}{V_\infty}(\sin\rho \sin w_o' + \cos\rho \sin w_o' \cos\beta) F_1 + (\frac{w_o}{V_\infty} \sin\rho - \frac{(r+u_d)}{V_\infty} \cos\rho \cos\beta) F_2 \end{cases}$$

$$H6 = \begin{cases} (\frac{(r+u_d)}{V_\infty} \cos w_o' \cos\rho \sin\beta + \frac{w_o}{V_\infty} \sin w_o' \cos\rho \sin\beta) G_1 \\ -\frac{e_3}{V_\infty}(\sin\rho \sin w_o' + \cos\rho \sin w_o' \cos\beta) G_1 + (\frac{w_o}{V_\infty} \sin\rho - \frac{(r+u_d)}{V_\infty} \cos\rho \cos\beta) G_2 \end{cases}$$

C_G = Slip rate

$$
C_{44} = \left\{
\begin{aligned}
&\frac{3}{2}\int_{R_H}^{R} (N4)\left(\frac{\ell}{R}\sin\beta\cos w_o' + \frac{(r+u_m)}{R}\sin\rho\sin\beta\cos w_o'\right.\\
&\qquad\left. + \frac{w_o}{R}\sin w_o'\sin\rho\sin\beta\right) f_4^2\,\frac{dr}{R}\\
&\frac{3}{2}\int_{R_H}^{R} (N4)\,\frac{e_1}{R}\left(\sin\rho\sin w_o'\cos\beta - \cos\rho\cos w_o'\right) f_4^2\,\frac{dr}{R}\\
&\frac{3}{2}\int_{R_H}^{R} (N5)\left(\frac{\ell}{R}\left(\sin\rho\cos\beta\cos w_o' + \sin w_o'\cos\rho\right) + \frac{(r+u_m)}{R}\cos\beta\cos w'\right.\\
&\qquad\left. + \frac{w_o}{R}\sin w_o'\cos\beta\right) f_4^2\,\frac{dr}{R}\\
&-\frac{3}{2}\int_{R_H}^{R} (N5)\,\frac{e_1}{R}\sin w_o'\sin\beta f_4^2\,\frac{dr}{R}\\
&+\frac{3}{2}\int_{R_H}^{R} (H4)\left(\frac{\ell}{R}\cos\beta + \frac{(r+u_m)}{R}\sin\rho\cos\beta + \frac{w_o}{R}\cos\rho\right) f_4^2\,\frac{dr}{R}\\
&-\frac{3}{2}\int_{R_H}^{R} (H5)\left(\frac{\ell}{R}\sin\rho\sin\beta + \frac{(r+u_m)}{R}\sin\beta\right) f_4^2\,\frac{dr}{R}\\
&+\frac{3}{2}\,j_{\dot{q}_4}\int_{R_H}^{R} (N1)\left(\frac{\ell}{R}\sin\beta\cos w_o' + \frac{(r+u_m)}{R}\sin\rho\sin\beta\cos w_o'\right.\\
&\qquad\left. + \frac{w_o}{R}\sin w_o'\sin\rho\sin\beta\right)\frac{r_N}{R} f_4\,\frac{dr}{R}\\
&+\frac{3}{2}\,j_{\dot{q}_4}\int_{R_H}^{R} (N1)\,\frac{e_1}{R}\left(\sin\rho\sin w_o'\cos\beta - \cos\rho\cos w_o'\right)\frac{r_N}{R} f_4\,\frac{dr}{R}\\
&+\frac{3}{2}\,j_{\dot{q}_4}\int_{R_H}^{R} (H1)\left(\frac{\ell}{R}\cos\beta + \frac{(r+u_m)}{R}\sin\rho\cos\beta + \frac{w_o}{R}\cos\rho\right)\frac{r_N}{R} f_4\,\frac{dr}{R}\\
&-\frac{3}{2}\,k_{\dot{q}_4}\int_{R_H}^{R} (N1)\left(\frac{\ell}{R}\left(\sin\rho\cos\beta\cos w_o' + \sin w_o'\cos\rho\right) + \frac{(r+u_m)}{R}\cos\beta\cos w_o'\right.\\
&\qquad\left. + \frac{w_o}{R}\sin w_o'\cos\beta\right)\frac{r_N}{R} f_4\,\frac{dr}{R}
\end{aligned}
\right.
$$

$$
\begin{cases}
+\frac{3}{2}k_{\dot{q}_4}\int_{R_H}^{R}(N1)\,\frac{e_1}{R}\sin w_o'\sin\beta\,\frac{r_N}{R}f_4\,\frac{dr}{R} \\
+\frac{3}{2}k_{\dot{q}_4}\int_{R_H}^{R}(H1)\,\left(\frac{\ell}{R}\sin\rho\sin\beta+\frac{(r+u_m)}{R}\sin\beta\right)\frac{r_N}{R}f_4\,\frac{dr}{R}
\end{cases}
$$

Stiffness coefficient matrix of the rotor

$$
k_{11}=\begin{cases}
-\frac{3}{q_\infty}\int_{R_H}^{R}\mu\Omega^2\frac{e^2}{R^2}\cos w_o'^2(\sin^2\beta+\sin^2\rho\cos^2\beta)f_1^2\,\frac{dr}{R} \\
+\frac{3}{q_\infty}\int_{R_H}^{R}\mu\Omega^2\left(\frac{e}{R}\right)^2(\cos^2\beta+\sin^2\rho\sin^2\beta)f_1^2\,\frac{dr}{R} \\
-\frac{6}{q_\infty}\int_{R_H}^{R}\mu\Omega^2\left(\frac{e}{R}\right)^2\sin\rho\cos^2\rho\cos\beta\sin w_o'\cos w_o'f_1^2\,\frac{dr}{R} \\
-\frac{3}{q_\infty}\int_{R_H}^{R}\mu\Omega^2\left(\frac{e}{R}\right)^2\cos^2\rho\sin^2 w_o'f_1^2\,\frac{dr}{R} \\
+\frac{3}{q_\infty}\int_{R_H}^{R}\mu\Omega^2\frac{e}{R}\frac{w_o}{R}\sin\beta\cos\beta(1-\sin^2\rho)f_1^2\,\frac{dr}{R} \\
+\frac{3}{q_\infty}\int_{R_H}^{R}\mu\Omega^2\frac{e}{R}\frac{(r+u_c)}{R}\sin\rho\cos\rho\sin\beta f_1^2\,\frac{dr}{R} \\
-\frac{3}{q_\infty}\int_{R_H}^{R}\mu\Omega^2\cos^2\rho\left(\frac{\partial u_c}{R\partial q_1}\right)^2\frac{dr}{R} \\
-\frac{3}{q_\infty}\int_{R_H}^{R}\mu\Omega^2\left(\frac{(r+u_c)}{R}\cos^2\rho-\frac{w_o}{R}\sin\rho\cos\rho\cos\beta+\frac{e}{R}\sin\rho\cos\rho\sin\beta\right)\frac{\partial^2 u_c}{R\partial q_1^2}\,\frac{dr}{R} \\
-\frac{3}{q_\infty}\int_{R_H}^{R}\frac{(I_2-I_3)}{R^2}\Omega^2(\sin\rho\sin w_o'-\cos\rho\cos w_o'\cos\beta)^2f_1^2\,\frac{dr}{R} \\
-\frac{3}{q_\infty}\int_{R_H}^{R}\frac{(I_2-I_3)}{R^2}\Omega^2\cos^2\rho\sin^2\beta f_1^2\,\frac{dr}{R}+\frac{3}{q_\infty}\int_{R_H}^{R}\frac{GJ}{R^4}f_1'^2\,\frac{dr}{R} \\
-3\int_{R_H}^{R}\frac{\Omega e_3}{V_\infty}F_2(\sin\rho\cos w_o'+\cos\rho\sin w_o'\cos\beta)\left(\frac{e_1}{R}f_1-\frac{\dot{u}_{m1}}{R}\sin w_o'\right)f_1\,\frac{dr}{R}
\end{cases}
$$

$$
\left\{
\begin{aligned}
&- 3 \int_{R_H}^{R} \frac{\Omega R}{V_\infty} \left(\frac{\partial u_d}{R\partial q_1}\right)\left(-\cos w_o' \cos\rho \sin\beta\ F_1 + \cos\rho\cos\beta\ F_2\right)\left(\frac{e_1}{R} f_1 \right.\\
&\qquad \left. - \frac{\dot{u}_{m1}}{R} \sin w_o'\right) \frac{dr}{R} - 3 \int_{R_H}^{R} F_4 \left(\frac{e_1}{R} f_1 - \frac{\dot{u}_{m1}}{R} \sin w_o'\right) \frac{dr}{R}\\
&+ 3 \int_{R_H}^{R} N_o \frac{\partial \dot{u}_{m1}}{R\partial q_1} \sin w_o' \frac{dr}{R} + 3 \int_{R_H}^{R} H_o \frac{e_1}{R} f_1^2 \frac{dr}{R}
\end{aligned}
\right.
$$

$$k_{12} = k_{12a} + k_{12b}$$

$$
k_{12a} = \left\{
\begin{aligned}
&\frac{3}{q_\infty} \int_{R_H}^{R} \mu\Omega^2 \left(\frac{e}{R}\right)^2 \left(\sin\beta\cos\beta\sin w_o'\left(1-\sin^2\rho\right) - \sin\rho\cos\rho\sin\beta\cos w_o'\right) f_1 f_2' \frac{dr}{R}\\
&- \frac{3}{q_\infty} \int_{R_H}^{R} \mu\Omega^2 \frac{e}{R} \frac{R_s}{R} \left(\cos w_o'\left(\sin^2\beta + \sin^2\rho\cos^2\beta\right)\right.\\
&\qquad \left. + \sin\rho\cos\rho\cos\beta\sin w_o'\right) f_1 f_2 \frac{dr}{R}\\
&+ \frac{3}{q_\infty} \int_{R_H}^{R} \mu\Omega^2 \frac{e}{R} \frac{w_o}{R} \left(\sin w_o'\left(\sin^2\beta + \sin^2\rho\cos^2\beta\right)\right.\\
&\qquad \left. - \sin\rho\cos\rho\cos\beta\cos w_o'\right) f_1 f_2' \frac{dr}{R}\\
&- \frac{3}{q_\infty} \int_{R_H}^{R} \mu\Omega^2 \frac{e}{R} \frac{(r+u_c)}{R} \left(\sin\rho\cos\rho\cos\beta\sin w_o' - \cos^2\rho\cos w_o'\right) f_1 f_2' \frac{dr}{R}\\
&- \frac{3}{q_\infty} \int_{R_H}^{R} \mu\Omega^2 \frac{\partial^2 u_c}{R\partial q_1 \partial q_2} \left(\frac{(r+u_c)}{R}\cos^2\rho - \left(\frac{w_o}{R}\cos\beta - \frac{e}{R}\sin\beta\right)\sin\rho\cos\beta\right) \frac{dr}{R}\\
&- \frac{3}{q_\infty} \int_{R_H}^{R} \mu\Omega^2 \frac{\partial u_c}{R\partial q_1} \frac{\partial u_c}{R\partial q_2} \cos^2\rho \frac{dr}{R}\\
&- \frac{3}{q_\infty} \int_{R_H}^{R} \frac{(I_2 - I_3)}{R^2} \Omega^2 \cos\rho\sin\beta \left(\sin\rho\cos w_o' + \cos\rho\sin w_o'\cos\beta\right) f_1 f_2' \frac{dr}{R}
\end{aligned}
\right.
$$

$$k_{12b} = \begin{cases} +3 \int_{R_H}^{R} (N7)\left(\frac{e_1}{R} f_1 - \frac{\dot{u}_{m1}}{R} \sin w_o'\right) \frac{dr}{R} \\ +3 \int_{R_H}^{R} N_o \frac{\partial \dot{u}_{m1}}{R \partial q_2} \sin w_o' \frac{dr}{R} + 3 \int_{R_H}^{R} N_o \frac{\dot{u}_{m1}}{R} \cos w_o' f_2' \frac{dr}{R} \end{cases}$$

where

$$N7 = \begin{cases} \left((\sin\rho\cos w_o' + \cos\rho \sin w_o' \cos\beta)(1-a) f_2' - \Omega \frac{(r+u_d)}{V_\infty} \sin w_o' \cos\rho \sin\beta f_2' \right. \\ \qquad \left. + \frac{\Omega R}{V_\infty} \cos w_o' \cos\rho \sin\beta \frac{\partial u_d}{R \partial q_2}\right) F_1 \\ \left(\frac{\Omega R}{V_\infty} \frac{R_s}{R} \sin w_o' \cos\rho \sin\beta f_2 + \frac{\Omega w_o}{V_\infty} \cos w_o' \cos\rho \sin\beta f_2' \right. \\ \qquad \left. + \frac{\Omega e_3}{V_\infty} \left(\sin\rho \sin w_o' - \cos\rho \cos w_o' \cos\beta\right) f_2'\right) F_1 \\ \qquad + \left(\frac{\Omega R}{V_\infty} \frac{R_s}{R} \sin\rho f_2 - \frac{\Omega R}{V_\infty} \frac{\partial u_d}{R \partial q_2} \cos\rho \cos\beta\right) F_2 \end{cases}$$

$N_o = \left[\left(\frac{W_e}{V_\infty}\right)^2 \frac{c}{R} C_n\right]$ evaluated at nominal value

$H_o = \left[\left(\frac{W_e}{V_\infty}\right) \frac{c}{R} C_t\right]$ evaluated at nominal value

$$k_{13} = k_{14} = 0$$

$$k_{21} = k_{12a} + k_{21b}$$

$$
k_{21b} = \begin{cases}
-3\int_{R_H}^{R}\frac{\Omega e_3}{V_\infty}\left(\sin\rho\cos w_o' + \cos\rho\sin w_o'\cos\beta\right)F_2\left(\frac{R_s}{R}\cos w_o' f_2 - \frac{\dot{u}_{m2}}{R}\sin w_o'\right)f_1\frac{dr}{R} \\
+3\int_{R_H}^{R}\frac{R\Omega}{V_\infty}\left(\frac{\partial u_d}{R\partial q_1}\right)\left(\cos w_o'\sin\beta F_1 - \cos\beta F_2\right)\cos\rho\left(\frac{R_s}{R}\cos w_o' f_2 - \frac{\dot{u}_{m2}}{R}\sin w_o'\right)\frac{dr}{R} \\
+3\int_{R_H}^{R} N_o\frac{\partial\dot{u}_{m2}}{R\partial q_1}\sin w_o'\frac{dr}{R} - 3\int_{R_H}^{R} F_4\left(\frac{R_s}{R}\cos w_o' f_2 - \frac{\dot{u}_{m2}}{R}\sin w_o'\right)\frac{dr}{R}
\end{cases}
$$

$$
k_{22} = \begin{cases}
-\frac{3}{q_\infty}\int_{R_H}^{R}\mu\Omega^2\left(\frac{R_s}{R}\right)^2\left(\sin^2\beta + \cos^2\beta\sin^2\rho\right)f_2^2\frac{dr}{R} \\
-\frac{3}{q_\infty}\int_{R_H}^{R}\mu\Omega^2\cos^2\rho\left(\frac{\partial u_c}{R\partial q_2}\right)^2\frac{dr}{R} \\
-\frac{3}{q_\infty}\int_{R_H}^{R}\mu\Omega^2\frac{\partial^2 u_c}{R\partial q_2^2}\left[\frac{(r+u_c)}{R}\cos^2\rho - \left(\frac{w_o}{R}\cos\beta - \frac{e}{R}\sin\beta\right)\sin\rho\cos\rho\right]\frac{dr}{R} \\
+\frac{3}{q_\infty}\int_{R_H}^{R}\frac{(I_1-I_3)}{R^2}\Omega^2\cos 2w_o'\left(\sin^2\rho - \cos^2\rho\cos^2\beta\right)f_2'^2\frac{dr}{R} \\
+\frac{12}{q_\infty}\int_{R_H}^{R}\frac{(I_1-I_3)}{R^2}\Omega^2\sin\rho\cos\rho\sin w_o'\cos w_o'\cos\beta f_2'^2\frac{dr}{R} \\
+\frac{3}{q_\infty}\int_{R_H}^{R}\frac{EI}{R^4}f_2''^2\frac{dr}{R} \\
+3\int_{R_H}^{R}(N7)\left(\frac{R_s}{R}f_2\cos w_o' - \frac{\dot{u}_{m2}}{R}\sin w_o'\right)\frac{dr}{R} \\
+3\int_{R_H}^{R} N_o\frac{R_s}{R}\sin w_o' f_2' f_2\frac{dr}{R} + 3\int_{R_H}^{R} N_o\frac{\partial\dot{u}_{m2}}{R\partial q_2}\sin w_o'\frac{dr}{R} \\
+3\int_{R_H}^{R} N_o\frac{\partial\dot{u}_{m2}}{R}\cos w_o' f_2'\frac{dr}{R}
\end{cases}
$$

$$k_{23} = k_{24} = 0$$

$$k_{31} = \left\{ \begin{array}{l}
-3\int_{R_H}^{R} \frac{\Omega e_3}{V_\infty}(\sin\rho\cos w_o' + \cos\rho\sin w_o'\cos\beta)F_2\left(\frac{(r+u_m)}{R}\cos w_o'\cos\rho\sin\beta \right. \\
\qquad \left. + \frac{w_o}{R}\sin w_o'\cos\rho\sin\beta + \frac{e_1}{R}(\sin\rho\cos w_o' + \cos\rho\sin w_o'\cos\beta)\right)f_1 f_3 \frac{dr}{R} \\
-3\int_{R_H}^{R} \frac{\Omega e_3}{V_\infty}(\sin\rho\cos w_o' + \cos\rho\sin w_o'\cos\beta)G_2\left(\frac{(r+u_m)}{R}\cos\rho\sin\beta \right. \\
\qquad \left. - \frac{w_o}{R}\sin\rho\right)f_1 f_3 \frac{dr}{R} \\
-3\int_{R_H}^{R}\left[\frac{\Omega R}{V_\infty}\left(\frac{\partial u_d}{R\partial q_1}\right)(-\cos w_o'\sin\beta F_1 + \cos\beta F_2)\cos\rho + F_4\right]\left(\frac{w_o}{R}\sin w_o'\cos\rho\sin\beta \right. \\
\qquad \left. + \left(\frac{r+u_m}{R}\right)\cos w_o'\cos\rho\sin\beta + \frac{e_1}{R}(\sin\rho\cos w_o' + \cos\rho\sin w_o'\cos\beta)\right)f_3 \frac{dr}{R} \\
-3\int_{R_H}^{R}\left[\frac{\Omega R}{V_\infty}\left(\frac{\partial u_d}{R\partial q_1}\right)(-\cos w_o'\sin\beta G_1 + \cos\beta G_2)\cos\rho \right. \\
\qquad \left. + G_4\right]\left(\frac{(r+u_m)}{R}\cos\rho\sin\beta - \frac{w_o}{R}\sin\rho\right)f_3 \frac{dr}{R} \\
-3\int_{R_H}^{R} N_o \frac{\partial u_m}{R\partial q_1}\cos w_o'\cos\rho\sin\beta f_3 \frac{dr}{R} - 3\int_{R_H}^{R} H_o \frac{\partial u_m}{R\partial q_1}\cos\rho\cos\beta f_3 \frac{dr}{R} \\
+3\int_{R_H}^{R} H_o \frac{e_1}{R}(\sin\rho\cos w_o' + \cos\rho\sin w_o'\cos\beta)f_1 f_3 \frac{dr}{R}
\end{array} \right.$$

$$
k_{32} = \begin{cases}
3\int_{R_H}^{R} (N7)\left(\frac{(r+u_m)}{R}\cos w_o'\cos\rho\sin\beta + \frac{w_o}{R}\sin w_o'\cos\rho\sin\beta\right)f_3\frac{dr}{R} \\
+ 3\int_{R_H}^{R} (N7)\frac{e_1}{R}\left(\sin\rho\cos w_o' + \cos\rho\sin w_o'\cos\beta\right)f_3\frac{dr}{R} \\
+ 3\int_{R_H}^{R} (H7)\left(\frac{(r+u_m)}{R}\cos\rho\sin\beta - \frac{w_o}{R}\sin\rho\right)f_3\frac{dr}{R} \\
- 3\int_{R_H}^{R} N_o\frac{\partial u_m}{R\partial q_2}\cos w_o'\cos\rho\sin\beta f_3\frac{dr}{R} \\
+ 3\int_{R_H}^{R} N_o\left(\frac{(r+u_m)}{R}f_2' - \frac{R_s}{R}f_2\right)\sin w_o'\cos\rho\sin\beta f_3\frac{dr}{R} \\
- 3\int_{R_H}^{R} N_o\frac{w_o}{R}\cos w_o'\cos\rho\sin\beta f_2' f_3\frac{dr}{R} \\
3\int_{R_H}^{R} N_o\frac{e_1}{R}\left(\sin\rho\sin w_o' - \cos\rho\cos w_o'\cos\beta\right)f_2' f_3\frac{dr}{R} \\
- 3\int_{R_H}^{R} H_o\frac{\partial u_m}{R\partial q_2}\cos\rho\cos\beta f_3\frac{dr}{R} + 3\int_{R_H}^{R} H_o\frac{R_s}{R}\sin\rho f_2 f_3\frac{dr}{R}
\end{cases}
$$

$$k_{33} = k_{34} = 0$$

$$k_{41} = k_{42} = k_{43} = 0$$

$$
k_{44} = \left\{
\begin{aligned}
&\frac{3}{2}\int_{R_H}^{R}(N2)\left(\frac{\ell}{R}\sin\beta\cos w_o' + \frac{(r+u_m)}{R}\sin\rho\sin\beta\cos w_o'\right.\\
&\qquad\left.+\frac{w_o}{R}\sin w_o'\sin\rho\sin\beta\right)f_4^2\frac{dr}{R}\\
&\frac{3}{2}\int_{R_H}^{R}(N2)\frac{e_1}{R}\left(\sin\rho\sin w_o'\cos\beta-\cos\rho\cos w_o'\right)f_4^2\frac{dr}{R}\\
&\frac{3}{2}\int_{R_H}^{R}(N3)\left(\frac{\ell}{R}\left(\sin\rho\cos\beta\cos w_o'+\sin w_o'\cos\rho\right)+\frac{(r+u_m)}{R}\cos\beta\cos w_o'\right.\\
&\qquad\left.+\frac{w_o}{R}\sin w_o'\cos\beta\right)f_4^2\frac{dr}{R} - \frac{3}{2}\int_{R_H}^{R}(N3)\frac{e_1}{R}\sin w_o'\sin\beta f_4^2\frac{dr}{R}\\
&-\frac{3}{2}\int_{R_H}^{R}(H3)\left(\frac{\ell}{R}\sin\rho\sin\beta+\frac{(r+u_m)}{R}\sin\beta\right)f_4^2\frac{dr}{R}\\
&+\frac{3}{2}\int_{R_H}^{R}(H2)\left(\frac{\ell}{R}\cos\beta+\frac{(r+u_m)}{R}\sin\rho\cos\beta+\frac{w_o}{R}\cos\rho\right)f_4^2\frac{dr}{R}\\
&+\frac{3}{2}j_{q_4}\int_{R_H}^{R}(N1)\left(\frac{\ell}{R}\sin\beta\cos w_o'+\frac{(r+u_m)}{R}\sin\rho\sin\beta\cos w_o'\right.\\
&\qquad\left.+\frac{w_o}{R}\sin w_o'\sin\rho\sin\beta\right)\frac{r_N}{R}f_4\frac{dr}{R}\\
&+\frac{3}{2}j_{q_4}\int_{R_H}^{R}(N1)\frac{e_1}{R}\left(\sin\rho\sin w_o'\cos\beta-\cos\rho\cos w_o'\right)\frac{r_N}{R}f_4\frac{dr}{R}\\
&+\frac{3}{2}j_{q_4}\int_{R_H}^{R}(H1)\left(\frac{\ell}{R}\cos\beta+\frac{(r+u_m)}{R}\sin\rho\cos\beta+\frac{w_o}{R}\cos\rho\right)\frac{r_N}{R}f_4\frac{dr}{R}\\
&-\frac{3}{2}k_{q_4}\int_{R_H}^{R}(N1)\left(\frac{\ell}{R}\left(\sin\rho\cos\beta\cos w_o'+\sin w_o'\cos\rho\right)+\frac{(r+u_m)}{R}\cos\beta\cos w_o'\right.\\
&\qquad\left.+\frac{w_o}{R}\sin w_o'\cos\beta-\frac{e_1}{R}\sin w_o'\sin\beta\right)\frac{r_N}{R}f_4\frac{dr}{R}\\
&+\frac{3}{2}k_{q_4}\int_{R_H}^{R}(H1)\left(\frac{\ell}{R}\sin\rho\sin\beta+\frac{(r+u_m)}{R}\sin\beta\right)\frac{r_N}{R}f_4\frac{dr}{R}
\end{aligned}
\right.
$$

Forcing function vector

$$
G_{01} = \left\{
\begin{aligned}
&\frac{3}{q_\infty}\int_{R_H}^{R}\mu\Omega^2\left(\frac{e}{R}\right)^2\left(\sin\beta\cos\beta\cos w_o'\left(1-\sin^2\rho\right)-\sin\rho\cos\rho\sin\beta\sin w_o'\right)f_1\frac{dr}{R}\\
&+\frac{3}{q_\infty}\int_{R_H}^{R}\mu\Omega^2\frac{e}{R}\frac{w_o}{R}\left(\cos w_o'\left(\sin^2\beta+\sin^2\rho\cos^2\beta\right)\right.\\
&\qquad\left.+\sin\rho\cos\rho\cos\beta\sin w_o'\right)f_1\frac{dr}{R}\\
&-\frac{3}{q_\infty}\int_{R_H}^{R}\mu\Omega^2\frac{e}{R}\frac{\left(r+u_c\right)}{R}\left(\cos^2\rho\sin w_o'+\sin\rho\cos\rho\cos\beta\cos w_o'\right)f_1\frac{dr}{R}\\
&+\frac{3}{q_\infty}\int_{R_H}^{R}\mu\Omega^2\frac{\partial u_c}{R\partial q_1}\left(\frac{\left(r+u_c\right)}{R}\cos^2\rho-\frac{w_o}{R}\sin\rho\cos\rho\cos\beta\right.\\
&\qquad\left.+\frac{e}{R}\sin\rho\cos\rho\sin\beta\right)\frac{dr}{R}\\
&+\frac{3}{q_\infty}\int_{R_H}^{R}\frac{\left(I_2-I_3\right)}{R^2}\Omega^2\cos\rho\sin\beta\left(\sin\rho\sin w_o'-\cos\rho\cos w_o'\cos\beta\right)f_1\frac{dr}{R}\\
&+3\int_{R_H}^{R}N_o\left(\frac{e_1}{R}f_1-\frac{\dot{u}_{m1}}{R}\sin w_o'\right)\frac{dr}{R}
\end{aligned}
\right.
$$

$$
G_{02} = \left\{
\begin{aligned}
&\frac{3}{q_\infty}\int_{R_H}^{R}\mu\Omega^2\frac{R_s}{R}\left(\frac{w_o}{R}\left(\sin^2\beta+\sin^2\rho\cos^2\beta\right)+\frac{e}{R}\frac{R_s}{R}\sin\beta\cos\beta\cos 2\rho\right)f_2\frac{dr}{R}\\
&\qquad-\frac{3}{q_\infty}\int_{R_H}^{R}\mu\Omega^2\frac{\left(r+u_c\right)}{R}\frac{R_s}{R}\sin\rho\cos\beta f_2\frac{dr}{R}\\
&+\frac{3}{q_\infty}\int_{R_H}^{R}\mu\Omega^2\frac{\partial u_c}{R\partial q_2}\left(\frac{\left(r+u_c\right)}{R}\cos^2\rho-\frac{w_o}{R}\sin\rho\cos\rho\cos\beta+\frac{e}{R}\sin\rho\cos\rho\sin\beta\right)\frac{dr}{R}\\
&+\frac{3}{q_\infty}\int_{R_H}^{R}\frac{R\left(I_2-I_3\right)}{R^2}\Omega^2\left(\sin\rho\cos\rho\cos\beta\cos 2w_o'\right.\\
&\qquad\left.+\sin w_o'\cos w_o'\left(\cos^2\rho\cos^2\beta-\sin^2\rho\right)\right)f_2'\frac{dr}{R}\\
&-\frac{3}{q_\infty}\int_{R_H}^{R}\frac{EI}{R^4}f_2''^2\frac{dr}{R}q_s+3\int_{R_H}^{R}N_o\left(\frac{R_s}{R}f_2\cos w_o'-\frac{\dot{u}_{m2}}{R}\sin w_o'\right)\frac{dr}{R}
\end{aligned}
\right.
$$

$$G_{03} = \begin{cases} 3 \int_{R_H}^{R} N_o \left[\frac{(r+u_m)}{R} \cos w_o' \cos\rho \sin\beta + \frac{w_o}{R} \sin w_o' \cos\rho \sin\beta \right. \\ \left. + \frac{e_1}{R}(\sin\rho \cos w_o' + \cos\rho \sin w_o' \cos\beta)\right] f_3 \frac{dr}{R} \\ + 3 \int_{R_H}^{R} H_o \left(\frac{(r+u_m)}{R} \cos\rho \sin\beta - \frac{w_o}{R} \sin\rho \right) f_3 \frac{dr}{R} - N_G T_{G_o} \end{cases}$$

where T_{G_o} = generator torque at nominal speed

$G_{04} = 0$

Summary of symbols used in this section

u_c = blade's radial displacement at center of mass

u_d = blade's radial displacement at mid-chord

u_m = blade's radial displacement at 1/4 blade chord

$$\dot{u}_\eta = \frac{\partial u_\eta}{\partial t}$$

$$\dot{u}_{\eta i} = \frac{\partial \dot{u}_\eta}{\partial \dot{q}_i} \text{ evaluated at nominal value}$$

where

η = c,d,n

i = 1,2,3,4

e = distance from mass center to shear center of blade cross section

e_1 = distance from 1/4 blade chord to shear center of blade cross section

e_2 = distance from 3/4 blade chord to shear center of blade cross section

e_3 = distance from mid blade chord to shear center of blade cross section

μ = blade's mass per unit length

$$N_o = \left(\frac{W_e}{V_\infty}\right)^2 C_n \frac{c}{R} \qquad \text{evaluated at nominal values}$$

$$H_o = \left(\frac{W_e}{V_\infty}\right)^2 C_t \frac{c}{R} \qquad \text{evaluated at nominal values}$$

$$N1 = (\sin\rho\sin w_o' - \cos\rho\cos w_o'\cos\beta)F_1 - \cos\rho\sin\beta F_2$$

$$N2 = \cos w_o'\sin\beta F_1 - \cos\beta F_2$$

$$N3 = (\cos\rho\sin w_o' + \sin\rho\cos w_o'\cos\beta)F_1 + \sin\rho\sin\beta F_2$$

$$N4 = \begin{cases} \left(\frac{\ell}{V_\infty}\sin\beta\cos w_o' + \frac{(r+u_d)}{V_\infty}\sin\rho\sin\beta\cos w_o' + \frac{w_o}{V_\infty}\sin w_o'\sin\rho\sin\beta\right)F_1 \\ + \frac{e_3}{V_\infty}(\cos\rho\cos w_o' - \sin\rho\sin w_o'\cos\beta)F_1 \\ - \left(\frac{\ell}{V_\infty}\cos\beta + \frac{(r+u_d)}{V_\infty}\sin\rho\cos\beta + \frac{w_o}{V_\infty}\cos\rho\right)F_2 \end{cases}$$

$$N5 = \begin{cases} \left(\frac{\ell}{V_\infty}(\sin\rho\cos\beta\cos w_o' + \sin w_o'\cos\rho) + \frac{(r+u_d)}{V_\infty}\cos\beta\cos w_o' + \frac{w_o}{V_\infty}\sin w_o'\cos\beta\right. \\ \left. + \frac{e_3}{V_\infty}\sin w_o'\sin\beta\right)F_1 \\ + \left(\frac{\ell}{V_\infty}\sin\rho\sin\beta + \frac{(r+u_d)}{V_\infty}\sin\beta\right)F_2 \end{cases}$$

$$N6 = \begin{cases} \left(\frac{(r+u_d)}{V_\infty}\cos w_o'\cos\rho\sin\beta + \frac{w_o}{V_\infty}\sin w_o'\cos\rho\sin\beta\right)F_1 \\ - \frac{e_3}{V_\infty}(\sin\rho\sin w_o' + \cos\rho\sin w_o'\cos\beta)F_1 + \left(\frac{w_o}{V_\infty}\sin\rho - \frac{(r+u_d)}{V_\infty}\cos\rho\cos\beta\right)F_2 \end{cases}$$

$$
N7 = \left\{
\begin{aligned}
&(\sin\rho\cos w_o' + \cos\rho\sin w_o'\cos\beta)\,(1-a)f_2' - \Omega\,\frac{(r+u_d)}{V_\infty}\sin w_o'\cos\rho\sin\beta f_2' \\
&\qquad = \frac{\Omega R}{V_\infty}\frac{\partial u_d}{R\partial q_2}\cos w_o'\cos\rho\sin\beta)F_1 \\
&+ (\frac{\Omega R}{V_\infty}\frac{R_s}{R}\sin w_o'\cos\rho\sin\beta\ f_2 + \frac{\Omega w_o}{V_\infty}\cos w_o'\cos\rho\sin\beta f_2' \\
&\qquad + \frac{\Omega e_3}{V_\infty}(\sin\rho\sin w_o' - \cos\rho\cos w_o'\cos\beta)f_2')F_1 \\
&+ (\frac{\Omega R}{V_\infty}\frac{R_s}{R}\sin\rho f_2 - \frac{\Omega R}{V_\infty}\frac{\partial u_d}{R\partial q_2}\cos\rho\cos\beta)F_2
\end{aligned}
\right.
$$

The expressions for H1, H2, H3, H4, H5, H6, and H7 are the same as N1, N2, N3, N4, N5, N6, and N7, respectively, except F_1 and F_2 in N_i terms are replaced by G_1 and G_2 in H_i terms.

APPENDIX V

COMPUTER CODE

A FORTRAN computer program is developed to handle the numerical values of the coefficients of the system's equations of motion. The code will calculate the axial induction factor along the blade at a particular tip speed ratio. At the same time it also calculates the integral terms for the variations of the axial induction factor with yaw and yaw rate. Then it calculates the power and thrust coefficient. Finally, the code calculates the constant coefficients in the equations of motion (mass, damping, stiffness coefficients, and forcing function).

The lift curve and drag curves are approximated to use in the computer code. The lift curve is approximated and can be described in a simple yet fairly accurate form by six parameters. The curve consists of four straight line segments as follows:

$$C_L = 2\pi m \sin(\alpha+\alpha_o) \qquad \alpha < \alpha_{C_{L_{max}}}$$

$$C_L = C_{L_{max}} \qquad \alpha_{C_{L_{max}}} < \alpha < \alpha_{BR}$$

$$C_L = C_{L_{flat}} \qquad \alpha_{BR} < \alpha < \alpha_{stall}$$

$$C_L = C_{L_{flat}} \frac{\sin(\frac{\pi}{2} - \alpha)}{\sin(\frac{\pi}{2} - \alpha_{stall})} \qquad \alpha > \alpha_{stall}$$

The six parameters are

m - lift curve slope divided by 2π

α_{L_o} - zero lift angle of attack

$\alpha_{C_{L_{max}}}$ - maximum lift coefficient

α_{BR} - angle at which C_L drops to $C_{L_{flat}}$

$C_{L_{flat}}$ - an approximate to the average C_L on the far side of the C_L curve, this can be adjusted up and down depending upon the characteristics of the airfoil

α_{stall} - angle at which C_L begins to decrease

The drag coefficient curve is also in multiple sections. Below $\alpha_{C_{L_{max}}}$, the drag is given by the following:

$$C_D = C_{D_o} \left(1 + C_\alpha \left(\frac{\alpha}{\alpha_{C_{L_{max}}}}\right)^n\right)$$

where C_α, n, and C_{D_o} are constants determined by the airfoil characteristics. If $\alpha > \alpha_{C_{L_{max}}}$ the drag coefficient can be represented by a single curve fit or a series of curve fits.

The axial induction factor "a" is calculated by equating momentum flux to blade force. There are six possible intersections of blade force and momentum relations due to two regions on momentum relations and three regions on blade force. Two regions on momentum relations are the region of parabolic curve when "a" < "$a_{critical}$" and the straight line when "a" > "$a_{critical}$". Three regions on blade force are the linear slope curve where the angle of attack is less than the angle at the maximum lift force, the flat part of lift curve ($C_{L_{max}}$ and $C_{L_{flat}}$), and the lift curve in the stall region. Once the particular region is identified, the solution is a straightforward procedure of finding where the momentum and blade element curves intersect. These intersections of blade force and momentum relations are shown in Figure V.1.

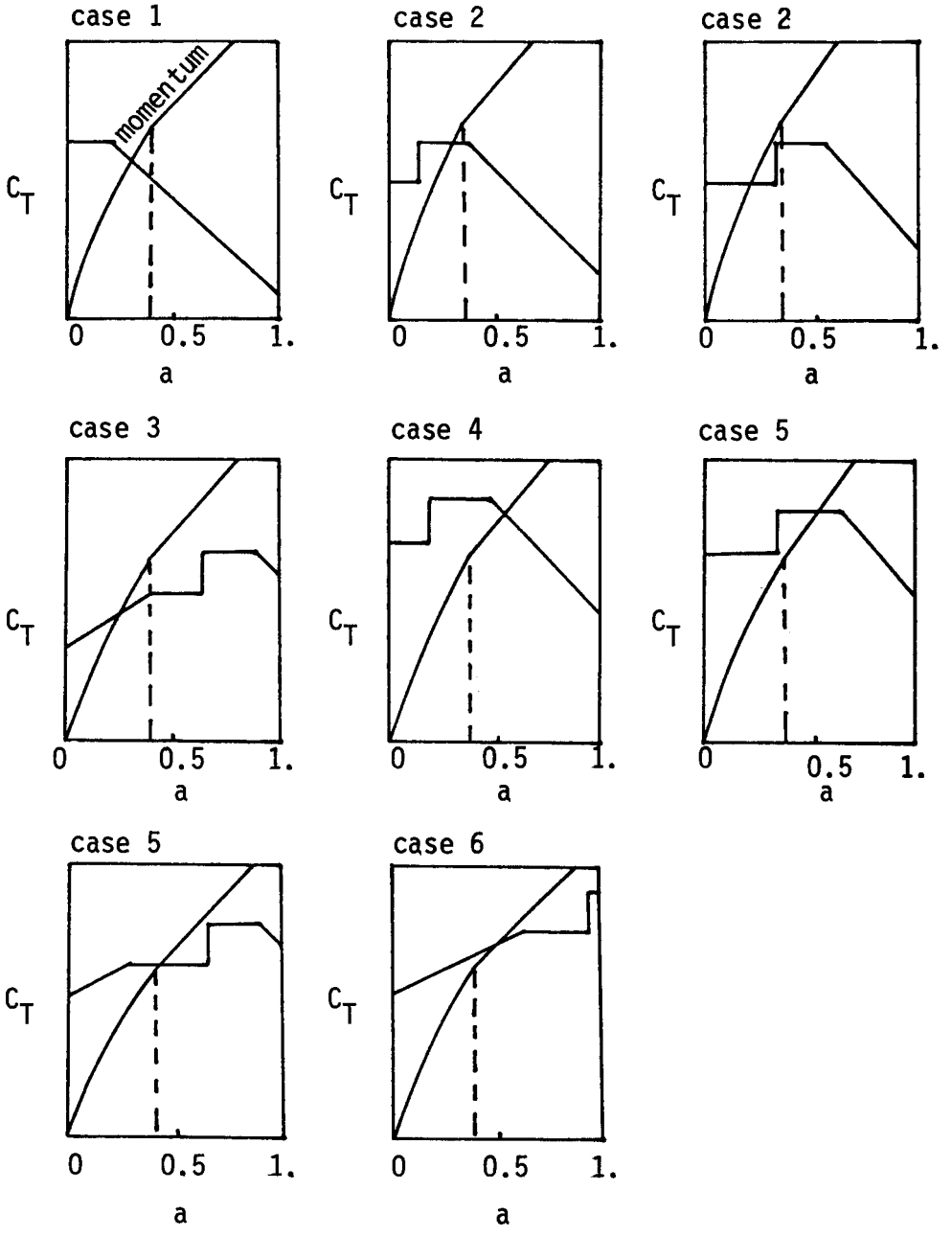

Figure V.1 Regions of operation for momentum calculations

A subroutine and two functions are developed to handle the inner integral term of the double integration. The inner integral terms are terms involving the derivative of flapwise deflection (radial displacement and its derivative). The composite Simpson's rule method is used for the numerical integration in the code.

Input Data

The input data for the program consists of the physical characteristics of the wind turbine rotor itself. They consist of physical airfoil data and operation variables. The physical airfoil data and operation variables are:

BCRR	chord to radius ratio at blade root (Bc/R)
B	number of blades
EM	slope of linear portion of lift curve/2π
DRR	dr/R
XMIN	tip speed ratio to start program
XMAX	last tip speed ratio - used to end the program
DBX	the increment of tip speed ratio
CD ZERO	minimum drag coefficient
CL MAX	maximum lift coefficient
CL FLAT	lift coefficient on the horizontal portion of the lift curve
ALPHA BREAK	angle of attack where the lift curve changes values, from the maximum value to CL FLAT, degrees
ALO	angle of attack at zero lift, degrees
AST	stall angle of attack, degrees
SI	coning angle, degrees

PITCH	prepitch angle, degrees
BETA ROOT	pretwist angle at blade root, degrees
DBETA	(βroot - βtip); twist angle change, degrees
RT	local radius at twist angle change from linear to constant twist
DCND	(c/R at chord change - c/R at tip), chord change ratio
RC	local radius at chord change from linear taper to constant chord
RH	hub radius
ESC	blade shear center position given as the ratio of the distance from the blade leading edge to the shear center and blade chord (e_s/c)
XCG	position of blade cross-section's center of mass given as the ratio of distance from blade leading edge to center of mass and blade chord (x_{cg}/c)
E	modulus of elasticity, psi
G	modulus of shear, psi
OMEGA	rotor speed, rad/sec
RHO	air density, slug/ft^3
YL	distance from the nacelle yaw axis to the center of the rotor, ft
R	blade tip radius, ft
M	number of integration steps in subroutine

Output

The output for the program is on a tape file entitled TAPE 1. On this file are written both the program operating conditions and program output. The following are the output quantities:

QS	nondimensional static tip deflection
CP	power coefficient
CT	thrust coefficient
$M_{\eta\eta}$	rotor mass coefficient where $\eta\eta$ is the indication of which variables it represents
$C_{\eta\eta}$	rotor damping coefficient
$K_{\eta\eta}$	rotor stiffness coefficient
HP	rotor forcing function of pitch equation
HF	rotor forcing function of flap equation
SKDEL	coefficient accounting for the variation of the axial induction factor with yaw, k_γ
SJDEL	coefficient accounting for the variation of the axial induction factor with yaw, j_γ
SKRDEL	coefficient accounting for the variation of the axial induction factor with yaw rate, $k_{\dot{\gamma}}$
SJRDEL	coefficient accounting for the variation of the axial induction factor with yaw rate, $j_{\dot{\gamma}}$

For $\eta\eta$ parameters

P	generalized coordinate in pitch
F	generalized coordinate in flap
O	generalized coordinate in speed
D	generalized coordinate in yaw

If the code is not suppressed, additional output quantities are printed on the output list. They are as follows:

PCR	local distance on the blade, r/R
A	axial induction factor
PHI	summation of angle of attack and pretwist angle
BETA	pretwist angle
ALPHA	angle of attack
CL	lift coefficient
CD	drag coefficient
BCR	local chord to radius ratio, Bc/R
CPB	power coefficient
CTB	thrust coefficient

For the tower shadow part in yaw equations, the additional quantities on the output list are:

$SM_{n\eta}$	mass coefficient in shadow region per unit shadow width/$(B/2\pi)$
$GC_{n\eta}$	damping coefficient in shadow region per unit shadow width/$(B/2\pi)$
$SK_{n\eta}$	stiffness coefficient in shadow region per unit shadow width/$(B/2\pi)$
CQO	forcing function per unit shadow width generated from the shadow/$(B/2\pi)$

The quantities from the tower shadow effect will be calculated when the magnitude of the velocity deficit is given. For example, if the velocity deficit value is 50%, the forcing function at tip speed ratio of 2 due to tower shadow is given as

$$\frac{B}{2\pi}\left[CQO\big|_{x=2} - (SF)^2\, CQO\big|_{x=4}\right] 2 \sin\frac{j}{2}$$

where j = width of the shadow segment (degree)

B = number of blades

x = tip speed ratio

SF = correction factor due to nondimensionalized value at different tip speed value [= 1 - (% velocity deficit)/100]

For the gravity effect, the gravity forces on the pitch equation for a single blade are listed as the components of sine and cosine of the azimuth angle.

GNCOS	Cosine component of the forcing function due to gravity
GNSIN	Sine component of the forcing function due to gravity
GPCOS	Cosine component of the k_{11} of a single blade due to gravity
GPSIN	Sine componet of the k_{11} of the single blade due to gravity
GFCOS	Cosine component of the k_{12} of a single blade due to gravity
GFSIN	Sine component of the k_{12} of a single blade due to gravity
GOCOS	Cosine component of the k_{13} of single blade due to gravity
GOSIN	Sine component of the k_{13} of a single blade due to gravity

The properties of the blade and shear center position are also listed in the output

ER	$\frac{e}{R}$
E1	$\frac{e_1}{R}$
E2	$\frac{e_2}{R}$
E3	$\frac{e_3}{R}$
AE	Modulus of elasticity, psi
AG	Shear modulus of rigidity, psi

The integration step sizes are shown as

N	Number of integration step sizes used in the main program
M	Number of integration step sizes used in subroutine (double integral)

Note

The code does not calculate some of the terms in the expression of the coefficient of rotor equations of motion. These terms have to be calculated by hand then added to the results of the computer code.

These terms are

C_G in C_{33} $\qquad$ $N_G T_{G_o}$ in G_{03}

$\frac{1}{q_\infty}(I_H + N_G^2 I_G) f_3^2$ in M_{33}

```
      PROGRAM AERO  (INPUT,OUTPUT,TAPE1)
      COMMON L,r,RS
      COMMON /STIFF/ AEI,EIO,AGJ,GJO,RHR,OS
      EXTERNAL TOM,TIM
C     ******************************************************************
C
C     THIS PROGRAM CALCULATES THE POWER COEFFICIENT AND WINDWISE
C     FORCE COEFFICIENT FOR A HORIZONTAL AXIS WIND TURBINE
C     AND GENERATES THE COEFFICIENTS OF EQUATION OF MOTION
C     OF THE TURBINE SYSTEM
C
C     DEVELOPED BY
C
C     R E WILSON
C     S. CHAIYAPINUNT
C     OREGON STATE UNIVERSITY
C     MARCH 1983
C
C
C     FILE ASSIGNMENTS
C
C         INPUT          FOR INPUT OF INDEPENDENT VARIABLES
C         OUTPUT         FOR PROGRAM MESSAGES TO THE USER
C         TAPE 1         FOR A LISTING OF THE PROGRAM OUTPUT
C
C
C     VARIABLES INPUT FROM TELETYPE
C
C     B         NUMBER OF BLADES
C     BCRR      DIMENSIONLESS CHORD TO RADIUS RATIO AT BLADE ROOT
C     EM        SLOPE OF LIFT COEFFICIENT CURVE
C     DRR        INCREMENTAL INTEGRATION STEP ALONG THE BLADE
C     CDO       MINIMUM DRAG COEFFICIENT
C     CLM       MAXIMUM LIFT COEFFICIENT
C     PTCH      PITCH ANGLE-IN DEGREES
C     BRT       TWIST ANGLE AT BLADE ROOT-IN DEGREES
C     DBTA      INCREMENAL TWIST ANGLE CHANGE -IN DEGREES
C     ALO       ANGLE OF ATTACK FOR ZERO LIFT
C     AST       STALL ANGLE OF ATTACK
C     SI        CONING ANGLE
C     RT        RADIAL POSITION AT WHICH TWIST ANGLE CHANGES
C     DCND      INCREMENTAL CHORD CHANGE RATIO
C     RC        RADIAL POSITION AT WHICH BLADE CHORD CHANGES
C     RH        HUB RADIAL POSITION
C     ABR       LIFT BREAK ANGLE OF ATTACK
C
C
C     OTHER VARIABLE ASSIGNMENTS
C
C     A         AXIAL INDUCTION FACTOR
C     CP        POWER COEFFICIENT
C     CT        WINDWISE FORCE COEFFICIENT
C     XL        LOCAL TIP SPEED RATIO
C     BETA      LOCAL TWIST ANGLE
C     CL        LOCAL LIFT COEFFICIENT
C     CD        LOCAL DRAG COEFFICIENT
C     BCR       LOCAL DIMENSIONLESS CHORD TO RADIUS RATIO
C     PHI       LOCAL ANGLE OF RELATIVE VELOCITY WITH ROTOR PLANE
C     ALPHA     LOCAL ANGLE OF ATTACK
C
C
C     ******************************************************************
      PI=3.1415926356
```

```
C     ******************************************************************
C
C     INDEPENDENT VARIABLE INPUT SECTION
C
C     ******************************************************************
      TIMIN=SECOND()
      PRINT1
      PRINT2
      READ*,B,BCRR,EM,DER,XMIN,XMAX,DBX
      PRINT 3
      READ*,CDO,CLM,CLFL,ABR
      PRINT 65
      READ*,ALO,AST,SI,PTCH,BRT,DBTA
      PRINT 66
      READ*,RT,DCND,RC,RH
      PRINT 67
67    FORMAT(' INPUT SHEAR CENTER POSITION ES/C, XCG( CENTER OF MASS')
      READ*,ESC,XCG
      PRINT 50
50    FORMAT('  INPUT E AND G ')
      READ*,AE,AG
      PRINT 51
51    FORMAT (' INPUT OMEGA,RHO,YL,R,M' )
      READ*,OM,RHO,YL,R,MM
      PRINT 68
      READ5,SUPP
  68  FORMAT('SUPPRESS INTERMED. OUTPUT? (Y)')
C     ******************************************************************
C
C     HEADINGS AND CALCULATION OF CONSTANTS
C
C     ******************************************************************
      WRITE(1,60)
      WRITE(1,19) B,BCRR,DCND,RT,RC,RH,BRT,DBTA
      WRITE(1,8)CLM,CLFL,EM,AST,ABR,ALO,CDO
      WRITE(1,9) XMIN,XMAX,DRR,SI
      CONVT=PI/180.
      AC=.38
      FAT=1.
      YL=YL/R
      SI=SI*CONVT
      CSI=COS(SI)
      SSI=SIN(SI)
      DBTA=DBTA*CONVT
      ABR=ABR*CONVT
      ALO=ALO*CONVT
      AST=AST*CONVT
      AMAX=PI/2.
      ZLOT=1.
      CD1=CLFL/ZLOT
      CD2=(CLFL/ZLOT)*(1.+SIN(AST))/(.5*SIN(2.*AST))
      ROSE=ATAN((.41/CLFL)**.87)
      EM1=CLFL/(SIN(AMAX-AST))
 200  WRITE(1,21)PTCH
      X=XMIN
      ANG=BRT*CONVT
      RTR=RT/R
      RCR=RC/R
      RHR=RH/R

  27  CONTINUE
      KK=0
      V=OM*R/X
```

```
      KL=1
      IM=1
      QS=.023
      DX=DRR*X
      DR=DRF*R
      TNUM=(R-RH)/DR
      NUM=TNUM
      N=NUM
      IF(NUM.NE.TNUM) N=NUM+1
      XL=X
C
C******INITIALIZED
C
      ZI1=ZI2=ZI3=ZI4=ZI5=ZI6=ZI7=ZI8=ZI9=ZI10=ZI11=ZI12=ZI13=ZI14=0.
      ZI15=ZI16=ZI17=ZI18=ZI19=0.
      ZMPP=ZMPF=ZMPO=ZMFF=ZMFO=ZMOO=ZMDD=ZCPP=ZCPF=ZCPO=ZCFP=ZCFF=0.
      ZCFO=ZCOP=ZCOF=ZCOO=ZCDZ=ZCD1=ZCD2=ZKPP=ZKPF=ZKPO=ZKFP=ZKFF=0.
      ZKFO=ZKOP=ZKOF=ZKOO=ZKDZ=ZKD1=ZKD2=ZHP=ZHF=ZHO=0.
      COO=SMDP=SMDF=SMDO=SMDD=SCDP=SCDF=SCDC=SCD1=SCDJ=SCDK=0.
      SKDP=SKDF=SKDO=SKD1=SKDJ=SKDK=0.
      SCPD1=SCPD2=SCFD1=SCFD2=SCOD1=SCOD2=0.
      SKPD1=SKPD2=SKFD1=SKFD2=SKOD1=SKOD2=0.
      S1=S2=S3=SS1=SS2=SS3=0.
      GNCOS=GNSIN=GPCOS=GPSIN=GFCOS=GFSIN=GOCOS=GOSIN=0.
      G=32.2
      GR=G/9
      ZDL1=ZDL2=ZDL3=ZDR1=ZDR2=ZDR3=ZDW1=ZDW2=ZDW3=0.
      CT=0.
      CP=0.
      AT=AP=ATB=0.
      APB=-X**3.*CDC*(BCRR-3*DCND)
      ZF=0.7
      Z9=COS(PI/2.*ZF)
      RE=SQRT((X*8**.6666)/(X*8**.6666+1.32))
      IF(X.LT.3.) RE=SQRT(8**.6666/(3**.6666+.44))
      GLUART=4.*(1.-2.*AC)
      KL=1
      NN=N+1
      JU=1
      I=1
C
C****** CHECK TO SEE IF NUMBER OF INTERVAL IS EVEN
C****** EVEN---1/3 RULE   ODD---3/8 RULE ON THE FIRST
C****** THREE INTERVALS
C
      KHALF=N/2
      IF((N-2*KHALF).EQ.0) IM=0
      IF(KL.EQ.1) GO TO 555
553   IF(SUPP.EQ.1HY) GO TO 555
      WRITE(1,15)
555   IF(KL.EQ.1) THEN
      NHALF=JU/2
      NTEST=JU-2*NHALF
      ELSE
      NHALF=I/2
      NTEST=I-2*NHALF
      ENDIF
      RLR=XL/X
      RLR2=RLR*RLR
      RLR3=RLR2*RLR
      RLR4=RLR3*RLR
C     ********************************************************************
C
```

```
C     CALCULATION OF LOCAL TWIST ANGLE AND
C     LOCAL CHORD TO RADIUS RATIO
C
C     ******************************************************************
      PCR=XL/X
      EA=(1.-PCR)/(1.-RE)
      EPSML=Z9**EA
      FBIG=2./PI*ACOS(EPSML)
      Z1=(1.-PCR)*10.
      Z1=(2.**Z1)-1.
      BCR=BCRR
      IF(RLR.GE.RCR) BCR=BCRR-B*DCND*(RLR-RCR)/(1.-RCR)
      IF(FBIG.NE.0.) BCRF=BCR/FBIG
      CR=BCR/B
      EP=(ESC-XCG)*CR
      E1=(ESC-.25)*CR
      E2=(0.75-ESC)*CR
      E3=(0.5-ESC)*CR
      CV=CR*R/V
      BETA=ANG
      IF(RLR.GE.RTR) BETA=ANG-DBTA*(RLR-RTR)/(1.-RTR)
      BETA=BETA+PTCH*CONVT
      IF(FBIG.NE.0.) EM2=EM1*BCRF*X*CSI/(2.*PI)
      STEL=BCR/B*(XL/X)
      AM=ASIN(CLM/(2.*PI*EM))-ALO
C     ******************************************************************
C
C     CALCULATION OF AXIAL INDUCTION FACTOR
C
C     ******************************************************************
      IF(RLR.EQ.1.) THEN
      CL=ALPHA=0.
      PHI=BETA
      A=1.
      ELSE
      G=4.*(1.-2.*AC)
      H=4.*AC*(1.-AC)-G*AC
      AB=BCRF*X*EM*CSI*(COS(BETA-ALO)-XL*SIN(BETA-ALO))-H
      A=AB/(BCRF*X*EM*CSI*COS(BETA-ALO)+G)
      PHI=ATAN((1.-A)/XL)
      ALPHA=PHI-BETA
      IF(A.GT.AC) GO TO 30
      B1=4.+BCRF*EM*X*CSI*COS(BETA-ALO)
      C1=BCRF*EM*X*CSI*(COS(BETA-ALO)-XL*SIN(BETA-ALO))
      A=(B1-SQRT(B1**2-16.*C1))/8.
      PHI=ATAN((1.-A)/XL)
      ALPHA=PHI-BETA
   30 CL=2.*PI*EM*SIN(ALPHA+ALO)
      IF(ABS(CL).LT.CLM) GO TO 500
      CL=(ABS(ALPHA)/ALPHA)*CLM
      IF(ABS(ALPHA).GT.ABR) CL=(ALPHA/ABS(ALPHA))*CLFL
      EN=BCRF*X*CL*CSI/(2.*PI)
      B2=(G*H+EN**2)/(G**2-EN**2)
      C2=(EN**2*(1.+XL**2)-H**2)/(G**2-EN**2)
      BOOM=B2**2+C2
       IF(BOOM.LT..0) A=0.
       IF(BOOM.LT..0) GO TO 32
      A=-B2+SQRT(B2**2+C2)
32    CONTINUE
      PHI=ATAN((1.-A)/XL)
      ALPHA=PHI-BETA
      IF(ABS(ALPHA).LE.ABR) CL=(ABS(ALPHA)/ALPHA)*CLM
      IF(ABS(ALPHA).GT.ABR) CL=(ALPHA/ABS(ALPHA))*CLFL
```

```
      IF(A.GT.AC) GO TO 35
      DO 31 K=1,5
      B3=BCRF*XL*X*CL*CSI*SQRT(1.+((1.-A)/XL)**2)/(2.*PI)
      A=(1.-SQRT(1.-B3))/2.
      PHI=ATAN((1.-A)/XL)
      ALPHA=PHI-BETA
      IF(ABS(ALPHA).GT.ABR) CL=(ALPHA/ABS(ALPHA))*CLFL
      IF(ABS(ALPHA).LE.ABR) CL=(ALPHA/ABS(ALPHA))*CLM
   31 CONTINUE
   35 CONTINUE
      IF(ALPHA.LT.AST) GO TO 500
      ETA=BETA+AMAX
      CETA=COS(ETA)
      SETA=SIN(ETA)
      EM4=BCRF*X/(2.*PI*SIN(AMAX-AST))
      A=(EM4*(XL*SETA-CETA)-H)/(G-EM4*CETA)
      PHI=ATAN((1.-A)/XL)
      ALPHA=PHI-BETA
      CL=EM1*SIN(AMAX-ALPHA)
      IF(A.GT.AC.AND.CL.LT.CLFL) GO TO 500
      B4=4.-EM2*COS(ETA)
      C4=EM2*(XL*SIN(ETA)-COS(ETA))
      A=(B4-SQRT(B4**2-16.*C4))/8.
      PHI=ATAN((1.-A)/XL)
      ALPHA=PHI-BETA
      CL=EM1*SIN(AMAX-ALPHA)
  500 ALPHA=PHI-BETA
      ENDIF
C     ******************************************************************
C
C     CALCULATION OF DRAG COEFFICIENT
C
C     ******************************************************************
      ABSAL=ABS(ALPHA)
      SA=SIN(ABSAL)
      COA=COS(ABSAL)
      SA2=SA*SA
      BOB=.20944
      BOB2=ABR
      IF(ABSAL.LT.BOB) CD=CD0*(1.+53.81*(ABSAL**2.))
      IF(ABSAL.LT.BOB) CDA=107.62*CD0*ABSAL
      IF(ABSAL.GE.BOB) CD=3.36*CD0-TAN(BOB)+TAN(ABSAL)
      IF(ABSAL.GE.BOB) CDA=1.+(TAN(ABSAL))**2.
      IF(ABSAL.GT.BOB2) CD=2.439*CLFL*(TAN(ABSAL)**2.15)
      IF(ABSAL.GT.BOB2) THEN
      CDA=5.24385*CLFL*(TAN(ABSAL))**1.15*(1.+(TAN(ABSAL))**2)
      ELSE
      ENDIF
      IF(ABSAL.GE.RCSE)CDA=CD1*(1.+(TAN(ABSAL))**2)
      IF(ABSAL.GE.RCSE) CD=CD1*TAN(ABSAL)
      IF(ABSAL.GE.AST) CD=CD2*SA2/(1.+SA)
      IF(ABSAL.GE.AST) CDA=CD2*(2*SA*COA+SA*SA*COA)/(1.+SA)**2
      CSP=COS(PHI)
      SNP=SIN(PHI)
      CAS=COS(ALPHA)
      SAS=SIN(ALPHA)
      CN=CL*CAS+CD*SAS
      CO=CL*SAS-CD*CAS
      CLA=2.*PI*EM
      IF(ABSAL.GT.AM) CLA=0.
      IF(ABSAL.GT.AST) CLA=-EM1*COS(AMAX-ABSAL)
      COP=CLA*SAS-CDA*CAS+CN
      CNP=CLA*CAS+CDA*SAS-CO
```

```
      CNA=CLA*CAS+CDA*SAS
      CTA=CLA*SAS-CDA*CAS
      DPHI=PHI/CONVT
      DAL=ALPHA/CONVT
      DBET=BETA/CONVT
      IF(KL.EQ.1) GO TO 20


      IF(RLR.EQ.1.) THEN
      AP=0.
      AT=0.
      ELSE
      AP=((1.-A)*CL-XL*CD)*XL**2.*SQRT(1.+((1.-A)/XL)**2.)*BCR
      AT=((1.-A)*CD+XL*CL)*XL*SQRT(1.+((1.-A)/XL)**2.)*BCR
      ENDIF
      CPB=CSI**3.*(AP+APB)*DX/(2.*PI*X)
      CTB=CSI**3.*(AT+ATB)*DX/(2.*PI*X)
      CT=CT+CTB
      CP=CP+CPB
      ATB=AT
      APB=AP
C
C*******PROPERTIES OF THE BLADE
C
20    AFACTO=0.84752/144.
      IF(RLR.LE.1..AND.RLR.GT.0.6545) THEN
      BI2=5.673*EXP(-3.313*RLR)
      BI3=67.3636*EXP(-2.0236*RLR)
      AMASS=15.*AFACTO*EXP(-1.3266*RLR)
      ELSE IF(RLR.LE.0.6545.AND.RLR.GT.0.3648) THEN
      BI2=2.111*EXP(-1.802*RLR)
      BI3=29.44*EXP(-0.76*RLR)
      AMASS=9.65*AFACTO*EXP(-0.6447*RLR)
      ELSE IF(RLR.LE.0.3648.AND.RLR.GT.0.1393) THEN
      BI2=4.5679*EXP(-4.8604*RLR)
      IF(RLR.GT.0.244) BI2=2.111*EXP(-1.802*RLR)
      BI3=11.3726*RLR**(-0.6585)
      AMASS=5.243*AFACTO*RLR**(-0.3695)
      ELSE
      BI2=2.3210
      BI3=41.924
      AMASS=10.89*AFACTO
      ENDIF
      BI1=BI2+BI3
      EI=BI2*AE
      EI0=2.321*AE
      GJ=BI1*AG
      GJ0=44.245*AG
C********CHANGE UNIT TO FEET
C
      AI1=AFACTO*BI1/(144.*R*R)
      AI2=AFACTO*BI2/(144.*R*R)
      AI3=AFACTO*BI3/(144.*R*R)
      EI=EI/(144.*R**4.)
      EI0=EI0/(144.*R**4.)
      GJ=GJ/(144.*R**4.)
      GJ0=GJ0/(144.*R**4.)
      AEI=AE*1./(144*R**4.)
      AGJ=AG*(21.)/(144.*R**4.)

C
C************
C
```

```
      QVEL=0.5*RHO*V*V
      FO=1.
      FD=1.
      RS=(1.-PHR)
      ZP=(RLR-RHR)/RS
      ZP2=ZP*ZP
      ZP3=ZP2*ZP
      ZP4=ZP3*ZP
      FF=6.*ZP2-4.*ZP3+ZP4
      FFP=12.*ZP-12.*ZP2+4.*ZP3
      FFPP=12.-24.*ZP+12.*ZP2
      FP=2.*ZP-ZP*ZP
      FPP=2.*(1.-ZP)
      FPH=0.
      FPHP=0.
C******ASSUME STATIC MODE SHAPE EQUAL DYNAMIC MODE SHAPE
C
      FFS=FF
      FFSP=FFP
      FFSPP=FFPP
      FFHS=FFH
      FFHSP=FFHP
      FFHSPP=FFHPP
      WR=FFS*QS*RS
      WP=FFSP*QS
      WPP=FFSPP*QS
      CW=COS(WP)
      SW=SIN(WP)
      C2W=CW*CW-SW*SW
      CB=COS(BETA)
      SB=SIN(BETA)
C
C********CORRECTION OF MODE SHAPE THAT BASED ON LENGTH OF THE BLADE
C********(R-RH) NOT ON THE RADIUS OF THE ROTOR ( CORRECTION FOR
C********MASS,DAMPING,STIFFNESS MATRICES )
C
      FF=FF*RS
      FFPP=FFPP/RS
      FPP=FPP/RS
C
      CALL SUMRCW(TCM,TIM,RLR,ER,E1,E3,UC,AUC,BUC,AAUC,ABUC,BBUC,AUM,AAU
     1M,ABUM,AUC,MM)
      UD=UM=UC
      UCPD=AUC
      UCFD=BUC
      UCFD=UMFD=BUC
      UMPD=AUM
      BUD=BUM=BUC
      AUCPD=AAUC
      AUMPD=AAUM
      BUCPD=AUCFD=ABUC
      BUMPD=AUMFD=ABUM
      BUCFD=BUMFD=BBUC
      BBUM=BBUC
      SB=SIN(BETA)
      CB=COS(BETA)
      DIS=(RLR+UC)*CSI-WR*SSI
      DYNA=6./(RHO*V*V)
C*****
C*******SOLVE FOR QS (STATIC TIP DEFLECTION)
C
      IF(KL.EQ.1) THEN
      BNORMA=-CSI*CB*(1.-A)+X*RLR*CSI*SB-X*E3*SSI
```

```
      BTANG=CSI*SB*(1.-A)+X*RLR*CSI*CB
      WNORM=(PNORMA*BNORMA+BTANG*BTANG)

      DS1=DYNA*AMASS*OM*OM*(ER*SB*CB*(1.-SSI*SSI)-RLR*SSI*CB)*FF*DRR
      DS2=DYNA*(AI1-AI2)*OM*OM*SSI*CSI*CB*FFP*DRR
      DS3=3.*WNORM*FF*CN*CR*DRR
C******* SINCE BUC=BBUC*QS
      PAUL=-BBUC
      DSS1=DYNA*AMASS*OM*OM*(RLR*CSI*CSI+ER*SSI*CSI*SB)*PAUL*DRR
      DSS2=-DYNA*AMASS*OM*OM*(SB*SB+(SSI*CB)**2.)*FF*FF*DRR
      DSS3=DYNA*2I*FFPP*FFPP*DRR
      IF(IM.EQ.1) THEN
      FEB=9./8.
      IF(JU.EQ.1.OR.JU.EQ.4) FEB=3./8.
      IF(JU.GE.4) IM=0
      ELSE

      FEB=2./3.
      IF(NTEST.EQ.0) FEB=4./3.
      IF(JU.EQ.1.OR.JU.EQ.NN) FEB=1./3.
      ENDIF
C**** START THE INTEGRATION
      S1=S1+FEB*DS1
      S2=S2+FEB*DS2
      S3=S3+FEB*DS3
      SS1=SS1+FEB*DSS1
      SS2=SS2+FEB*DSS2
      SS3=SS3+FEB*DSS3
      XL=XL-DX
      RLR=XL/X
      IF(RLR.LT.RHR) THEN
      RLR=RHR
      XL=RHR*X
      DRR=(TNUM-NUM)*DRR
      ELSE
      ENDIF
      JU=JU+1
      IF(JU.LE.NN) GO TO 555
      ELSE
      ENDIF
      IF(KL.EQ.1) THEN

      QS=(S1+S2+S3)/(SS1+SS2+SS3)
      WRITE(1,510) QS
      KL=KL+1
      XL=X
      DRR=DX/X
      IF((N-2*KHALF).EQ.0) THEN
      IM=0
      ELSE
      IM=1
      ENDIF
      GO TO 553
      ELSE
      ENDIF
C*****SOME COFACTORS
      PART1=SSI*SW-CSI*CW*CB
      PART2=CSI*SB
      PART3=CSI*CW-SSI*SW*CB
      PART4=(RLR+UM)*CW+WR*SW
      PART5=(RLR+UM)*SW-WR*CW
      PART6=CSI*SW+SSI*CW*CB
      PART7=R/V*(YL*SB*CW+(RLR+UD)*SSI*SB*CW+WR*SW*SSI*SB+E3*PART3)
```

```
      PART8=R/V*(YL*C3+(RLR+UD)*SSI*CB+WR*CSI)
      PART9=R/V*(YL*PART6+(RLR+UD)*CB*CW+WR*SW*CB+E3*SW*SB)
      PART10=R/V*(YL*SSI*SB+(RLR+UD)*SB)
      PART11=WR*SB*CSI+ER*CSI*CB
      PART12=SSI*CW+CSI*SW*CB
      PART13=WR*SSI*SB+ER*CB*SSI
      TLF1=(YL*SB*SW+(RLR+UM)*SSI*SB*SW-WR*CW*SSI*SB-E1*PART6)*FFP
      TLF1=TLF1-SW*SSI*SB*FF-UM*SSI*SB*CW
      PAL1=(RLR+UC)*CSI-WR*SSI*CB+ER*SSI*SB
      PAL2=YL+(RLR+UC)*SSI+WR*CSI*CB-ER*SB*CSI

C
      TAIL1=(RLR+UM)*CW*CSI*SB+WR*SW*CSI*SB+E1*PART12
      TAIL2=(RLR+UM)*CSI*SB-WR*SSI
      TAIL3=YL*SB*CW+(RLR+UM)*SSI*SB*CW+WR*SW*SSI*SB-E1*PART3
      TAIL4=YL*PART6+(RLR+UM)*CB*CW+WR*SW*CB-E1*SW*SB
      TAIL5=YL*CB+(RLR+UM)*SSI*CB+WR*CSI
      TAIL6=YL*SSI*SB+(RLR+UM)*SB
C
      WT=CSI*SB*(1.-A)+X*((RLR+UD)*CSI*CB-WR*SSI)
      WN=-PART1*(1.-A)-X*((RLR+UD)*CW*CSI*SB+WR*SW*CSI*SB-E3*PART12)
      WE2=WN*WN+WT*WT
      WTC=WE2*CO*CR
      WNC=WE2*CN*CR
      F1=CR*(2.*CN*WN+CNP*WT)
      F2=CR*(2.*CN*WT-CNP*WN)
      G1=CR*(2.*CO*WN+COP*WT)
      G2=CR*(2.*CO*WT-COP*WN)
      F4=CR*WE2*CNA*FP
      G4=CR*WE2*CTA*FP
      HELP2=AUD*(-CW*CSI*SB*G1+CSI*CB*G2)
      WP2=X*E3*PART12*FP
      WF11=-PART12*(1.-A)*FFP
      WF12=X*(RLR+UD)*SW*CSI*SB*FFP-X*SW*CSI*SB*FF-X*WR*CW*CSI*SB*FFP
      WF13=-X*E3*PART1*FFP-X*AUD*CW*CSI*SB
      WF1=WF11+WF12+WF13
      WF2=-X*(SSI*FF-AUD*CSI*CB)
      WO1=((RLR+UD)*CW*CSI*SB+WR*SW*CSI*SB-E3*(SSI*SW+CSI*SW*CB))*R*FO/V
      WO2=(WR*SSI-(RLR+UD)*CSI*CB)*R*FO/V
      WD1=(YL*SB*CW+(RLR+UD)*SSI*SB*CW+WR*SW*SSI*SB+E3*PART3)*R/V
      WD2=R/V*(YL*CB+(RLR+UD)*SSI*CB+WR*CSI)
      WD3=R/V*(YL*(SSI*CB*CW+SW*CSI)+(RLR+UD)*CB*CW+WR*SW*CB+E3*SW*SB)
      WD4=R/V*(YL*SSI*SB+(RLR+UD)*SB)
      WND1=PART1*F1-PART2*F2
      WTD1=PART1*G1-PART2*G2
      WND2=PART6*F1+SSI*SB*F2
      WND3=CW*SB*F1-CB*F2
      WTD2=PART6*G1+SSI*SB*G2
      WTD3=CW*SB*G1-CB*G2
      WNDD2=WD3*F1+WD4*F2
      WNDD3=WD1*F1-WD2*F2
      WTDD2=WD3*G1+WD4*G2
      WTDD3=WD1*G1-WD2*G2
C*****FIND THE INTEGRAL COEFFICIENTS OF YAW AND YAW RATE
C
      SAM=(1.5/PI)
      DCTDA=4.*(1.-2.*A)
      DZI1=DCTDA*DIS*DIS*DIS*DRR*FBIG*CSI
      IF(A.LT.AC) GO TO 901
      DZI1=(GLUART/DCTDA)*DZI1
901   ADZI2=(PART1*F1-PART2*F2)*(E1*PART3-PART4*SSI*SB)
      BDZI2=+(PART1*G1-PART2*G2)*(PART5*PART3-PART4*PART6)
      DZI2=SAM*(ADZI2+BDZI2)*DIS*DRR
```

```
      ADZI3=(PART1*F1-PART2*F2)*(-E1*SW*SB+PART4*CB)
      BDZI3=-(PART1*G1-PART2*G2)*(PART5*SW*SB+PART4*CW*SB)
      DZI3=SAM*(ADZI3+BDZI3)*DIS*DRR
      DZI4=SAM*(CW*SB*F1-CB*F2)*(E1*PART3-PART4*SSI*SB)*FD*DRR
      DZI5=SAM*(PART6*F1+SSI*SB*F2)*(E1*SW*SB-PART4*CB)*FD*DRR
      DZI6=+SAM*(CW*SB*G1-CB*G2)*(PART5*PART3-PART4*PART6)*FD*DRR
      DZI7=+SAM*(PART6*G1+SSI*SB*G2)*(PART4*CW*SB+PART5*SW*SB)*FD*DRR
      DZI8=SAM*(PART7*F1-PART8*F2)*(E1*PART3-PART4*SSI*SB)*FD*DRR
      DZI9=-SAM*(PART9*F1+PART10*F2)*(PART4*CB-E1*SW*SB)*FD*DRR
      DZI10=+SAM*(PART7*G1-PART8*G2)*(PART5*PART3-PART4*PART6)*FD*DRR
      DZI11=+SAM*(PART9*G1+PART10*G2)*(PART4*CW*SB+PART5*SW*SB)*FD*DRR
      DZI12=SAM*(CW*SB*F1-CB*F2)*(E1*SW*SB-PART4*CB)*FD*DRR
      DZI13=SAM*(PART6*F1+SSI*SB*F2)*(-E1*PART3+PART4*SSI*SB)*FD*DRR
      DZI14=+SAM*(CW*SB*G1-CB*G2)*(PART5*SW*SB+PART4*CW*SB)*FD*DRR
      DZI15=-SAM*(PART6*G1+SSI*SB*G2)*(PART5*PART3-PART4*PART6)*FD*DRR
      DZI16=SAM*(PART7*F1-PART8*F2)*(E1*SW*SB-PART4*CB)*FD*DRR
      DZI17=-SAM*(PART9*F1+PART10*F2)*(E1*PART3-PART4*SSI*SB)*FD*DRR
      DZI18=+SAM*(PART7*G1-PART8*G2)*(PART5*SW*SB+PART4*CW*SB)*FD*DRR
      DZI19=-SAM*(PART9*G1+PART10*G2)*(PART5*PART3-PART6*PART4)*FD*DRR
C*****MASS MATRIX
      QVEL=0.5*RHO*V*V
      DYNA=(3./QVEL)
      DZMPP1=(UCPD*UCPD-2.*UCPD*ER*SW*FP+ER*ER*FP*FP)*AMASS+AI1*FP*FP
      DZMPP=DYNA*DZMPP1*DRR
      DZMFF=DYNA*(AMASS*(UCFD*UCFD+FF*FF)+AI2*FFP*FFP)*DRR
      O1=(WR*WR*(SB*SB+(SSI*CB)**2.)+ER*ER*(CB*CB+(SSI*SB)**2.))
      O2=(RLR+UC)**2.*CSI*CSI+2.*(RLR+UC)*SSI*CSI*(ER*SB-WR*CB)
      O3=2.*WR*ER*SB*CB*CSI*CSI
      O4=AI1*(SSI*CW+CSI*CB*SW)**2.+AI2*CSI*CSI*SB*SB+AI3*PART1**2.
      DZMOO=DYNA*(AMASS*(O1+O2+O3)+O4)*FO*FO*DRR
      DD1=2.*YL*YL+4.*YL*WR*CSI*CB+4.*YL*(RLR+UC)*SSI-4.*YL*ER*CSI*SB
      DD2=WR*WR*(1.+(CSI*CB)**2.)+ER*ER*(1.+(SB*CSI)**2.)
      DD3=(RLR+UC)**2.*(1.+SSI*SSI)-2.*ER*WR*SB*CB*(1.-SSI*SSI)
      DD4=2.*(RLR+UC)*WR*SSI*CSI*CB-2.*(RLR+UC)*ER*SSI*CSI*SB
      DD5=(CSI*CW)**2.+(SSI*SW*CB)**2.+(SW*SB)**2.-2.*SSI*CSI*SW*CW*CB
      DD6=((SSI*SB)**2.+CB*CB)*AI2
      DD7=(CSI*SW)**2.+(SSI*CW*CB)**2.+(CW*SB)**2.+2.*SW*CW*SSI*CSI*CB
      DZMDD=DYNA*(AMASS*(DD1+DD2+DD3+DD4)+AI1*DD5+DD6+AI3*DD7)*FD*FD*DRR
      DZMPF=DYNA*AMASS*(UCPD*UCFD-UCFD*ER*SW*FP+ER*CW*FF*FP)*DRR
      PO1=PART11*(-UCPD+ER*SW*FP)+ER*CW*((RLR+UC)*CSI*SB+ER*SSI)*FP
      PO2=AI1*(SSI*CW+CSI*CB*SW)*FP
      DZMPO=DYNA*(AMASS*PO1+PO2)*FO*DRR
      ZFO1=-UCFD*PART11+((RLR+UC)*SB*CSI+ER*SSI)*FF
      ZFO2=AI2*CSI*CB*FFP
      DZMFO=DYNA*(AMASS*ZFO1+ZFO2)*FO*DRR
C
C*****DAMPING COEFFICIENTS MATRIX
C
      CPP1=AUCPD*PART11+UCPD*ER*CSI*CW*SB*FP-AUC*ER*CW*SB*CSI*FP
      CPP2=-ER*WR*SSI*FP*FP+ER*(RLR+UC)*CB*CSI*FP*FP
      CPP3=3.*WT*CR*FP*(CNA*E2*(E1*FP-UMPD*SW)+PI/8.*CR*CR*R)/V
      DZCPP=(DYNA*(AMASS*OM*(CPP1+CPP2))+CPP3)*DRR
      CPF1=AUCFD*PART11+UCFD*ER*CSI*SB*CW*FP+ER*SB*SW*CSI*FF*FP
      CPF2=ER*(RLR+UC)*SW*SB*CSI*FFP*FP+ER*ER*SSI*SW*FFP*FP
      CPF3=-ER*CW*PART11*FFP*FP
      CPF4=(AI2-AI3)*OM*PART1*FFP*FP
      CPF5=3.*F1/V*(-R*UDFD*SW+CW*FF*R)*(E1*FP-UMPD*SW)
      DZCPF=(DYNA*(AMASS*OM*(CPF1+CPF2+CPF3)-CPF4)+CPF5)*DRR
      CPO1=ER*ER*(SSI*CSI*SB*SW-SB*CB*CW*(1.-SSI*SSI))*FP
      CPO2=-ER*WR*(CW*(SB*SB+(SSI*CB)**2.)+SSI*CSI*CB*SW)*FP
      CPO3=ER*(RLR+UC)*(CSI*CSI*SW+SSI*CSI*CB*CW)*FP
      CPO4=AUC*((RLR+UC)*CSI*CSI-WR*SSI*CSI*CB+ER*SSI*CSI*SB)
      CPO5=-(AI2-AI3)*OM*CSI*SB*PART1*FP
```

```
      CPO6=3.*(WO1*F1+WO2*F2)*(F1*FP-UMPD*SW)
      DZCPO=(2.*DYNA*(AMASS*OM*(CPO1+CPO2+CPO3+CPO4)+CPO5)*FO+CPO6)*DRR
      CFP1=BUCPD*PART11+UCPD*SB*CSI*FF+ER*(RLR+UC)*SB*SW*FFP*FP
      CFP2=ER*ER*SSI*SW*FFP*FP+ER*SB*CB*SSI*CW*FF*FP-ER*BUC*CW*SB*CSI*FP
      CFP3=ER*CW*PART11*FFP*FP-ER*SW*SB*CSI*FP*FF
      CFP4=AI1*OM*PART1*FFP*FP
      CFP5=3.*WT*CR*CNA*E2*(FF*CW-UMFD*SW)*FP*R/V
      DZCFP=(DYNA*(AMASS*OM*(CFP1+CFP2+CFP3)+CFP4)+CFP5)*DRR
      DZCFF=DYNA*(AMASS*OM*(BUCFD*PART11+UCFD*SB*CSI*FF))
      DZCFF=(DZCFF+3.*F1/V*(-R*UDFD*SW+CW*FF*R)*(FF*CW-UMFD*SW))*DRR
      CFO1=WR*(SB*SB+(SSI*CB)**2.)+ER*SB*CB*(1.-SSI*SSI)-(RLR+UC)*SSI*CB
      CFO2=((RLR+UC)*CSI*CSI-WR*SSI*CSI*CB+ER*SSI*CSI*SB)*AUC
      CFO3=(AI2-AI3)*OM*(SSI*CSI*CB*C2W+SW*CW*((CSI*CB)**2.-SSI*SSI))
      CFO4=3.*(WO1*F1+WO2*F2)*(FF*CW-UMFD*SW)
      DZCFO=(-2.*DYNA*(AMASS*OM*(CFO1*FF+CFO2)*FO+CFO3*FFP*FO)+CFO4)*DRR
      DZCOP=3.*WT*CR*(E2*R*(CNA*TAIL1+CTA*TAIL2)+PI/8.*CR*CR*R*PART12)/V
      DZCOP=DZCOP*FP*FO*DRR
      DZCOF=3./V*(-R*UDFD*SW+CW*FF*R)*(F1*TAIL1+G1*TAIL2)*FO*DRR
      DZCCO=3.*((WO1*F1+WO2*F2)*TAIL1+(WO1*G1+WO2*G2)*TAIL2)*FO*DRR
      CDD1=((WD1*F1-WD2*F2)*TAIL3+(WD3*F1+WD4*F2)*TAIL4)*FO*FO
      CDD2=(+(WD1*G1-WD2*G2)*TAIL5-(WD3*G1+WD4*G2)*TAIL6)*FO*FO
      DZCDZ=1.5*(CDD1+CDD2)*DRR
      DZCD1=(PART1*F1-PART2*F2)*TAIL3+(PART1*G1-PART2*G2)*TAIL5
      DZCD1=1.5*DZCD1*DIS*FO*DRR
      DZCD2=(PART1*F1-PART2*F2)*TAIL4-(PART1*G1-PART2*G2)*TAIL6
      DZCD2=1.5*DZCD2*DIS*FO*DRR
C
C*****STIFFNESS COEFFICIENTS MATRIX
C
      HELP=AUC*(-CW*CSI*SB*F1+CSI*CB*F2)
      PP1=-ER*ER*(CW*CW*(SB*SB+(SSI*CB)**2.)-(CB*CB+(SSI*SB)**2.))
      PP2=-ER*ER*CSI*CSI*(2.*SSI*CB*SW*CW+SW*SW)
      PP3=ER*WR*SB*CB*(1.-SSI*SSI)+ER*(RLR+UC)*SSI*CSI*SB
      PP4=-AUC*AUC*CSI*CSI-AAUC*((RLR+UC)*CSI*CSI-SSI*CSI*(WR*CB-ER*SB))
      PP5=GJ*FPP*FPP
      PP6=3.*(-X*HELP-WP2*F2-WE2*CR*CNA*FP)*(E1*FP-UMPD*SW)
      PP7=3.*(WN0*SW*AUMPD+WTJ*F1*FP*FP)
      DZKPP=(DYNA*(AMASS*OM*OM*((PP1+PP2+PP3)*FP*FP+PP4)+PP5))
      PP8=(AI2-AI3)*OM*OM*(SSI*SW-CSI*CW*CB)**2*FP*FP
      PP9=(AI2-AI3)*OM*OM*CSI*CSI*SB*SB*FP*FP
      DZKPP=DZKPP+DYNA*(PP8+PP9)
      DZKPP=(DZKPP+PP6+PP7)*DRR
      PF1=ER*ER*SB*(CB*SW*(1.-SSI*SSI)-SSI*CSI*CW)*FFP*FP
      PF2=-ER*(CW*(SB*SB+(SSI*CB)**2.)+SSI*CSI*CB*SW)*FF*FP
      PF3=ER*WR*(SW*(SB*SB+(SSI*CB)**2.)-CW*SSI*CSI*CB)*FFP*FP
      PF4=-ER*(RLR+UC)*(SSI*CSI*CB*SW-CSI*CSI*CW)*FFP*FP
      PF5=-AUC*BUC*CSI*CSI-ABUC*((RLR+UC)*CSI*CSI-SSI*CSI*(WR*CB-ER*SB))
      PF6=-(AI2-AI3)*OM*OM*CSI*SB*PART12*FFP*FP
      PF7=-3.*(WF1*F1+WF2*F2)*(E1*FP-UMPD*SW)
      PF8=3.*WN0*(BUMPD*SW+UMPD*CW*FFP)
      DZKPF=(DYNA*(AMASS*OM*OM*(PF1+PF2+PF3+PF4+PF5)+PF6)+PF7+PF8)*DRR
      ZFP1=3.*(-X*HELP-WP2*F2)*(FF*CW-UMFD*SW)+3.*AUMFD*WN0*SW
      ZFP1=ZFP1-3.*WE2*CR*CNA*FP*(FF*CW-UMFD*SW)
      DZKFP=(DYNA*(AMASS*OM*OM*(PF1+PF2+PF3+PF4+PF5)+PF6)+ZFP1)*DRR
      ZFF1=-(SB*SB+(CB*SSI)**2.)*FF*FF-CSI*CSI*BUC*BUC
      ZFF2=-((RLR+UC)*CSI*CSI-SSI*CSI*(WR*CB-ER*SB))*BBUC
      ZFF3=(AI1-AI3)*OM*OM*C2W*(SSI*SSI-(CSI*CB)**2.)*FFP*FFP
      ZFF4=4.*(AI1-AI3)*OM*OM*SSI*CSI*SW*CW*CB*FFP*FFP
      ZFF5=EI*FFPP*FFPP
      ZFF6=-3.*((WF1*F1+WF2*F2)*(FF*CW-UMFD*SW))
      ZFF7=3.*WN0*(SW*FF*FFP+SW*BUMFD+UMFD*CW*FFP)
      DZKFF=DYNA*(AMASS*OM*OM*(ZFF1+ZFF2)+ZFF3+ZFF4+ZFF5)
      DZKFF=(DZKFF+ZFF6+ZFF7)*DRR
```

```
      OP1=-WP2*FO*(F2*TAIL1+G2*TAIL2)-WNO*AUM*CW*CSI*SB*FC
      OP1=OP1-(F4*TAIL1+G4*TAIL2)*FO
      OP2=-WTO*(AUM*CSI*CB*FO-PART12*FP*FC*E1)
      OP3=(-X*HELP*TAIL1-A*AUD*(-CW*CSI*SB*G1+CSI*CB*G2)*TAIL2)*FO
      DZKOP=3.*(OP1+OP2+OP3)*DRR
      OF1=-(WF1*F1+WF2*F2)*TAIL1*FO-(WF1*G1+WF2*G2)*TAIL2*FO
      OF2=WNO*CSI*SB*(SW*(RLR+UM)*FFP-AUM*CW-WR*CW*FFP-FF*SW)*FO
      OF3=WNO*E1*PART1*FFP*FO-WTO*(AUM*CSI*CB-SSI*FF)*FC
      DZKOF=3.*(OF1+OF2+OF3)*DRR
      ZDD1=((CW*SB*F1-CB*F2)*TAIL3+(PART6*F1+SSI*SB*F2)*TAIL4)*FD*FD
      ZDD2=(+(CW*SB*G1-CB*G2)*TAIL5-(PART6*G1+SSI*SB*G2)*TAIL6)*FD*FD
      DZKDZ=1.5*(ZDD1+ZDD2)*DRR
      DZKD1=(PART1*F1-PART2*F2)*TAIL3+(PART1*G1-PART2*G2)*TAIL5
      DZKD1=1.5*DZKD1*DIS*FD*DRR
      DZKD2=(PART1*F1-PART2*F2)*TAIL4-(PART1*G1-PART2*G2)*TAIL6
      DZKD2=1.5*DZKD2*DIS*FD*DRR

C
C***** FORCING FUNCTIONS
C
      HP1=ER*ER*(SB*CB*CW*(1.-SSI*SSI)-SSI*CSI*SB*SW)*FP
      HP2=ER*WF*(CW*(SB*SB+(SSI*CB)**2.)+SSI*CSI*CB*SW)*FP
      HP3=-ER*(RLR+UC)*(CSI*CSI*SW+SSI*CSI*CB*CW)*FP
      HP4=AUC*((RLR+UC)*CSI*CSI-WR*SSI*CSI*CB+ER*SSI*CSI*SB)
      HP5=(AI2-AI3)*OM*OM*CSI*SB*PART1*FP
      HP6=3.*WNO*(E1*FP-UMPO*SW)
      DZHP=(DYNA*(AMASS*OM*OM*(HP1+HP2+HP3+HP4)+HP5)+HP6)*DRR
      HF1=WR*(SB*SB+(SSI*CB)**2.)+ER*SB*CB*(1.-SSI*SSI)-(RLR+UC)*SSI*CB
      HF2=BUC*((RLR+UC)*CSI*CSI-WR*SSI*CSI*CB+ER*SSI*CSI*SB)
      HF3=(AI1-AI3)*OM*OM*(SSI*CSI*CB*C2W+SW*CW*((CSI*CB)**2.-SSI*SSI))
      HF4=-EI*FFPP*FFPP*OS
      HF5=3.*WNO*(FF*CW-UMFO*SW)
      DZHF=(DYNA*(AMASS*OM*OM*(HF1*FF+HF2)+HF3*FFP+HF4)+HF5)*DRR
      DZHO=3.*(WNO*TAIL1-WTO*TAIL2)*FO*DRR
********  EFFECT OF TOWER SHADOW
**********
      DCOO=-(WNO*TAIL3+WTO*TAIL5)*FD*DRR
      DZSMP1=-UCPO*PART13+ER*CW*SB*(YL+(RLR+UC)*SSI)*FP-ER*ER*CW*CSI*FP
      DZSMDP=(AMASS*DZSMP1-AI1*PART3*FP)*FO*DRR/OVEL
      DZSMF1=-UCFO*PART13+SB*(YL+(RLR+UC)*SSI)*FF-ER*CSI*FF
      DZSMDF=(AMASS*DZSMF1+AI2*SSI*SB*FFP)*FD*DRR/OVEL
      DZSMO1=(AMASS*PAL1*PAL2-AI1*PART12*PART3-AI2*CSI*SSI*SB*SB)
      DZSMDO=(DZSMO1+AI3*PART1*PART6)*FO*FC*DRR/OVEL
      ZSMD1=(YL*CSI-WR*CB+ER*SB)**2+(YL*SSI+(RLR+UC))**2
      ZSMD2=-(PART13**2+PAL2**2+PART11**2)
      ZSMD3=AI1*(SW*SB)**2+AI2*CB*CB+AI3*(CW*SB)**2
      ZSMD4=-(AI1*PART3**2+AI2*(SSI*SB)**2+AI3*PART6**2)
      DZSMDD=(AMASS*(ZSMD1+ZSMD2)+ZSMD3+ZSMD4)*FO*FD*DRR/OVEL
C
      ZSCP1=-CR*E2*R*WT*FP*(CNA*TAIL3+CTA*TAIL5)*FD/V
      ZSCP2=-PI/8.*WT*CR*CR*CV*FP*PART3*FD
      DSCDP=(ZSCP1+ZSCP2)*DRR
      ZSCP3=((AUC*CSI-ER*PART6*FP)*PAL2+PAL1*(AUC*SSI-ER*PART1*FP))
      ZSCP4=(AI3-AI2)*(SB*SW*(CSI*CSI-SSI*SSI)+2.*SSI*CSI*CW*SB*CB)*FP
      ZSCP5=-WNDD3*(E1*FP-UMPO*SW)*FD
      DSCPD2=-WND1*DIS*(E1*FP-UMPO*SW)*DRR
      DSCPD1=(ZSCP5+OM*(AMASS*ZSCP3+ZSCP4)*FD/OVEL)*DRR
      DSCDF=(R*UDFO*SW-CW*FF*R)/V*(F1*TAIL3+G1*TAIL5)*FD*DRR
      ZSDF2=AMASS*OM*((BUC*CSI-SSI*CB*FF)*PAL2+PAL1*(BUC*SSI+CSI*CB*FF))
      ZSDF3=-(AI1-AI3)*OM*CB*FFP
      ZSDF4=-WNDD3*(FF*CW-UMFO*SW)*FD*DRR
      DSCFD2=-WND1*DIS*(FF*CW-UMFO*SW)*DRR
      DSCFD1=ZSDF4+(-ZSDF2+ZSDF3)*FD*DRR/OVEL
```

```
      DSCDO=-((WO1*F1+WO2*F2)*TAIL3+(WC1*G1+WO2*G2)*TAIL5)*FD*DRR
      DSCO2=-((WR*SB+ER+CB)*YL+(WR*CB-ER*SB)*PART11+(RLR+UC)*PART13)*FO
      DSCO3=((AI1-AI3)*(SW*CW*SB*SSI-CW*CW*CSI*SB*CB)-AI2*CSI*SB*CB)*FO
      DSCO4=-(WNDD3*TAIL1+WTDD3*TAIL2)*FO*FD*DRR
      DSCDD2=-(WND1*TAIL1+WTD1*TAIL2)*DIS*FO*DRR
      DSCDD1=DSCO4+(AMASS*DSCO2+DSCO3)*UM*FD*DRR/QVEL
      DSDD1=(-WNDD2*TAIL4+WNDD3*TAIL3+WTDD2*TAIL5+WTDD3*TAIL5)*FD*FD*DRR
      DSDDJ=(WND1*TAIL3+WTD1*TAIL5)*FD*DIS*DRR
      DSDDK=(WND1*TAIL4-WTD1*TAIL6)*DIS*FD*DRR
C
      DSKP1=(WTO*(E1*PART3*FP+AUM*SSI*CB)+WNO*AUM*SSI*SB*CW)*FD*DRR
      DSKP2=((WP2*F2+X*HELP+F4)*TAIL3+(WP2*G2+X*HELP2+G4)*TAIL5)*FD*DRR
      DSKP2=DSKP2+WE2*CR*FP*(CNA*TAIL3+CTA*TAIL5)*FD*DRR
      DSKDP=DSKP1+DSKP2
      DSKF1=(-WNO*TLF1+WTO*BUM*SSI*CB)*FD*DRR
      DSKF2=((WF1*F1+WF2*F2)*TAIL3+(WF1*G1+WF2*G2)*TAIL5)*FD*DRR
      DSKDF=DSKF1+DSKF2
      DSKDO=(-WNO*TAIL4+WTO*TAIL6)*FD*DRR
      DSKD1=(-WND2*TAIL4+WND3*TAIL3+WTD2*TAIL6+WTD3*TAIL5)*FD*FD*DRR
      DSKDJ=(WND1*TAIL3+WTD1*TAIL5)*DIS*FD*DRR
      DSKDK=(WND1*TAIL4-WTD1*TAIL6)*DIS*FD*DRR
      DSKPD1=-WND3*(E1*FP-UMPD*SW)*FD*DRR
      DSKPD2=-WND1*DIS*(E1*FP-UMPD*SW)*DRR
      DSKFD1=-WND3*(FF*CW-UMFD*SW)*FD*DRR
      DSKFD2=-WND1*DIS*(FF*CW-UMFD*SW)*DRR
      DSKOD1=-(WND1*TAIL1+WTD1*TAIL2)*FD*FO*DRR
      DSKOD2=-(WND1*TAIL1+WTD1*TAIL2)*DIS*FO*DRR

C*****
C******* GRAVITY TERMS
C*****
      DGNCOS=AMASS*GR*((UCPD-ER*SW*FP)*CSI-ER*SSI*CB*CW*FP)*DRR/QVEL
      DGNSIN=-AMASS*GR*ER*CW*SB*DRR/QVEL
      DGPCOS=AMASS*GR*(AUCPD*CSI-ER*SSI*SB*FP*FP)*DRR/QVEL
      DGPSIN=AMASS*GR*ER*CB*FP*FP*DRR/QVEL
      DGFCOS=AMASS*GR*((BUCPD-ER*CW*FP*FFP)*CSI+ER*SSI*CB*SW*FP*FFP)*DRR
      DGFCOS=DGFCOS/QVEL
      DGFSIN=AMASS*GR*ER*SW*SB*FP*FFP*DRR/QVEL
      DGOCOS=-AMASS*GR*ER*CW*SB*FP*FO*DRR/QVEL
      DGOSIN=AMASS*GR*(ER*SSI*CB*CW*FP-UCPD*CSI)*FO*DRR/QVEL
      IF(IM.EQ.1) THEN
      FEB=9./8.
      IF(I.EQ.1.OR.I.EQ.4) FEB=3./8.
      IF(I.GE.4) IM=0
      ELSE

      FEB=2./3.
      IF(NTEST.EQ.0) FEB=4./3.
      IF(I.EQ.1.OR.I.EQ.NN) FEB=1./3.
      ENDIF
C*****START THE SIMPSON INTEGRATION
      ZI1=ZI1+FEB*DZI1
      ZI2=ZI2+FEB*(DZI2)
      ZI3=ZI3+FEB*(DZI3)
      ZI4=ZI4+FEB*(DZI4)
      ZI5=ZI5+FEB*(DZI5)
      ZI6=ZI6+FEB*(DZI6)
      ZI7=ZI7+FEB*(DZI7)
      ZI8=ZI8+FEB*(DZI8)
      ZI9=ZI9+FEB*(DZI9)
      ZI10=ZI10+FEB*(DZI10)
      ZI11=ZI11+FEB*(DZI11)
      ZI12=ZI12+FEB*(DZI12)
```

```
ZI13=ZI13+FEB*(DZI13)
ZI14=ZI14+FEB*(DZI14)
ZI15=ZI15+FEB*(DZI15)
ZI16=ZI16+FEB*(DZI16)
ZI17=ZI17+FEB*(DZI17)
ZI18=ZI18+FEB*(DZI18)
ZI19=ZI19+FEB*(DZI19)
ZMPP=ZMPP+FEB*(DZMPP)
ZMPF=ZMPF+FEB*(DZMPF)
ZMPO=ZMPO+FEB*(DZMPO)
ZMFF=ZMFF+FEB*(DZMFF)
ZMOO=ZMOO+FEB*(DZMOO)
ZMOO=ZMOO+FEB*(DZMOO)
ZMFO=ZMFO+FEB*(DZMFO)
ZCPP=ZCPP+FEB*(DZCPP)
ZCPF=ZCPF+FEB*(DZCPF)
ZCPO=ZCPO+FEB*(DZCPO)
ZCFP=ZCFP+FEB*(DZCFP)
ZCFF=ZCFF+FEB*(DZCFF)
ZCFO=ZCFO+FEB*(DZCFO)
ZCOP=ZCOP+FEB*(DZCOP)
ZCOF=ZCOF+FEB*(DZCOF)
ZCOO=ZCOO+FEB*(DZCOO)
ZCOZ=ZCOZ+FEB*(DZCOZ)
ZCO1=ZCO1+FEB*(DZCO1)
ZCO2=ZCO2+FEB*(DZCO2)
ZKPP=ZKPP+FEB*(DZKPP)
ZKPF=ZKPF+FEB*(DZKPF)
ZKFP=ZKFP+FEB*(DZKFP)
ZKFF=ZKFF+FEB*(DZKFF)
ZKOZ=ZKOZ+FEB*(DZKOZ)
ZKOP=ZKOP+FEB*DZKOP
ZKOF=ZKOF+FEB*DZKOF
ZKO1=ZKO1+FEB*(DZKO1)
ZKO2=ZKO2+FEB*(DZKO2)
ZHP=ZHP+FEB*(DZHP)
ZHF=ZHF+FEB*(DZHF)
COO=COO+FFB*DCOO
SMOP=SMOP+FEB*DZSMOP
SMOF=SMOF+FEB*DZSMOF
SMOO=SMOO+FEB*DZSMOO
SMOO=SMOO+FEB*DZSMOO
SCOP=SCOP+FEB*DSCOP
SCOF=SCOF+FEB*DSCOF
SCOO=SCOO+FEB*DSCOO
SCO1=SCO1+FEB*DSCO1
SCOJ=SCOJ+FEB*DSCOJ
SCOK=SCOK+FEB*DSCOK
SKOP=SKOP+FEB*DSKOP
SKOF=SKOF+FEB*DSKOF
SKOO=SKOO+FEB*DSKOO
SKO1=SKO1+FEB*DSKO1
SKOJ=SKOJ+FEB*DSKOJ
SKOK=SKOK+FEB*DSKOK
SCPO1=SCPO1+FEB*DSCPO1
SCPO2=SCPO2+FEB*DSCPO2
SCFO1=SCFO1+FFB*DSCFO1
SCFO2=SCFO2+FEB*DSCFO2
SCOO1=SCOO1+FEB*DSCOO1
SCOO2=SCOO2+FEB*DSCOO2
SKPO1=SKPO1+FEB*DSKPO1
SKPO2=SKPO2+FEB*DSKPO2
SKFO1=SKFO1+FEB*DSKFO1
```

```
      SKFD2=SKFC2+FEB*DSKFD2
      SKOD1=SKOC1+FEB*DSKOD1
      SKOD2=SKOC2+FEB*DSKOD2
      GNCOS=GNCCS+FEB*DGNCOS
      GNSIN=GNSIN+FEB*DGNSIN
      GPCOS=GPCOS+FEB*DGPCOS
      GPSIN=GPSIN+FEB*DGPSIN
      GFCOS=GFCCS+FEB*DGFCOS
      GFSIN=GFSIN+FEB*DGFSIN
      GOCOS=GOCCS+FEB*DGOCOS
      GOSIN=GOSIN+FEB*DGOSIN
      ZHO=ZHO+FEB*(DZHO)
C
      IF(SUPP.EQ.1HY) GO TO 43
      IF(RLR.EQ.RHR) GO TO 554
      IF(KK.LT.5) GO TO 43
554   WRITE(1,16)RLR,A,DPHI,DBET,DAL,CL,CD,BCR,CPB,CTB
      KK=0
43    CONTINUE
      KK=KK+1
      XL=XL-DX
      RLR=XL/X
      I=I+1
      IF(RLR.LT.RHR) THEN
      RLR=RHR
      XL=RHR*X
      DRR=(TNUM-NUM)*DRR
      ELSE
      ENDIF
      IF(I.LE.NN) GO TO 555
C
C******CALCULATE THE YAW AND YAW RATE VARIATION
C
      IF(RLR.EQ.1.) THEN
      SKDEL=SJDEL=SKRDEL=SJRDEL=0.
      ELSE
73    DENO=(ZI1-ZI3)**2+ZI2*ZI2
      SKDEL=((ZI4+ZI5+ZI6+ZI7)*(ZI1-ZI3)-ZI2*(ZI12+ZI13+ZI14+ZI15))/DENO
      SJDEL=((ZI4+ZI5+ZI6+ZI7)*ZI2+(ZI1-ZI3)*(ZI12+ZI13+ZI14+ZI15))/DENO
      SJDEL=-SJDEL
      SKRDEL=(ZI8+ZI9+ZI10+ZI11)*(ZI1-ZI3)
      SKRDEL=(SKRDEL-ZI2*(ZI16+ZI17+ZI18+ZI19))/DENO
      SJRDEL=(ZI8+ZI9+ZI10+ZI11)*ZI2
      SJRDEL=-(SJRDEL+(ZI1-ZI3)*(ZI16+ZI17+ZI18+ZI19))/DENO
      ENDIF
      ZCDD=ZCDZ+SJRDEL*ZCD1-SKRDEL*ZCD2
      ZKDD=ZKDZ+SJDEL*ZKD1-SKDEL*ZKD2
      SCDD=SCD1+SJRDEL*SCDJ+SKRDEL*SCDK
      SKDD=SKD1+SJDEL*SKDJ+SKDEL*SKDK
      SCPD=SCPD1+SJRDEL*SCPD2
      SCFD=SCFD1+SJRDEL*SCFD2
      SCOD=SCOD1+SJRDEL*SCOD2
      SKPD=SKPD1+SJDEL*SKPD2
      SKFD=SKFD1+SJDEL*SKFD2
      SKOD=SKOD1+SJDEL*SKOD2
C
C*******CORRECTION FOR MASS COEF. DUE TO TOWER SHADOW SO IT IS IN
C*******FORM OF (MIJ-MIJS)
      SMDP=-SMDP
      SMDF=-SMDF
      SMDO=-SMDO
      SMDD=-SMDD
      WRITE(1,700)LR,E1,E2,E3,AE,AG
```

```
      WRITE(1,402)N,MM
      WRITE(1,509) CP,CT
      WRITE(1,505)
      WRITE(1,405) ZMPP,ZMPF,ZMPO,ZMFF,ZMFO,ZMOO,ZMOO
      WRITE(1,506)
      WRITE(1,406) ZCPP,ZCPF,ZCPO,ZCFP,ZCFF,ZCFO,ZCOP,ZCOF,ZCOO,ZCOO
      WRITE(1,507)
      WRITE(1,405) ZKPP,ZKPF,ZKFP,ZKFF,ZKOP,ZKOF,ZKOO
      WRITE(1,508)
      WRITE(1,408) ZHP,ZHF
      WRITE(1,407) SKOEL,SJOEL,SKROEL,SJROEL
      WRITE(1,513)
      WRITE(1,514) GNCOS,GNSIN,GPCOS,GPSIN,GFCOS,GFSIN,GOCOS,GOSIN
      WRITE(1,515) SMOP,SMOF,SMOO,SMOO
      WRITE(1,516) SCOP,SCOF,SCOO,SCOO
      WRITE(1,517) SKOP,SKOF,SKOO,SKOO
      WRITE(1,311) SCPO,SCFO,SCOO
      WRITE(1,312) SKPO,SKFO,SKOO
      WRITE(1,518) COO

      DRR=DX/X
      X=X+DBX
      IF(X.GT.XMAX) GO TO 40
      GO TO 27
40    CONTINUE
      PRINT 4
      READ5,DANSR
      IF(DANSR.NE.1HY) GO TO 300
      PRINT 6
      READ*,PITCH
      GO TO 200
C     ******************************************************************
C
C     FORMAT STATEMENTS
C
C     ******************************************************************
   1  FORMAT(*  FORCES INPUT SEQUENCE*)
   2  FORMAT(* WRITE B,BCRR,EM,DRR,XMIN,XMAX,DBX*)
  65  FORMAT(* WRITE ALC,AST,SI,PITCH,BETA FOOT,DBETA*)
  66  FORMAT(* WRITE RT,DCND,RC,RH*)
   3  FORMAT(* WRITE CD ZERO, CL MAX, CL FLAT, ALPHA BREAK*)
  4   FORMAT(*DO YOU WANT ANOTHER PITCH ANGLE? (Y)*)
   5  FORMAT(A1)
   6  FORMAT(*INPUT PITCH ANGLE*)
  8   FORMAT(15X,*AERODYNAMIC DATA*//,6X,*CLM*,6X,*CLFL*,8X,*M*,8X,*AST*
     1,7X,*ABR*,7X,*ALC*,7X,*CDO*/7F10.3/)
   9  FORMAT(15X,*OPERATIONAL VARIABLES*//5X,*XMIN*,6X,*XMAX*,7X,*DRR*,
     18X,*SI*/4F10.3/)
  19  FORMAT(15X,*PHYSICAL AIRFOIL DATA*//,7X,*B*,7X,*BCRR*,6X,*DCND*
     1,7X,*RT*,8X,*RC*,8X,*RH*,8X,*BRT*,6X,*DBTA*/8F10.3/)
  60  FORMAT(////25X,*PROGRAM OPERATING CONDITIONS*/)
  21  FORMAT(///25X,*PROGRAM FORCES OUTPUT AT PITCH =*,F7.3,* DEGREES*)
  15  FORMAT(////,6X,*PCR*,8X,*A*,8X,*PHI*,8X,*BETA*,
     15X,*ALPHA*,7X,*CL*,7X,*CD*,7X,*BCR*,7X,*CPR*,7X,*CTR*)
  16  FORMAT(2F10.4,6F10.3,4X,2F9.5)
 100  FORMAT(//,5X,*THIS RUN USED*,F9.3,3X,*SECONDS*)
407   FORMAT(/,3X,*SKOEL*,12X,*SJOEL*,12X,*SKROEL*,12X,*SJROEL*/,
     14(3X,G12.6))
405   FORMAT (7(3X,G12.6))
406   FORMAT(10(1X,G12.6))
408   FORMAT(3(4X,G12.6))
402   FORMAT(4),*  N = *,I3,*    MM = *,I3)
505   FORMAT(//,6X,*MPP*,12X,*MPF*,12X,*MPO*,12X,*MFF*,12X,*MFO*,12X
```

```
     1,'MOO',12X,'MOD')
506   FORMAT(//,6X,'CPP',11X,'CPF',11X,'CPO',11X,'CFP',11X,'CFF',11X,
     1'CFO',11X,'COP',11X,'COF',11X,'COO',11X,'COD')
507   FORMAT(//,6X,'KPP',12X,'KPF',12X,'KFP',12X,'KFF',12X,'KOP',12X,
     1'KOF',12X,'KOD')
508   FORMAT(//,6X,'HP',12X,'HF',12X,'HO')
509   FORMAT(/,3X,'CP=  ',F10.5,8X,' CT=  ',F10.5)
510   FORMAT(/,1X,'  QS  =  ',G12.6)
513   FORMAT(//,2X,'GNCOS',9X,'GNSIN',9X,'GPCOS',9X,'GPSIN',9X,'GFCOS',
     19X,'GFSIN',9X,'GOCOS',9X,'GOSIN')
514   FORMAT(8(1X,G12.6))
515   FORMAT(/,4X,'SMDP = ',G12.6,' SMDF = ',G12.6,' SMDO = ',G12.6,'
     1SMDD = ',G12.6)
516   FORMAT(/,4X,'SCDP = ',G12.6,' SCDF = ',G12.6,' SCDO = ',G12.6,'
     1SCDD = ',G12.6)
517   FORMAT(/,4X,'SKDP = ',G12.6,' SKDF = ',G12.6,' SKDO = ',G12.6,'
     1SKDD = ',G12.6)
518   FORMAT(/,4X,'CQS = ',G12.6)
311   FORMAT(/,4X,'SCPD = ',G12.6,' SCFD = ',G12.6,' SCOD = ',G12.6)
312   FORMAT(/,4X,'SKPD = ',G12.6,' SKFD = ',G12.6,' SKOD = ',G12.6)
700   FORMAT(/,8X,' ER',9X,'E1',9X,'E2',9X,'E3',9X,'AE',9X,'AG'
     1/,2X,6(G12.6,2X))
  300 TIMOUT=SECOND()-TIMIN
      WRITE(1,100) TIMOUT
      STOP
      END
      SUBROUTINE SUMROW(TOM,TIM,RLR,ER,E1,E3,UC,AUC,BUC,AAUC,ABUC,BBUC,A
     1UM,AAUM,ABUM,AUD,MM)
      COMMON L,F,RS
      COMMON /STIFF/ EI,EIC,GJ,GJD,RHR,QS
C
      UC=AUC=AAUC=ABUC=BBUC=AUM=AAUM=ABUM=AUD=0.
      ALOW=RHR
      AHIGH=(RLR-RHR)/RS
      N=MM
      DRS=(AHIGH-ALOW)/N
      DRS3=DRS/3.
      RLS=ALOW
      K=N+1
      DO 10 I=1,K
      IHALF=I/2
      ITEST=I-2*IHALF


      ZP=RLS
      ZP2=ZP*ZP
      ZP3=ZP2*ZP
      ZP4=ZP3*ZP
      FF=6.*ZP2-4.*ZP3+ZP4
      FFP=12.*ZP-12.*ZP2+4.*ZP3
      FFPP=12.-24.*ZP+12.*ZP2
      FP=2.*ZP-ZP2
      FPP=2.*(1.-ZP)
      WR=FF*QS*RS
      WP=FFP*QS
      WPP=FFPP*QS
      CW=COS(WP)
      SW=SIN(WP)
      DUC=-0.5*WP*WP*RS
      TOM0=TOM(ER,CW,SW,FP,FPP,WPP)
      TOM1=TOM(E1,CW,SW,FP,FPP,WPP)
      EE3=-E3
      TOM3=TOM(EE3,CW,SW,FP,FPP,WPP)
```

```
      DAUC=-WP*TOMC
      DAUM=-WP*TOM1
      DAUD=-WP*TOM3
      DAAUC=-TOMC*TOMC/RS
      DAAUM=-TOM1*TOM1/RS
      TIMC=TIM(ER,CW,SW,FP,FPP,WPP,FFP,FFPP)
      TIM1=TIM(E1,CW,SW,FP,FPP,WPP,FFP,FFPP)
      DABUC=WP*TIMC-FFP*TOMC
      DABUM=WP*TIM1-FFP*TOM1
      DBBUC=-FFF*FFP*RS
      FEB=C.
      IF(ITEST.EQ.C) FEB=1.
      IF(I.EQ.1.OR.I.EQ.K) FEB=1.
      UC=UC+FEB*DUC*DRS3
      AUC=AUC+FEB*DAUC*DRS3
      AUM=AUM+FEB*DAUM*DRS3
      AUD=AUD+FEB*DAUD*DRS3
      AAUC=AAUC+FEB*DAAUC*DRS3
      AAUM=AAUM+FEB*DAAUM*DRS3
      ABUC=ABUC+FEB*DABUC*DRS3
      ABUM=ABUM+FEB*DABUM*DRS3
      BBUC=BBUC+FEB*DBBUC*DRS3
      BUC=BBUC*QS
      RLS=RLS+DRS
10    CONTINUE
      RETURN
      END
      FUNCTION TOM(A,B,C,D,E,F)
      COMMON L,F,RS
      TOM=A*B*E-A*C*F*D
      RETURN
      END
      FUNCTION TIM(A,B,C,D,E,F,G,H)
      COMMON L,F,RS
      TIM=A*C*E*G+A*F*B*D*G+A*C*D*H
      RETURN
      END
```

★ U.S. Government Printing Office 1984 - 779-093/9278 Reg. 8